Title
Phenological and Physiological Response of Vitis Vinifera to Elevated Temperature and Carbon Dioxide

Author
Clemens, Molly Elizabeth

Publication Date
2022

Peer reviewed|Thesis/dissertation

Phenological and Physiological Response of *Vitis Vinifera* to Elevated Temperature and Carbon Dioxide

By

MOLLY ELIZABETH CLEMENS

DISSERTATION

Submitted in partial satisfaction of the requirement for the degree of

DOCTOR OF PHILOSOPHY

in

Ecology

in the

OFFICE OF GRADUATE STUDIES

of the

UNIVERSITY OF CALIFORNIA, DAVIS

And

SAN DIEGO STATE UNIVERSITY

Approved:

_____

Walter Oechel, Chair

_____

Andrew Walker

_____

Kyaw Tha Paw U

Committee in Charge

2022

Table of Contents

ABSTRACT

From an ecological perspective, grape production is a result of the many tiered interactions between vine, soil, pest, cultivation, and climate. Globally, vineyards are facing year-round changes in climate that impact growth and maturation, driven by an increase in atmospheric carbon dioxide from anthropogenic emissions. Carbon dioxide is not only contributing to the overall warming of the planet, for grapevine, it also fuels unwanted growth, drives an increase in pest pressure through carbon-nitrogen imbalances, and sometimes unfavorably alters the response of stomata. The potential for an increase in water use efficiency is likely transient, and concurrently limited by water availability. A major finding from the literature synthesis was the impact of advancing grapevine phenology, which is altered by both temperature and carbon dioxide.

A subsequent field based phenological study using an experimental vineyard site at the University of California, Davis was used to create a model of grapevine phenology for the three major lifecycle stages: budburst, flowering, and veraison for 137 varieties over four years. The timing of the primary stages of grapevine phenology were modelled in terms of total growing degree days and used coefficient of variation as a proxy for sensitivity to climate, grouping the cultivars by genetically determined geographic origin. The estimates of each stage for every variety contributes to our understanding of alternative varieties, which can inform future selection for breeding and planting. The general intercept for these models was offset by geographic origin of the varieties, utility of the varieties as a table or wine grape, and for the stage of veraison, was also impacted by the number of days that reached temperatures of 40°C or more.

Understanding that elevated carbon dioxide will likely increase drought events in major winegrape growing regions, we investigated one potential mitigation strategy via genetic transformation of grapevine for drought resistance. The CRISPR/Cas9 system was applied to functionally characterize and modify the stomatal density gene, VvEPFL9-1, in *Vitis vinifera c.v.* Sugraone. After successful transformation, the analysis of stomata density revealed that in edited plants the number of stomata was significantly reduced compared to the wild type control, demonstrating for the first time the role of EPFL9 in a perennial fruit crop. Two edited lines were then assessed for growth, photosynthesis, stomatal conductance, and water use efficiency in the greenhouse at both controlled ambient conditions and in a natural dry-down experiment. Intrinsic water-use efficiency was significantly impacted under both well-watered and drought conditions, confirming reduced stomatal density as a preferable trait under future drier environmental conditions. These results show the potential of manipulating stomatal density for optimizing grapevine responses under changing climate conditions.

A common thread from each of these studies is that alternative varieties of grapevine are needed in the major winegrape growing areas as climate change increases the risk of high heat events and drought. Potential mitigation strategies are planting alternative varieties with more resilience to climate change and/or cultivating new material from the expansive selection of available material. We can strengthen the vineyard system by introducing more diverse cultivars, with an ideal candidate fitting the profile of heat and drought tolerant, late ripening, with strong pest resistance. We identified groups of varieties with common geographic origins that would make suitable candidates for further research based on their low sensitivity to climate, and we demonstrated that well known varieties can be modified to have increased drought resistance.

Acknowledgments

I would like to first and foremost thank my wonderful mentor Walt, who believed in me and encouraged the pursuit of grapevine research. Walt inspired me to study grapes in the most beautiful places in the world by sending me for a field season in the Alaskan tundra.

I would like to thank Lorenza Dalla Costa, who inspired me with her excellence and dedication. Lorenza mentored me as a scientist and as a woman in science, and I could not have accomplished my PhD without her guidance and encouragement. I owe a debt of gratitude to Lizzie Wolkovich for her constant mentorship and guidance throughout my PhD, but especially for the encouragement at the beginning of my thesis. She taught me to be thorough, patient, and reassured me during some of the toughest moments of my dissertation. I would also like to thank Sarah Cookson for her mentorship through the Chateaubriand Fellowship, for guiding me through technical skills and providing the opportunity of a lifetime to work at the ISVV.

I could not have achieved my research goals without the incredible team at the San Diego State University Santa Margarita Ecological Reserve team, with a special thank you to Pablo Bryant, Jamie Bourdon, and my good friend Beth Cobb who spent long hours helping to bring the experimental vineyard to life. I also owe my sincere gratitude to my friend and colleague Clarissa Reyes for her patience and help with my data collection and analysis. A sincere thank you to my graduate committee members Andy Walker and Kyaw Tha Paw U for your thoughtful comments and constructive reviews.

Funding sources: San Diego State University, University of California Davis, Fondazione Edmund Mach, University Graduate Fellowship, ARCS, and Chateaubriand Foundation.

List of Figures and Tables

INTRODUCTION

Presented here is the cumulative research on the response of grapevine within different climate change scenarios, specifically, rising levels of atmospheric carbon dioxide, temperature, and drought. Global warming increases the frequency of extreme high-temperature events and consequent severe drought scenarios and thus may constitute a threat to modern viticulture (Van Leeuwen et al., 2019). Global warming affects grapevine not only by increasing growing season temperatures, but also by impacting pest pressure, soil water availability, carbon:nitrogen ratios, and the resulting chemical composition of wine. Additionally, elevated carbon dioxide causes advances in phenology, which compound significantly over seasons, with the long-term carbon storage increasing after each growing season (Edwards et al. 2017). Synthesizing the ecological impacts of elevated carbon dioxide on the system of vineyards highlights the profound impact global warming will have on grapevine phenology and subsequent harvest.

Grape growers have been keeping detailed records of harvest dates for centuries (Labbé et al. 2019), and the predicted advances in phenology are creating a challenge for growers. In order for farmers to explore alternative late ripening varieties, we need a quantification of the sensitivity to climate change of international varieties in California. There are between 6,000 – 10,000 genetically different varieties of grapevine (Galet 2015). As part of an ongoing research project at the University of California Davis, I recorded the phenological timing of 137 different grapevine varieties and compared this timing across 4 years of varying climate. We modeled the response of the grapevines to temperature and included a variable for days over 40°C to estimate sensitivity to extreme heat. Grouping the varieties by geographic origin and by utility (wine or table) also increased the accuracy of the phenological prediction. This provided perspective on how the vast differences between grapevine varieties contributed to their responses to

temperature, and therefore avenues for selective breeding. Many grape growers are legally required to grow specific varieties, which is not the case in California. As a leader in the global market, California could demonstrate the utility of growing alternative varieties as a mitigation to global warming (Wolkovich et al. 2018).

Furthermore, the commitment to grapevine varieties (either legal or cultural) inspired the research of a targeted genetic transformation to incorporate drought resistance into eminent varieties. One of the mechanisms that plants can activate in response to environmental stresses is the stomatal regulation of transpiration. The highly conserved hormonal peptides of the epidermal patterning factor family (EPF and EPF-Like) are known in model plants to be responsible for regulating stomatal development during leaf formation (Lu et al. 2019). In particular, *EPFL9* (also known as STOMAGEN) promotes stomatal development (Kondo et al., 2010). I studied the role of *VvEPFL9* in determining stomatal density in grapevine and determined that stomatal features such as density and distribution are a promising target for designing climate change-resilient crops. *Vitis vinifera* genotypes with reduced stomatal density and, in turn, greater intrinsic water use efficiency, may in fact be desirable to improve plant water conservation under current and future climate scenarios (Arrizabalaga-Arriazu et al. 2021).

The overarching goal of this thesis is to predict the response of grapevines to future climate conditions. The synthesis of current literature on grapevine grown under elevated carbon dioxide levels indicates the major threats include shifts in phenology and drought stress. Modelling the phenological response of 137 varieties over four growing seasons in Northern California created a reference for phenological timing and sensitivity to change in temperature. Furthermore, I transformed grapevine for reduced stomatal density to test the concept of climate change resilient grapevine. I stress that genetic transformation should be used as one tool among

many, and this targeted agroecological approach can be used in tandem with exploiting existing grapevine material, which is vast and diverse.

References:

Arrizabalaga-Arriazu M., Morales F., Irigoyen J.J., Hilbert G., & Pascual I. (2021). Growth and physiology of four *Vitis vinifera* L. cv. Tempranillo clones under future warming and water deficit regimes. *Australian Journal of Grape Wine Research* 27: 295–307.

Edwards E, Unwin D, Kilmister R & Treeby M. (2017). Multi-seasonal effects of warming and elevated CO_2 on the physiology, growth and production of mature, field grown, Shiraz grapevines. *OENO One* 51: 127-132.

Galet, P. *Dictionnaire Encyclopédique des Cépages et de leur Synonymes* (Édition Libres et Solidaire, Paris, 2015).

Kondo T., Kajita R., Miyazaki A., Hokoyama M., Nakamura-Miura T., Mizuno S., Masuda Y., Irie K., Tanaka Y., & Takada S. (2010). Stomatal density is controlled by a mesophyll-derived signaling molecule. *Plant Cell Physiol* 51: 1–8.

Labbé, T., Pfister, C., Brönnimann, S., Rousseau, D., Franke, J., & Bois, B. (2019). The longest homogeneous series of grape harvest dates, Beaune 1354–2018, and its significance for the understanding of past and present climate. *Climate of the Past*, *15*(4), 1485-1501.

Lu J., He J., Zhou X., Zhong J., Li J., Liang Y.K. (2019). Homologous genes of epidermal patterning factor regulate stomatal development in rice. *Journal of Plant Physiology* 234–235: 18–27.

Van Leeuwen C., Destrac-Irvine A., Dubernet M., Duchêne E., Gowdy M., Marguerit E., Pieri P., Parker A., De Rességuier L., & Ollat N. (2019). An update on the impact of climate change in viticulture and potential adaptations. *Agronomy* 9: 1–20.

Wolkovich, E. M., García de Cortázar-Atauri, I., Morales-Castilla, I., Nicholas, K. A., & Lacombe, T. (2018). From Pinot to Xinomavro in the world's future wine-growing regions. *Nature Climate Change*, 8(1), 29-37.

CHAPTER 1

The Effects of Elevated Atmospheric Carbon Dioxide on the Vineyard System of *Vitis vinifera*: A Review

Authors: Molly E Clemens, Alessandra Zuniga, Walter Oechel

Am J Enol Vitic. November 2021: ajev.2021.21029; published ahead of print November 11, 2021

DOI: 10.5344/ajev.2021.21029

Abstract

Global atmospheric carbon dioxide concentrations will continue increasing throughout the next century, with profound impacts on agriculture. The literature concerning the effects of climate change on viticulture has largely focused on the isolated impacts of variables such as temperature and soil water deficit. Likewise, the research on the effects of elevated atmospheric CO_2 on grapevines is stunted at the categorical level, chiefly because of the difficulty of experimentally controlling the gaseous environment in situ for the years necessary to replicate the vineyard system in a future climate condition. Despite numerous studies on the short-term influence of environmental and cultural factors on grapevine development at elevated carbon dioxide, the long-term impacts remain poorly understood. The lack of field based elevated CO_2 experiments in the United States is an added challenge to predicting viticultural changes, particularly in California. This review focuses on the systemic impact of atmospheric CO_2 on *Vitis vinifera*, synthesizing physiological, phenological, and plant-pest interactions. Major findings from this synthesis inform of a predicted increase in pest pressure, advanced phenological timing, transient increase in water use efficiency for grapevine, and changes in

grape berry chemistry. While water use efficiency is highly desirable, the prediction for current winegrape growing regions is a transient increase in water use efficiency subsequently limited by a lack of available soil water. Grapevine is influenced by the negative synergistic effects of heat, drought, and elevated CO_2, which will alter cultural practices including harvest and pest/disease control, with downstream effects on winemaking. Several options for adaptation are discussed including leaf removal, planting alternative varieties and selective breeding of new varieties.

Introduction

Rising atmospheric carbon dioxide levels are well documented by the International Panels on climate change, and carbon dioxide is expected to reach levels between 530 and 720 mg/L by the year 2100 according to intermediate scenarios (IPCC 2014). The last time Earth experienced levels of carbon dioxide consistently above 400 mg/L was the early Miocene era, approximately 23 million years ago (Pearson and Palmer 2000). The earliest agriculture was cultivated between 23,000 and 12,000 years ago (Weiss et al. 2004), with the earliest grape domestication estimated between 6,000 and 9,000 years ago (Terral et al. 2010). Grapevine has historically been sensitive to changes in climate, including the "Little Ice Age" in Europe (Mariani et al. 2018) and the more recent heat waves of the 21st century (Galat Giorgi et al. 2019, Venios et al. 2020, Bertamini et al. 2021).

While grapevine is typically cultivated in regions with wet winters and dry summers, increasing events of severe water stress will impede growth and reduce quality and yield in grapevine under climate change (Chaves et al. 2010, Mosedale et al. 2016, Scholasch and Rienth 2019, Morales-Castilla et al. 2020). Mean climate projections underestimate the impact of

climate change on grapevine, in particular the impact of extreme temperature spikes/drops in areas growing premier winegrapes, currently characterized by few days with extreme heat or cold (White et al. 2006, Parker et al. 2020). While vines in Mediterranean areas will have to adapt to a more variable climate, elevated CO_2 will compound the effects of heat and drought stress at a global scale, impacting the quality and quantity of grapevine yield (Jones et al. 2005, Schultz 2010, Mosedale et al. 2016, Van Leeuwen and Darriet 2016, Bertamini et al. 2021). Carbon dioxide levels present a relatively novel challenge as they have been increasing at an unprecedented rate since the start of the Industrial Revolution (IPCC 2014).

Winegrapes are one of the most culturally and economically important crops worldwide, with an annual production of 60 million tons of fruit annually, the highest monetary value of fruit crops, and wine being part of the UNESCO intangible cultural heritage of humanity (Vivier and Pretorius 2002, Owens 2008, Ponti et al. 2018, Delrot et al. 2020, Santos et al. 2020). While wild grapevines can be very resilient to abiotic stress, domesticated winegrapes are far more sensitive; a result of the meticulous conservation of berry phenotype with emphasis on flavor over stress tolerance since 400 BC (Terral et al. 2010, Mariani et al. 2018). While this careful preservation of grape berry phenotype benefits the culture and industry of winegrape growing, as an ecological system the vineyard is vulnerable to a changing climate and elevated atmospheric CO_2 levels (Jones 2005).

Heat, elevated carbon dioxide, and limited water availability are necessary for cultivating quality grapes, however, studies on their interactive effects indicate these will have a negative synergistic impact on grapevine (Lobell et al. 2006, Edwards et al. 2017, Galat Giorgi et al. 2019). The variety-specific responses to these environmental conditions introduces further variability to any study of grapevine response to future climate (Wohlfahrt et al. 2017), while

variability in viticultural production is often viewed as undesirable. The varying physiology of cultivars and the long-term perennial nature of grapevine creates a challenging subject for adaptation studies; we expect that any adaptation will be much slower than that of annual crops (Lobell et al. 2006, Venios et al. 2020).

This review synthesizes recent literature published on the direct effects of elevated carbon dioxide on grapevine physiology, as well as the indirect effects on phenology and ecological responses of grapevines, including studies of the interactive effects of climate variables. This synthesis focused on literature specific to grapevine, and in addition, included studies on Arabidopsis to explore relevant hypotheses illustrating mechanisms of carbon dynamics in C3 plants. Results were compared from the four predominant experimental approaches; growth chambers, greenhouses, open top chambers, and Free Air CO_2 Enrichment (FACE), all evaluated for predictive value. Finally, this review concludes by discussing potential research necessary for understanding the future of growing grapevine with elevated CO_2 and adaptive viticultural management.

Physiology

The physiological advantage of increased atmospheric carbon available for crops such as grapevine must be weighed against other factors likely to cooccur in the context of climate change, including water scarcity and temperature increases (Gray et al. 2016, Faralli et al. 2017). The literature asserts that the RUBISCO of C3 plants, including grapevines, are currently limited by ambient CO_2 substrate (Long and Drake 1992, Ainsworth and Rogers 2007) and any increases should stimulate carbon assimilation rates and increase vegetative growth (Bowes 1993), in the

absence of other stressors. However, grapevine specific studies provide evidence for down regulation of net photosynthesis as vines acclimate to higher carbon environments (Salazar-Parra et al. 2015, Rangel da Silva et al. 2017). Salazar-Parra et al. (2012) observed a transient increase in maximum photosynthesis in grapevine at elevated CO_2, but this effect dissipated over time. A short-term study in a temperature gradient greenhouse at 700 mg/L CO_2 showed grapevine photosynthesis increased around the time of veraison (Arrizabalaga-Arriazu et al. 2020), however studies of this duration are more reflective of a high dose of carbon enrichment rather than simulating future climate scenarios.

One possible explanation for photosynthetic down regulation, i.e. acclimation, is lowered capacity of the photochemical machinery due to reductions in nitrogen concentrations in the leaf (Luo et al. 1994, Moutinho-Pereira et al. 2009), limiting the activity of the enzyme RUBISCO. Species that are not nitrogen fixing such as grapevine are more likely to experience acclimation in elevated CO_2 environments because of limited RUBISCO content (Ainsworth et al. 2002). The nitrogen dilution effect is well documented in other crop species, therefore in grapevine, nitrogen use efficiency could increase in elevated CO_2 environments because RUBISCO acclimation allows for nitrogen to be redistributed for other growth in the vine, however, FACE experiments documented nitrogen gains lower than predicted (Leaky et al. 2009).

The long-term impact of elevated CO_2 on rates of grapevine photosynthesis has been shown to be dependent on other climate factors such as temperature and water availability (Wohlfahrt et al. 2018). Water scarcity, a concomitant climate change variable with elevated CO_2, can impact the carbon storage in trunks of vines, as demonstrated in fruit tree orchards, and in turn, drought stress can be partially relieved in elevated CO_2 scenarios (Paudel et al. 2018). Three general physiological responses will benefit grapevine in an elevated CO_2 climate with

limited water availability; starting with partial stomatal closure limiting water loss, a subsequent increase in soil water content as transpiration decreases, and an increase of starch storage to provide for drought recovery (Salazar-Parra et al. 2015, Paudel et al. 2018). Acclimation to elevated CO_2 will decrease rates of assimilation, while starch reserves increase, as the carbon sink may be driving rates of photosynthesis rather than carbon availability driving metabolism (Li et al. 2021). Therefore, the widespread observed reduction in stomatal conductance and density (Rangel da Silva et al. 2017, Kizildeniz et al. 2018) may have a greater impact on grapevine water use efficiency (WUE) from decreasing transpiration rather than increasing carbon assimilation.

In the past ten years, grapevine physiology research under elevated CO_2 has focused on the impacts on WUE defined as carbon assimilated per unit of water transpired. Grapevine relies on stomatal aperture to facilitate cooling and CO_2 uptake, releasing latent heat as the plant reaches physiological temperature thresholds; however, closure is essential to avoid detrimental water loss, heat damage, and reduced photosynthate production (Martínez-Lüscher et al. 2016b). With higher levels of carbon dioxide in the atmosphere, stomata can facilitate a lower water per CO_2 molecular exchange, increasing the leaf level WUE (Figure 1). An early study of grapevine under elevated CO_2 treatment for one season found no significant effect on stomatal conductance (g_s) and transpiration (Moutinho-Pereira et al. 2009). Subsequently, a study using 650 mg/L in a similar open top chamber treatment found g_s and transpiration decreased at elevated CO_2 (Edwards et al.2017). In contrast, at only at 500 mg/L, higher g_s and transpiration rates were observed in grapevines in a consistently elevated CO_2 environment for three consecutive seasons (Wohlfahrt et al. 2018). On a morphological level, multiple studies have documented the reduction in stomatal density in several varieties of grapevine (Moutinho-Pereira et al. 2009,

Rogiers et al. 2011, Rangel da Silva et al. 2017). Scaling intrinsic water use efficiency to the whole plant level will require documenting changes in microclimate as well as morphology, such as stomatal density and leaf area (Medrano et al. 2015).

Water use efficiency predictions are further complicated by the results of combination studies of elevated temperature, reduced soil water availability, and elevated CO_2, which reveal synergistic effects. In an open top chamber (OTC) study, combining temperature and CO_2 did not result in g_s being significantly reduced, contrary to results of elevated CO_2 alone (Edwards et al. 2017). When latent heat is trapped, overheating subsequently decreases the activity of RUBISCO activase, for most plants at temperatures higher than 37°C (Crafts-Brandner and Salvucci 2000), and in grapevine between 35-40°C, varying by species (Luo et al. 2011, Salazar-Parra et al. 2012). The elevated CO_2 and temperature treatments showed an increase in transpiration (Edwards et al. 2016), and the effects of drought were only temporarily delayed (Rangel da Silva et al. 2017). Temperature and elevated CO_2 had an additive effect on plant leaf area for multiple grapevine clones (Arrizabalaga-Arriazu et al. 2020), highlighting that overall higher leaf area without increased WUE could be detrimental for heat stressed vines. Measurements of predawn water potential were more negative in vines at elevated CO_2, indicating the demand for soil water availability of vines with increased productivity (Wohlfahrt et al. 2018). Notedly, the production of fine roots was positively impacted by an elevated CO_2 treatment, which would theoretically increase water absorption of water available (Reddy et al. 2018).

There remain inconsistent predictions of the effects of elevated CO_2 on grapevine whole plant water use efficiency, which seem to be contingent upon other factors such as soil water availability, temperature, and variety of grapevine. With the evidence from these studies of

elevated CO_2 and combination studies of soil water availability and temperature, grapevines most likely will not benefit from a long-term increase in photosynthesis under elevated CO_2. The lack of soil water available and biological temperature thresholds for RUBISCO will limit the gains in photosynthesis, and more likely the vines will struggle to release latent heat as temperatures rise.

Phenology

Grapevine phenology is categorized into four life cycle stages of periodic development: budburst, flowering, veraison, and maturation. The grapevine phenological cycle is a two-year process; bud formation occurs in the first year which develop into shoots in the second year. Therefore, clusters are significantly impacted by the previous year's climate (Vasconcelos et al. 2009). For grapevine grown at elevated CO_2, advances in phenology compound significantly over seasons (Edwards et al. 2017). This is likely the result of stored carbon photosynthate from the productive previous year. As a result, it can take several years to observe the effects of elevated CO_2 on grapevine phenology (Edwards et al. 2017), which leads to the question of: "To what extent does elevated CO_2 impact the timing of phenological stages over the long-term?"

Studies of Arabidopsis, another C3 flowering plant, provide insight to the mechanisms of phenological changes observed in grapevine. Excess carbohydrates may act similarly to phytohormones to delay the upregulation of genes involved in flowering time, as well as cell wall invertases in the meristem that downregulate photosynthesis under treatments of elevated CO_2, which leads to earlier flowering (Springer and Ward 2007). For grapevine, it is possible that excess photosynthate could trigger early flowering through the transfer of carbohydrates

from leaves. One of the most robust findings to support this hypothesis is that growth under elevated CO_2 results in increased carbohydrate reserves in plants (Kizildeniz et al. 2021).

The sugars produced by photosynthesis contribute only a fraction of the source of carbon needed for rapid growth and development from budbreak to flowering and sugar accumulation in berries at veraison, the remaining needed for these growth spurts is mobilized from long-term storage of total nonstructural carbohydrates (TNC) in trunks and roots (Zufferey et al. 2012). Over several growing seasons, storage of carbohydrates in the trunk will be impacted by elevated CO_2 (Lebon et al. 2008) and could therefore contribute to shifts in phenology. In a greenhouse study of fruiting cuttings where sugar accumulation in berries was measured, elevated CO_2 increased the rate of ripening correlated with the photosynthetic rate (and was only slightly mediated by UV-B treatments) (Martínez-Lüscher et al. 2015). The effect of elevated CO_2 on phenology was greater than the treatment of temperature elevated by 4°C (Martínez-Lüscher et al. 2016b). Therefore, an increase in total nonstructural carbohydrates could be a driver of advances in phenology long term, on its own, as well as with concomitant increases in growing season temperatures.

Carbohydrate reserves regulate the growth and differentiation of flowers, which only occurs after the grapevine shoot is resource independent from the rest of the vine (Lebon et al. 2008, Vasconcelos et al. 2009). These findings suggest that with an increase in carbon reserves stored as starch in roots, trunks and canes, second season shoots may grow faster and achieve independence earlier in the growing season. This could contribute to early flowering as a result of lifted competition for resources between vegetative and reproductive growth. In contrast, long-term studies in grapevine decreasing the leaf to fruit ratios (measured as light-exposed leaf area to fruit) decreased essential reserves of the TNC in the roots (Zufferey et al. 2012). The

well-known viticultural technique of strategic leaf removal has been shown to delay maturation, highlighting the importance of carbon availability for phenological development (Poni et al. 2006, Parker 2012, Parker et al. 2014).

While the mechanism for phenological shifts in grapevine grown under elevated CO_2 is under-studied, these shifts have been quantified using FACE experiments. The combination of elevated CO_2 and temperature in OTC caused an advance in flowering time by three days and veraison by two weeks (Edwards et al. 2016). The impact of elevated CO_2 on phenological timing is greatest during the period between fruit set to veraison and this impact increases when combined with a temperature treatment (Martínez-Lüscher et al. 2016a, Arrizabalaga-Arriazu et al. 2020). During fruit set, elevated CO_2 treatments with and without temperature treatments increased total soluble solids (hastening maturation), as well as decreased anthocyanins and malic acid concentration, which would contribute to an earlier veraison and harvest (Salazar-Parra et al. 2010). However, the impact of high temperature may have a greater impact on this phenological period (Arrizabalaga-Arriazu et al. 2020).

The quality of fruit harvested is the utmost concern when considering advanced phenology. Grapevines vulnerable to frost damage will suffer from early budburst, with subsequent losses in yield (Fraga et al. 2016). One consequence of increased shoot vigor at elevated CO_2 is the expected increase in bud fertility, which will likely increase the number of flowers per vine (Figure 1) (Delrot et al. 2020, Bindi et al. 2001). Changes in cluster density and phenological timing impact the carefully articulated annual harvest. Unbalanced sugar/acid ratios resulting from early harvest decrease the quality of grapes and wine produced, discussed further in the "Berry and Wine Chemistry" section below (Jones et al. 2005, Jones 2013). Shifting the lifecycle of grapevine will have a global impact on winegrape production.

Figure 1

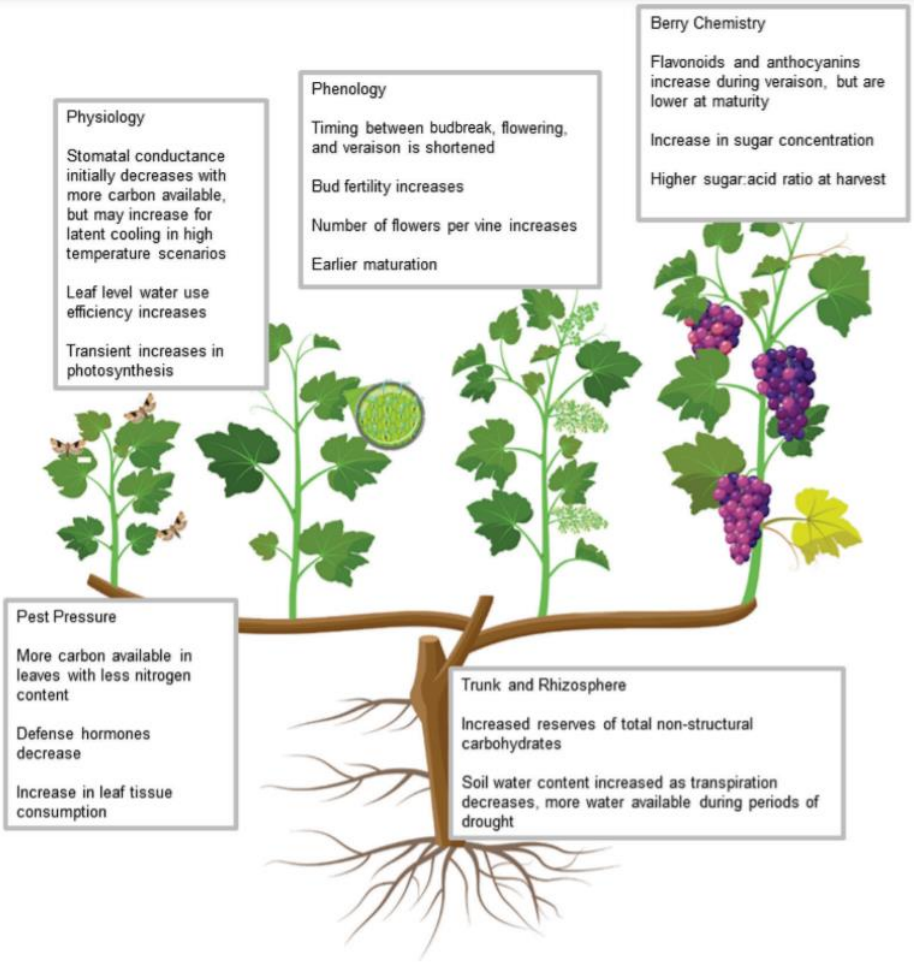

Figure 1 At a biophysiological level, elevated carbon dioxide (CO_2) affects the production and storage of sugars (total nonstructural carbohydrates) and the balance of growth. Indirect effects of rising CO_2 levels catalyze top-down effects of increased carbon:nitrogen (C:N) ratios with subsequent increases in herbivory. Grapevine phenology is a sensitive two-year cycle of growth spurts and acid degradation before harvest, with profound effects on grape berry quality when the timing is shifted. Intrinsic water use efficiency (WUE) at the leaf level increases as stomatal conductance decreases and more carbon is available per water molecule lost. However, WUE at the whole plant level depends on soil water available, which will vary depending on microclimate and future climate conditions.

Berry and Wine Chemistry

Fruit composition is a major area of concern for growers and winemakers alike, especially aromatic compounds. The changes in pest interactions, physiology, and timing of veraison in response to elevated CO_2 will collectively impact the resulting grape and wine quality (Ollat et al. 2017). For successful wines, in the grape berry there is a balance of acid and sugar at harvest. Increasing atmospheric carbon available impacts the balance as ripening

advances and sugar accumulation is accelerated (Martínez de Toda et al. 2014). Flavonoids and anthocyanins are important for the flavor, color, and mouthfeel of wine. The molecular analysis from the original Italian FACE experiments showed increases in total flavonoids, total anthocyanins, and total non-anthocyanin flavonoids in the wine produced with carbon enriched grapes grown at 700 mg/L (Bindi et al. 2001), which typically would affect the color and mouthfeel of wine. Interestingly, a subsequent experiment using 500 mg/L CO_2 open top chambers determined there were significant increases in ethyl 2-methylbutyrate (apple), isoamyl acetate (burnt), ethyl hexanoate (apple, pineapple), ethyl octanoate (fruit/fat), butyric acid (rancid), and isovaleric acid (rancid) concentrations and a significant decrease in ethyl acetate (fruity) concentration in wines produced from enriched CO_2 grapes after one year (Gonçalves et al. 2008), which contribute to the balance of floral and fruity characteristics in wines (Francis 2012). In the second year they found lower methionol (raw potato), 1-octanol (alcohol), and 4-ethylguaiacol (smoke), and they found higher ethyl lactate (butter) and linalool (floral) concentrations, although these changes in berry chemistry did not appear to significantly affect the quality of wine produced (Gonçalves et al. 2008). These results agree with early studies led by Bindi et al. (2001) that did not find significant effects on the quality of wine produced from grapes grown at elevated CO_2 (Table 1).

Although the changes observed in compounds contributing to flavor have been noted as so far insignificant for quality, a major concern for winemakers is the increase in alcohol content resulting from an increase in sugar concentrations in berries, as a result of higher CO_2 concentrations (Van Leeuwen and Darriet 2016, Teslić et al. 2018, Delrot et al. 2020, Ubeda et al. 2020). In the past, winemakers have added sugar to the fermentation to increase the final alcohol percentage (chaptalization where legal), depending on legal regulations for winemaking.

However, in recent years winemakers have begun removing sugar through processes like reverse osmosis in order to prevent alcohol levels from rising (Christmann et al. 2017, Delrot et al. 2020). Overall, elevated CO_2 is altering the balance of sugar accumulation, the levels tartaric and malic acids in berries and wine, and the impact on wine quality continues to be investigated (Table 1) (Gonçalves et al. 2008, Pons et al. 2017).

The most recent FACE studies on grapes continue to evaluate the berry chemistry and quality developing over years of exposure to elevated CO_2. The VineyardFACE in Germany analyzed must from grapes after pressing and did not find a significant increase in sugar content from conditions of carbon enrichment (Wohlfahrt et al. 2018). The Gonçalves et al. (2008) study also concluded that changes in water availability and heat stress could change their predictions in wine quality. We should expect that with the shifts in phenology and physiological changes to berries, early harvest will impact the quality of grapes in terms of reaching maturation too quickly (Martínez-Lüscher et al. 2016a). Viticulturists could also anticipate altered physiological demands to have long-term impacts on berry quality (Pons et al.2017).

Pest and Disease Pressure

In contrast to the ecological pressures discussed above, the rates of some fungal infections may be reduced in elevated CO_2 scenarios. With higher carbon allocation to roots, grapevine mycorrhizal colonization may be promoted by elevated CO_2 (Torres et al. 2018), which has been shown to protect grapevine against the nematode *Xiphinema index* by stimulating defense gene response (Hao et al. 2012). A study of elevated CO_2 on several varieties of grapevine seedlings showed a reduced severity of the infection of *Xanthomonas campestris* pv

viticola, a vector of bacterial canker in immature grapevine (Table 1) (Conceição et al. 2017). This may be the result of lower stomatal conductance (gs); with stomatal aperture reduced, there is less opportunity for bacteria to invade the leaf pores (Conceição et al. 2017, Kizildeniz et al. 2018). Also, researchers recorded a reduced instance and severity of powdery mildew infection in cv Barbera, at elevated CO_2 (Table 1) (Pugliese et al. 2010). The Geisenheim VineyardFACE site recorded changes in the bunch architecture but did not see an increase in the frequency of *B. cinera*, botrytis bunch rot, a necrotrophic fungus, occurrence (Wohlfahrt et al. 2018).

Changes in leaf chemistry phenotype, specifically carbon content, (e.g. higher soluble carbohydrates due to higher carbon dioxide levels), will increase the pressure of grapevine pests in future climates. Increasing available carbon dioxide, without a concomitant increase in nutrient levels in the soil, leads to an increase in C:N ratios in leaves (Figure 1) (Hunter 2001, Ainsworth and Long 2004, Moutinho-Pereira et al. 2009, Arrizabalaga-Arriazu et al. 2020, Kizildeniz et al. 2021). Insects consume at higher rates when nitrogen has been diluted to meet their nitrogen intake needs and chewing insect pests will generally eat more leaf tissue in elevated carbon dioxide scenarios (Hunter 2001). Elevated CO_2 increased individual survival rates and increased the fecundity of female mealybugs, which eat phloem of grapevine damaging the temporal and perennial plant tissue (Bordeu et al. 2012, Schulze-Sylvester and Reineke 2019, Schulze-Sylvester, Corronca and Paris 2021). The European grapevine moth, *Lobesia botrana*, is a major problem for European vineyards, affecting both the berries and flowers of grapevines; and has already invaded North and South American vineyards (Reineke and Selim 2019). *L. botrana* is also responsible for spreading Ochratoxin A-producing *Aspergillus* fungi, which typically spikes in occurrence during hotter and drier years (Mondani et al. 2020). At higher temperatures simulating future climate conditions, *L. botrana* female growth rate and pupal mass

increased (Iltis et al. 2018), while researchers found a down regulation of expression of ethylene-responsive factors, which suggests grapevines can become more vulnerable to herbivory or abiotic stress under future climate change as these are the major stress and defense response factors (Reineke and Selim 2019).

A comprehensive study of soil and elevated CO_2 showed the decomposition pathway is altered by the carbon-, nitrogen-, and phosphorus-acquiring enzymes in the soil with a significant increase in nematode density (Thakur et al. 2019). More than 4,000 plant-parasitic nematodes exist, posing a well-known global issue for grapevine, reducing total crop production by 8.8-14.6%, and one of the worst threats from the nematode *Xiphinema index* is GLRV (Grapevine Leaf Roll Virus) (Andret-Link et al. 2017). Under elevated CO_2 conditions, if ethylene is suppressed and salicylic acid is increased, it is likely that grapevine will struggle with an increase in pest and disease vectors such as nematodes and fungi (Reineke and Selim 2019). Grapevines largely rely on human intervention for defense against pests and diseases (Pertot et al. 2017), and this reliance could increase in future climates. Consider the grapevine "immune system" as weakened in terms of chemical defense, but some altered carbon dynamics under elevated CO_2 may be beneficial for reducing severity of pest pressure.

Discussion

An anticipated management solution to phenological shifts is planting later ripening and stress tolerant alternative varieties. Government response to climate change will determine the actions European growers are allowed to take to adapt to climate change, considering the current trials of alternative varieties planted in small diversity blocks in France as a positive example

(Morales-Castilla et al. 2020). Ancient varieties being tested in temperature gradient greenhouses in Spain for response to combination stresses of drought, heat, and elevated CO_2 showed greater resiliency to stress and did not shift phenological timing, although this was a short-term experiment (Antolín et al. 2021, Goicoechea et al. 2021). In some cases, alternative varieties may be hybrid crosses between existing cultivars and later ripening varieties. However, hypothetical crosses between very late ripening varieties were modelled and still struggle to be late-ripening enough to endure the predicted 23-day shift and potential increase of 7°C expected by the end of this century for major wine grape growing areas (Duchêne et al. 2010). Alternative varieties can be identified by oenological and ecological principals that make them suitable candidates for replacing existing cultivars, such as flavor profile and ability to survive long term through stressful climate change conditions (Antolín et al. 2021, Goicoechea et al. 2021). The challenge of adapting new varieties is highlighted by current popular varieties struggling with increases in growing season temperatures (Jones 2021), however a combination of diversity block trials and greenhouse experiments will guide predictions of the best alternatives (Wolkovich et al. 2018).

Our present knowledge of grapevine climate niches is limited relative to the vast diversity of cultivars (Duchêne et al. 2010). With California as an example, there are many potential late ripening varieties suitable as alternatives to early ripening Chardonnay that have yet to be tested in diversity blocks (Wolkovich et al. 2018). Even clones can have a varied response to climate change variables (Arrizabalaga-Arriazu et al. 2020). Varieties with heat and drought tolerance traits are a starting point for elevated CO_2 studies, as we expand from understanding the mechanisms of change into exploring mitigation strategies. Exploring the vast diversity of grapevine using diversity plots is a straightforward ecological approach, which could be

enhanced by evaluating the success of plants under several biotic and abiotic stresses predicted for the future.

Many studies on the impacts of leaf removal suggest that manipulating canopy cover is an effective way to mitigate phenological shifts caused by climate change (Martínez de Toda et al. 2014, Parker 2012). Leaf removal at pre-bloom positively influences cell division in inflorescence, by reducing sugar transport and decreasing flower fertility, which mitigates cluster compactness (Lebon et al. 2008, VanderWeide et al. 2021). Not only can leaf removal aid in delaying phenology, but other positive impacts also include increasing acid to sugar ratio at harvest, increasing production of anthocyanins and flavonoids, and decreasing incidence of bunch rot disease (Kliewer and Smart 1989, Martínez de Toda et al. 2014, VanderWeide et al. 2021).

Ecologists generally study a system's responses and interactions, and viticulturists need this system perspective for the challenges presented by climate change. Our understanding of the effects of elevated CO_2 on the vineyard system is profoundly complicated by the interactive effects of other biotic and abiotic stressors. From an ecological perspective, long-term FACE studies are the most realistic predictors of response to elevated CO_2. Advocating for long-term agroecological studies is necessary to evaluate the top-down and bottom-up impacts of higher carbon availability on pest/disease interactions, grapevine growth and phenology dynamics, and the resulting quality of wine produced.

Grapevine physiology will be impacted by elevated carbon dioxide, increasing temperatures, and extreme heat events during the growing season (De Cortázar-Atauri et al. 2017, Ugaglia et al. 2019). FACE experiments highlight the necessity of water availability for grapevines to take advantage of increased carbon dioxide for productivity. Soil water availability impacts the

opening of stomata, and in the case of VineyardFACE, the vines had increased g_s with more CO_2 available (Wohlfahrt et al. 2018). Grapevines may need more water under future climate conditions of elevated CO_2 and temperature, while precipitation is expected to decrease in most of the wine growing regions of the world. Desiccation threatens vines through water loss from latent cooling under elevated temperature, resulting in higher cumulative water loss even when operating at higher water use efficiency. The modulating response of stomata documented across literature is dependent on the soil water availability and temperature regimes (Arrizabalaga-Arriazu et al. 2020). In this synthesis, the varying levels of CO_2, ambient temperatures, and duration of these experiments could have contributed to these contrasting results of stomatal behavior, as well as the conditions of the chambers and greenhouses, versus FACE infrastructure.

Physiological response to abiotic stresses in future climate change conditions is likely to weaken grapevine, creating a vulnerability for biotic stresses such as pests. Overall, chewing pest pressure is anticipated to increase as carbon dioxide and temperature increase (Reineke and Selim 2019). It is unknown whether pest pressure can be compensated by the predicted increase in foliar growth and the effect of lower nutrient density on the populations of pests. The growing season for grapes may require drastic changes in viticultural practices to manage pests, alleviate heat and drought stress, and predict harvest dates. Fungal infections are responsible for a majority of crop damage; therefore, it is critical to clarify if fungal infection will decrease in the future for predictions of grapevine yield.

One of the biggest challenges for grape growers will be the shifts in phenological timing, with the potential for frost at early budbreak, alterations in cluster formation and density, and compromising harvest with early maturation. Many of the short-term experiments described here

did not find significant effects on phenology and yield, while long term studies account for acclimation and compounding effects of seasonal exposure to elevated carbon dioxide. Predictions of overall vineyard response to climate change are more accurate when experiments are field based, multi-seasonal, and combine the variables of water availability and temperature.

Table 1: Studies of carbon enrichment with grapevine, using temperature growth chambers (GC), greenhouse (GH), temperature gradient greenhouses (TGG), open top chambers (OTC) and Free Air Carbon Enrichment (FACE) with significant findings are summarized here. The contrast in results for photosynthetic response is likely due to the duration of the studies and the material used (fruiting cuttings for the Salazar-Parra et al. 2015 study versus field grown vines for Wohlfahrt et al. 2017, 2018). Photosynthesis (Anet) increased in response to elevated CO2 in all of these studies. However, the downstream impact on phenology has unclear results, as the Edwards FACE studies (2016, 2017) showed a significant impact on the timing of veraison, while the more recent temperature gradient greenhouse study by Arrizabalaga-Arriazu et al. 2020 did not. Few studies document long-term impacts on phenology, and there have been no studies in the United States using FACE.

Table 1

Citation	eCO_2 levels (mg/L)	Method	Notable Results	Location
Bindi et al. 2001	550 and 700	FACE	↑ vegetative growth – No significant impact on wine quality (20 year old vines)[a]	Italy
Gonçalves et al. 2008	500	OTC	– No significant impact on wine quality	Portugal
Moutinho-Pereira et al. 2009	500	OTC	↑ Photosynthesis (A_{net}) ↑ Intrinsic water use efficiency (A/gs) ↑ Leaf thickness ↑ Mg concentration ↑ C/N, K/N and Mg/N ratios ↓ Stomatal density and N concentration	Portugal
Pugliese et al. 2010	800	GC	↓ Chlorophyll content ↑ Instance and severity of powdery mildew increased for cv. Moscato ↓ Instance and severity of powdery mildew increased for cv. Barbera	Italy
Salazar-Parra et al. 2012	700	GH	↓ Reactive Oxygen Species – No significant change in photosynthetic pigments	Spain

Salazar-Parra et al. 2015	700	TGG	➖ No effect on photosynthetic rates ⬇ Stomatal conductance and transpiration at 20 days	Spain
Martínez-Lüscher et al. 2015	700	GH	⬆ Photosynthesis (A_{net}) ⬆ Dark respiration ⬇ Photorespiration ⬆ Chlorophyll a and b content ⬆ Ripening rates	Spain
Martínez-Lüscher et al. 2016a	700	TGG	⬆ Advanced phenology with and without combination of elevated temperature, with cultivar specific response	Spain
Edwards et al. 2016, 2017	650	OTC	⬆ Anthesis and veraison advanced in the third season ⬆ Light saturated assimilation (A_{sat})	Australia
Rangel da Silva et al. 2017	800	GC	⬇ 18% reduction in leaf nitrogen content ⬇ 25% reduction in stomatal density ⬆ Generally increased drought tolerance	USA
Conceição et al. 2017	770	GC	⬇ Decreased infection of bacterial disease of *Xanthomonas campestris* pv *viticola*	Brazil
Wohlfahrt et al. 2017, 2018	480 - 500 (+20% ambient)	FACE	⬆ Photosynthesis (A_{net}) ⬆ intrinsic water use efficiency (A/gs) pre-dawn leaf water potential ⬆ bunch compactness, weight, and length ⬇ Ethylene signals and ethylene responsive factors	Germany

Kizildeniz et al. 2018	700	TGG	↓ g_s, with additive effect of temperature and drought ↑ Stimulated more vegetative than reproductive growth – WUE increases did not compensate for water stress	Spain
Reineke and Selim 2019	500	FACE	↓ ethylene signalling hormones ↑ defensive compounds, including salicylic acid ↑ vulnerability to moth *L. botrana*	Germany
Arrizabalaga-Arriazu et al. 2020	700	TGG	– Phenology and cluster traits not significantly impacted ↑ Increased leaf area at maturity ↑ Photosynthesis (A_{net}) ↓ Stomatal conductance (g_s)	Spain
			↑ indicates increase ↓ indicates decrease – indicated no change	

Conclusion

A combination of the impacts of pest pressure, phenology, and physiology predict a much different future environment for growing grapes. Elevated carbon dioxide is a pervasive threat to the vineyard system because it fuels undesirable growth. Grapevine will sustain the impacts of elevated carbon dioxide for generations, as a perennial crop with a rich memory and sensitive expression of climate. We can strengthen the vineyard system by introducing more diverse cultivars, with an ideal candidate fitting the profile of heat and drought tolerant, late ripening, with strong pest resistance.

References

Ainsworth EA, Davey PA, Bernacchi CJ, Dermody OC, Heaton EA, Moore DJ, Morgan PB, Naidu SL, Yoo Ra HS, Zhu XG and Curtis PS. 2002. A meta-analysis of elevated CO_2 effects on soybean (*Glycine max*) physiology, growth and yield. Glob Chang Biol 8: 695-709.

Ainsworth EA and Long SP. 2004. What have we learned from 15 years of free-air CO_2 enrichment (FACE)? A meta-analytic review of the responses of photosynthesis, canopy properties and plant production to rising CO_2. New Phytol 165: 351-372.

Ainsworth EA and Rogers A. 2007. The response of photosynthesis and stomatal conductance to rising [CO_2]: mechanisms and environmental interactions. Plant Cell Environ 3:258-70.

Andret-Link P, Marmonier A, Belval L, Hleibieh K, Ritzenthaler C and Demangeat G. 2017. Ectoparasitic nematode vectors of grapevine viruses. In Grapevine Viruses: Molecular Biology, Diagnostics and Management. Pp. 505-529. Springer, Cham.

Antolín MC, Toledo M, Pascual I, Irigoyen JJ, Goicoechea N. 2021. The exploitation of local *Vitis vinifera* L. biodiversity as a valuable tool to cope with climate change maintaining berry quality. Plants 10: 71.

Arrizabalaga-Arriazu M, Morales F, Irigoyen JJ, Hilbert G, Pascual I. 2020. Growth performance and carbon partitioning of grapevine Tempranillo clones under simulated climate change scenarios: Elevated CO_2 and temperature. J Plant Physiol: 153-226.

Bertamini M, Faralli M, Varotto C, Grando MS, and Cappellin L. 2021. Leaf Monoterpene Emission Limits Photosynthetic Downregulation under Heat Stress in Field-Grown Grapevine. Plants 10: 181.

Bindi M, Fibbi L and Miglietta F. 2001. Free Air CO_2 Enrichment (FACE) of grapevine (*Vitis vinifera* L.): II. Growth and quality of grape and wine in response to elevated CO_2 concentrations. Eur J Agron 14: 145-155.

Bordeu E, Troncoso DO, Zaviezo T. 2012. Influence of mealybug (*Pseudococcus* spp.)-infested bunches on wine quality in Carmenere and Chardonnay grapes. Int J Food Sci Tech 47:232–239.

Bowes G. 1993. Facing the inevitable – plants and increasing atmospheric CO_2. Annu Rev Plant Physiol 44: 309–332.

Chaves M, Zarrouk O, Francisco R, Costa M, Santos T, Regalado P, Rodrigues L and Lopes M. 2010. Grapevine under deficit irrigation: hints from physiological and molecular data. Ann. Bot. 105: 661-676.

Christmann M, Schmitt M, and Pasch L. 2017. Managing climate change: Optimising cool climate wine styles: Impact of dramatic climatic change on traditional viticultural and oenological practices. Wine Viti J 32: 20-22.

Conceição JL, Angelotti F, Peixoto AR and Ghini R. 2017. Infection by *Xanthomonas campestris* pv. *viticola* under temperature increase and carbon dioxide concentrations. Com Sci 8:214-20.

Crafts-Brandner SJ and Salvucci ME. 2000. Rubisco activase constrains the photosynthetic potential of leaves at high temperature and CO_2. Proc Natl Acad Sci 97: 13430-13435.

De Cortázar-Atauri IG, Duchêne E, Destrac-Irvine A, Barbeau G, De Rességuier L, Lacombe T, Parker A, Saurin N and Van Leeuwen C. 2017. Grapevine phenology in France: from past observations to future evolutions in the context of climate change. OENO One 51:115-126.

Delrot S, Grimplet J, Carbonell-Bejerano P, Schwandner A, Bert PF, Bavaresco L, Dalla Costa L, Di Gaspero G, Duchêne E, Hausmann L and Malnoy M. 2020. Genetic and Genomic Approaches for Adaptation of Grapevine to Climate Change. Genomic Designing Climate-Smart Fruit Crops: 157-270.

Duchêne E, Huard F, Dumas V, Schneider C and Merdinoglu D. 2010. The challenge of adapting grapevine varieties to climate change. Clim Res 41:193-204.

Edwards EJ, Unwin DJ, Sommer KJ, Downey MO and Mollah M. 2016. The response of commercially managed, field grown, grapevines (*Vitis vinifera* L.) to a simulated future climate consisting of elevated CO_2 in combination with elevated air temperature. Acta Hortic: 103-110.

Edwards E, Unwin D, Kilmister R and Treeby M. 2017. Multi-seasonal effects of warming and elevated CO_2 on the physiology, growth and production of mature, field grown, Shiraz grapevines. OENO One 51: 127-132.

Faralli M, Grove IG, Hare MC, Kettlewell PS, Fiorani F. 2017. Rising CO_2 from historical concentrations enhances the physiological performance of *Brassica napus* seedlings under optimal water supply but not under reduced water availability. Plant Cell Environ 40:317-25.

Fraga H, De Cortázar Atauri IG, Malheiro AC and Santos JA. 2016. Modelling climate change impacts on viticultural yield, phenology and stress conditions in Europe. Glob Chang Biol 22: 3774-3788.

Francis L. 2012. Fermentation-derived aroma compounds and grape-derived monoterpenes. Appl Microbiol Biotechnol 96:601-618.

Galat Giorgi E, Sadras VO, Keller M and Perez Peña J. 2019. Interactive effects of high temperature and water deficit on Malbec grapevines. Aust J Grape Wine Res 25: 345-356.

Goicoechea N, Jiménez L, Prieto E, Gogorcena Y, Pascual I, Irigoyen JJ and Antolín MC. 2021. Assessment of Nutritional and Quality Properties of Leaves and Musts in Three Local Spanish Grapevine Varieties Undergoing Controlled Climate Change Scenarios. Plants 10: 1198.

Gonçalves B, Falco V, Moutinho-Pereira J, Bacelar E, Peixoto F and Correia C. 2008. Effects of elevated CO_2 on grapevine (*Vitis vinifera* L.): volatile composition, phenolic content, and in vitro antioxidant activity of red wine. J Ag Food Chem 57: 265-273.

Gray SB, Dermody O, Klein SP, Locke AM, Mcgrath JM, Paul RE, Rosenthal DM, Ruiz-Vera UM, Siebers MH, Strellner R, Ainsworth EA. 2016. Intensifying drought eliminates the expected benefits of elevated carbon dioxide for soybean. Nature Plants 9:1-8.

Hao Z, Fayolle L, van Tuinen D, Chatagnier O, Li X, Gianinazzi S, Gianinazzi-Pearson V. 2012. Local and systemic mycorrhiza-induced protection against the ectoparasitic nematode

Xiphinema index involves priming of defence gene responses in grapevine. J. Exp. Bot. 63:3657-72.

Hunter MD. 2001. Effects of elevated atmospheric carbon dioxide on insect–plant interactions. Agric For Entomol 3: 153-159.

Iltis C, Martel G, Thiéry D, Moreau J and Louâpre P. 2018. When warmer means weaker: high temperatures reduce behavioural and immune defenses of the larvae of a major grapevine pest. J Pest Sci 91: 1315-1326.

Intergovernmental Panel on Climate Change (IPCC). 2014. Climate change 2014: Synthesis report: Contribution of Working Groups I, II and III to the fifth assessment report of the Intergovernmental Panel on Climate Change.

Jones GV. 2013. Winegrape phenology. In Phenology: An integrative environmental science. Springer, Dordrecht: 563-584

Jones GV. 2021. Wine Production and Climate Change. In World Scientific Encyclopedia of Climate Change: Case Studies of Climate Risk, Action, and Opportunity Volume 2: pp. 177-184.

Jones GV, White MA, Cooper OR and Storchmann K. 2005. Climate change and global wine quality. Climatic Change 73:319-343.

Kizildeniz T, Irigoyen JJ, Pascual I and Morales F. 2018. Simulating the impact of climate change (elevated CO_2 and temperature, and water deficit) on the growth of red and white Tempranillo grapevine in three consecutive growing seasons (2013–2015). Agr Water Manage 202: 220-230.

Kizildeniz T, Pascual I, Irigoyen JJ and Morales F. 2021. Future CO_2, warming and water deficit impact white and red Tempranillo grapevine: Photosynthetic acclimation to elevated CO_2 and biomass allocation. Physiol Plant.

Kliewer W and Smart R. 1989. Canopy manipulation for optimizing vine microclimate, crop yield and composition of grapes C.J. Wright (Ed.), Manipulation of Fruiting, Butterworth & Co. Publishers. 275-291.

Leakey AD, Ainsworth EA, Bernacchi CJ, Rogers A, Long SP and Ort DR. 2009. Elevated CO_2 effects on plant carbon, nitrogen, and water relations: six important lessons from FACE. J Exp Bot :2859-76.

Lebon G,Wojnarowiez G, Holzapfel B, Fontaine F, Vaillant-Gaveau N, Clément C. 2008. Sugars and flowering in the grapevine (*Vitis vinifera L.*). J Exp Bot 59:2565-2578.

Li YM, Forney C, Bondada B, Leng F and Xie ZS. 2021. The Molecular Regulation of Carbon Sink Strength in Grapevine (Vitis vinifera L.). Front Plant Sci:11.

Lobell DB, Field CB, Cahill KN and Bonfils C. 2006. Impacts of future climate change on California perennial crop yields: Model projections with climate and crop uncertainties. Agric For Meteorol 141: 208-218.

Long SP and Drake BG. 1992. Photosynthetic CO_2 assimilation and rising atmospheric CO_2 concentrations. Crop Photosynthesis: spatial and temporal determinants. Elsevier: 69 – 101.

Luo Y, Field CB and Mooney HA. 1994. Predicting responses of photosynthesis and root fraction to elevated CO_2: interactions among carbon, nitrogen and growth. Plant Cell Enviro 17: 1195–1204.

Luo HB, Ma L, Xi HF, Duan W, Li SH, Loescher W, Wang JF, Wang LJ. 2011. Photosynthetic responses to heat treatments at different temperatures and following recovery in grapevine (*Vitis amurensis* L.) leaves. PLoS One: 23-33.

Mariani L, Cola G, Maghradze D, Failla O and Zavatti F. 2018. Influence of climate cycles on grapevine domestication and ancient migrations in Eurasia. Sci Total Enviro 635:1240-1254.

Martínez-Lüscher J, Morales F, Sánchez-Díaz M, Delrot S, Aguirreolea J, Gomès E, Pascual I. 2015. Climate change conditions (elevated CO_2 and temperature) and UV-B radiation affect grapevine (*Vitis vinifera* cv. Tempranillo) leaf carbon assimilation, altering fruit ripening rates. Plant Science 236:168-76.

Martínez-Lüscher J, Kizildeniz T, Vučetić V, Dai Z, Luedeling E, van Leeuwen C, Gomès E, Pascual I, Irigoyen JJ, Morales F and Delrot S. 2016b. Sensitivity of grapevine phenology to water availability, temperature and CO_2 concentration. Front Enviro Science 4:48.

Martínez-Lüscher J, Sánchez-Díaz M, Delrot S, Aguirreolea J, Pascual I and Gomès E. 2016a. Ultraviolet-B alleviates the uncoupling effect of elevated CO_2 and increased temperature on grape berry (*Vitis vinifera* cv. Tempranillo) anthocyanin and sugar accumulation. Aust J Grape Wine Res 22: 87–95.

Martínez de Toda F, Sancha JC, Zheng W and Balda P. 2014. Leaf area reduction by trimming, a growing technique to restore the anthocyanins: sugars ratio decoupled by the warming climate. Vitis 53:189–192.

Medrano H, Tomás M, Martorell S, Flexas J, Hernández E, Rosselló J, Pou A, Escalona JM, Bota J. 2015. From leaf to whole-plant water use efficiency (WUE) in complex canopies: Limitations of leaf WUE as a selection target. Crop J. 3:220-8.

Mondani L, Palumbo R, Tsitsigiannis D, Perdikis D, Mazzoni E, Battilani P. 2020. Pest management and ochratoxin a contamination in grapes: A review. Toxins 12:303.

Morales-Castilla I, de Cortázar-Atauri IG, Cook BI, Lacombe T, Parker A, Van Leeuwen C, Nicholas KA and Wolkovich EM. 2020. Diversity buffers winegrowing regions from climate change losses. Proc Natl Acad Sci.

Mosedale JR, Abernethy KE, Smart RE, Wilson RJ and Maclean IM. 2016. Climate change impacts and adaptive strategies: lessons from the grapevine. Glob Chang Biol 22:3814-3828.

Moutinho-Pereira J, Alves BG, Bacelar E, Cunha JB, Couro J and Correia CM. 2009. Effects of elevated CO_2, on grapevine (*Vitis vinifera* L.): Physiological and yield attributes. Vitis 48: 159-165.

Ollat N, Van Leeuwen C, de Cortazar Atauri IG and Touzard JM. 2017. The challenging issue of climate change for sustainable grape and wine production. OENO One 51:59-60.

Owens CL. 2008. Grapes. Temperate Fruit Crop Breeding. pp. 197-233 Springer, Dordrecht.

Parker A. 2012. Modelling phenology and maturation of the grapevine *Vitis vinifera L.*: varietal differences and the role of leaf area to fruit weight ratio manipulations (Doctoral dissertation, Lincoln University).

Parker AK, Hofmann RW, van Leeuwen C, McLachlan ARG and Trought MCT. 2014. Leaf area to fruit mass ratio determines the time of veraison in Sauvignon Blanc and Pinot Noir grapevines. Aust J Grape Wine Res 20: 422–431.

Parker LE, McElrone AJ, Ostoja SM and Forrestel EJ. 2020. Extreme heat effects on perennial crops and strategies for sustaining future production. Plant Sci 295: 110397.

Paudel I, Halpern M, Wagner Y, Raveh E, Yermiyahu U, Hoch G and Klein T. 2018. Elevated CO_2 compensates for drought effects in lemon saplings via stomatal downregulation, increased soil moisture, and increased wood carbon storage. Enviro Exp Bot 148:117-127.

Pearson PN and Palmer MR. 2000. Atmospheric carbon dioxide concentrations over the past 60 million years. Nature: 695.

Pertot I, Caffi T, Rossi V, Mugnai L, Hoffmann C, Grando MS, Gary C, Lafond D, Duso C, Thiery D and Mazzoni V. 2017. A critical review of plant protection tools for reducing pesticide use on grapevine and new perspectives for the implementation of IPM in viticulture. Crop Prot 97: 70-84.

Poni S, Casalini L, Bernizzoni F, Civardi S. and Intrieri C. 2006. Effects of early defoliation on shoot photosynthesis, yield components, and grape composition. Am J Enol Vitic 57: 397-407.

Pons A, Allamy L, Schüttler A, Rauhut D, Thibon C and Darriet P. 2017. What is the expected impact of climate change on wine aroma compounds and their precursors in grape? OENO One 51: 141-146.

Ponti L, Gutierrez AP, Boggia A and Neteler M, 2018. Analysis of grape production in the face of climate change. Climate 6: 20.

Pugliese MA, Gullino ML, Garibaldil A. 2010. Effects of elevated CO_2 and temperature on interactions of grapevine and powdery mildew: first results under phytotron conditions. J Plant Dis Prot117:9-14.

Rangel da Silva J, Patterson AE, Rodriguez WP, Campostrini E, and Griffin KL. 2017. Photosynthetic acclimation to CO_2 combined with partial root-zone drying results in improved water use efficiency, drought tolerance, and leaf carbon balance of grapevines (*Vitis labrusca*). Environ Exp Bot 134:82–95.

Reddy LS, Reddy AGK, Vanaja M, Maruthi V and Latha KV. 2018. Effect of elevated CO_2 and temperature on root length and root diameter of cuttings of grape varieties under face and fate facilities. Plant Arch 18:661-664.

Reineke A and Selim M. 2019. Elevated atmospheric CO_2 concentrations alter grapevine (*Vitis vinifera*) systemic transcriptional response to European grapevine moth (*Lobesia botrana*) herbivory. Sci Rep 9:1-12.

Rogiers SY, Hardie WJ and Smith JP. 2011. Stomatal density of grapevine leaves (*Vitis vinifera* L.) responds to soil temperature and atmospheric carbon dioxide. Aust J Grape Wine Res 17:147–152.

Salazar-Parra CS, Aguirreolea J, Sánchez-Díaz M, Irigoyen JJ and Morales F. 2010. Effects of climate change scenarios on Tempranillo grapevine (*Vitis vinifera L*.) ripening: response to a combination of elevated CO_2 and temperature, and moderate drought. Plant Soil 337: 179-191.

Salazar-Parra C, Aguirreolea J, Sanchez-Diaz M, Irigoyen JJ and Morales F. 2012. Photosynthetic response of Tempranillo grapevine to climate change scenarios. Annals Appl Bio 161: 277 – 292.

Salazar-Parra C, Aranjuelo I, Pascual I, Erice G, Sanz-Saenz A, Aguirreolea J, Sanchez-Diaz M, Irigoyen JJ and Morales F. 2015. Carbon balance, partitioning and photosynthetic acclimation in fruit-bearing grapevine (*Vitis vinifera* L. cv. Tempranillo) grown under simulated climate change (elevated CO_2, elevated temperature, and moderate drought) scenarios in temperature gradient greenhouses. J Plant Physiol 174:97 – 109.

Santos JA, Fraga H, Malheiro AC, Moutinho-Pereira J, Dinis LT, Correia C, Moriondo M, Leolini L, Dibari C, Costafreda-Aumedes S and Kartschall T. 2020. A review of the potential climate change impacts and adaptation options for European viticulture. Appl Sci 10:3092.

Scholasch T, Rienth M. 2019. Review of water deficit mediated changes in vine and berry physiology; Consequences for the optimization of irrigation strategies. OENO One 18: 53.

Schultz HR and Stoll M. 2010. Some critical issues in environmental physiology of grapevines: future challenges and current limitations. Aust. J. Grape Wine Res. 16:4-24.

Schulze-Sylvester M, Corronca JA and Paris CI. 2021. Vine mealybugs disrupt biomass allocation in grapevine. OENO One 55:93-103.

Schulze-Sylvester M and Reineke A. 2019. Elevated CO_2 levels impact fitness traits of vine mealybug *Planococcus ficus* Signoret, but not its parasitoid *Leptomastix dactylopii* Howard. Agronomy 9: 326.

Springer CJ and Ward JK. 2007. Flowering time and elevated atmospheric CO_2. New Phytol 176:243-255.

Thakur MP, Del Real IM, Cesarz S, Steinauer K, Reich PB, Hobbie S, Ciobanu M, Rich R, Worm K and Eisenhauer N. 2019. Soil microbial, nematode, and enzymatic responses to elevated CO_2, N fertilization, warming, and reduced precipitation. Soil Bio Biochem 135:184-193.

Terral JF, Tabard E, Bouby L, Ivorra S, Pastor T, Figueiral I, Picq S, Chevance JB, Jung C, Fabre I and Tardy C. 2010. Evolution and history of grapevine (*Vitis vinifera*) under domestication: new morphometric perspectives to understand seed domestication syndrome and reveal origins of ancient European cultivars. Annals Bot 105: 443-455.

Teslić N, Zinzani G, Parpinello GP and Versari A. 2018. Climate change trends, grape production, and potential alcohol concentration in wine from the “Romagna Sangiovese” appellation area (Italy). Theor App Climat 131:793-803.

Torres N, Antolín MC and Goicoechea N. 2018. Arbuscular mycorrhizal symbiosis as a promising resource for improving berry quality in grapevines under changing environments. Front Plant Sci 9:897.

Ubeda C, Hornedo-Ortega R, Cerezo AB, Garcia-Parrilla MC and Troncoso AM. 2020. Chemical hazards in grapes and wine, climate change and challenges to face. Food Chemistry 314: 126-222.

Ugaglia AA, Cardebat JM and Jiao L. 2019. The French Wine Industry. The Palgrave Handbook of Wine Industry Economics: 17-46.

Vasconcelos MC, Greven M, Winefield CS, Trought MC and Raw V. 2009. The flowering process of *Vitis vinifera*: a review. Am J Enol Vitic 60:411-434.

VanderWeide J, Gottschalk C, Schultze SR, Nasrollahiazar E, Poni S and Sabbatini P. 2021. Impacts of pre-bloom leaf removal on wine grape production and quality parameters: A systematic review and meta-analysis. Front Plant Sci: 11.

Van Leeuwen C and Darriet P. 2016. The impact of climate change on viticulture and wine quality. J Wine Econ 11:150-167.

Venios X, Korkas E, Nisiotou A and Banilas G. 2020. Grapevine Responses to Heat Stress and Global Warming. Plants 9: 1754.

Vivier MA and Pretorius IS. 2002. Genetically tailored grapevines for the wine industry. Trends Biot 20:472-478.

Weiss E, Kislev ME, Simchoni O and Nadel D. 2004. Small-grained wild grasses as staple food at the 23,000-year-old site of Ohalo II, Israel. Econ Bot 58:125-134.

White MA, Diffenbaugh NS, Jones GV, Pal JS, Giorgi F. 2006. Extreme heat reduces and shifts United States premium wine production in the 21st century. Proc Natl Acad Sci 30:17-22.

Wohlfahrt Y, Tittmann S and Stoll M. 2017. Physiological and yield performance of *Vitis vinifera* L. cvs. (Riesling and Cabernet Sauvignon) under Free Air Carbon Dioxide Enrichment (FACE). Conference: GiESCO 20th International Meeting 2017, At Mendoza, Argentina.

Wohlfahrt Y, Smith JP, Tittmann S, Honermeier B and Stoll M. 2018. Primary productivity and physiological responses of *Vitis vinifera* L. cvs. under Free Air Carbon Dioxide Enrichment (FACE). Eur J Agr 101: 149-162.

Wolkovich EM, de Cortázar-Atauri IG, Morales-Castilla I, Nicholas KA and Lacombe T. 2018. From Pinot to Xinomavro in the world's future wine-growing regions. Nat Clim Change 8: 29-37.

Zufferey V, Murisier F, Vivin P, Belcher S, Lorenzini F, Spring JL and Viret O. 2012. Carbohydrate reserves in grapevine (*Vitis vinifera* L.'Chasselas'): the influence of the leaf to fruit ratio. Vitis 51:103-110.

Chapter 2

Modelled Phenological Sensitivity of Grapevine

Molly Clemens[1], Geoffrey Legault[2], Andrew Walker[3], Elizabeth Wolkovich[4]

[1] San Diego State University and University of California Davis, Joint Doctoral Program Ecology
[2]University of British Columbia, Department of Forest and Conservation Sciences
[3]University of California, Davis, Department of Viticulture and Enology
[4]University of British Columbia, Department of Forest and Conservation Sciences

Abstract

The growing season temperatures in many of the world's premiere winegrape growing regions are increasing. Climate change is predicted to advance the phenology of grapevines, with significant impacts on harvest dates. This study examines the approximate sensitivity of 137 varieties grown in at the University of California, Davis with phenological data taken over four years. Grapevine sensitivity is not linear through the major phenophases (budburst, flowering, and veraison) as the vine matures from vegetative to reproductive growth. The model presented include the genetically determined geographic origins of each variety as well as detailed climate data to explore how important these are when predicting response of international varieties grown in California. This study addresses (1) whether varieties grouped by geographic origin have unique and quantifiable sensitivity to climate change (2) the impact of extreme heat on the three stages of grapevine phenology and (3) which of these three stages is most impacted by extreme heat events. We identified the estimated number of growing degree days for each variety to achieve budburst, flowering, and veraison, as well as the coefficient of variation for each group when planted in Northern California.

Introduction

Climate change is increasing the growing season temperatures in many of the world's most important winegrape growing regions. According to the most recent IPCC Assessment Report, Climate Change 2021, global warming is expected to exceed 1.5°C - 2°C during this century (Zhongming et al. 2021). Warming caused by anthropogenic greenhouse gas emissions advances phenology in hundreds of plant species, with increased consequences for perennial crops (Estrella et al., 2007; Franks and Weis, 2008; Wang et al., 2018; Droulia and Charalampopoulos, 2021). Climate warming has already altered the phenology (e.g. lifecycle timing such as budburst) of many plant species globally, including the phenology of valuable crop plants such as grapevine (Franks and Weis, 2008; Webb et al. 2011; Jones 2013; van Leeuwen et al., 2019; Droulia and Charalampopoulos, 2021; Cameron et al., 2022). Winegrapes, a globally important crop both economically and culturally, have become an important indicator of climate change, with well documented advancing phenology, shorter periods between phenological stages (Jones 2013), and large inter-annual variability (Jones and Davis, 2000; Cameron et al., 2022).

Adapting to climate change has become a global priority, and the wine industry is likewise looking for more accurate predictive measures of phenology and strategies for future planting. Culturally and economically, grapevine is one of the most valuable crops in the world, evidenced by an annual production of 60 million tons of fruit (Owens 2008), with varieties that have been cultivated for thousands of years, selected for color, flavor, and phenological timing (Terral *et al.*, 2009).

Grape growth and qualities are sensitive to growing season climate fluctuations, and there is a direct link between warming temperatures and early harvest dates (Cook and Wolkovich, 2016). Earlier ripening forces farmers to harvest grapes at optimal sugar levels during warmer

periods of the summer. Harvest should ideally occur later during a cooler period of the growing season after the berry has accumulated an appropriate balance of acids of sugars. Early harvesting decreases the quality of wine, evidenced by early ripening significantly altering berry chemical composition (Duchêne and Schneider, 2005). Higher year-round temperatures impact varieties with chilling requirements, such as California's premiere wine grape, Chardonnay (Caffarra *et al.*, 2010; Webb, Whetton, and Barlow, 2007; Monteverde and De Sales, 2020).

Globally, there have been shifts of 1-2 weeks for winegrape growing regions (Wolkovich *et al.*, 2017; Cameron et al., 2021). In Europe, the growing season has lengthened by about 11 days over the last 30 years, which will impact grape berry and wine quality (Jones and Davis, 2000; Coombe and Iland, 2005; Bernáth et al., 2021). Early budburst threatens frost damage during volatile Spring temperatures (De Rosa et al., 2021; Dinu et al., 2021). At present, the winegrape crop in Bordeaux has a month earlier harvest than it did 50 years ago (Webb, Whetton, and Barlow, 2007).

Models of warming indicate that increases in temperature are not uniform globally and that warming has increased in the major winegrowing areas of California and Western Europe more than South America and Australia during the past 50 years (Jones 2007; Cameron et al., 2021). The phenological shifts resulting from growing season temperature increases are documented internationally, and models predicting phenology using temperature are becoming more precise (Parker *et al.*, 2011; Pipan 2021; Costa et al., 2019; Cameron et al., 2022). A multitude of studies both observational and experimental have identified an acceleration of phenology and decrease in periods between stages in response to warming growing seasons (Duchêne and Schneider, 2005; Jones *et al.*, 2005; Webb, Whetton, and Barlow, 2007; Petrie and Sadras, 2008; Duchêne *et al.*, 2010), but some show trends of the intervals between each stage widening (Jones and

Davis, 2000). Previous grapevine modeling which quantified relative sensitivity of many varieties combined records of phenology across variable microclimates and conditions (Parker *et al.*, 2013; Parker et al., 2021; Cameron et al., 2022). Comparing phenological timing from different vineyards done does not capture the influence of the microclimate and microhabitat; elevation, management, soil type, and a multitude of other environmental factors can impact flowering time (Rathcke and Lacey, 1985; Hunter et al., 2021; Verdugo-Vásquez et al., 2021). The ampelography vineyard at University of California Davis allows for attributing the variation in phenology to the specific sensitivity of cultivars to changes in climate, rather than soil type, irrigation method, pruning, or other major sources of variability found when comparing multiple vineyards.

Temperature is the main driver of phenological development for grapes; heat accumulation impacts the biochemistry important for cell growth (Zapata *et al.*, 2017; Moncur *et al.*, 1989). A study of 15 cultivars in Australia documented a plateau in growth between 22-29°C (Cameron et al., 2022). For many plant species, higher temperatures can stagnate growth, and we expect that some varieties of grapevine would be sensitive to temperatures greater than 40°C (Wang and Engel, 1998). In extreme cases, beyond inducing premature veraison, heat stress will cause loss of berries, inactivate enzymes, and reduce development of flavors critical for wine quality (Mullins *et al.*, 1997). Many grapevine models do not include information on high temperature impacts (Duchêne *et al.*, 2010; Caffara *et al.*, 2010; Parker *et al.*, 2011; Zapata *et al.*, 2017). We integrate into our models a measure of extreme heat to determine its effect on veraison, the stage most likely impacted by these events.

In this study, we examined variability in the phenological responses of 137 varieties of *Vitis vinifera* over a 5-year period. We examined variability in the timing, in terms of growing degree

days, of the three major phenological stages: budburst, flowering, and veraison. Our data provide an updated reference to the last major study of variety-level phenological responses in California, which examined 114 varieties nearly 40 years ago (McIntyre *et al.*, 1982). We also compare traditional *Vitis vinifera* species with hybrids grown at the University of California Davis, originally cultivated by Harold Olmo. Overall, this study offers a comprehensive look at international varieties planted in California their relative phenological response to climate. This study aims to evaluate a wide range of cultivars to identify regions with lower sensitivity to climate change that may be used in adaptation, either through breeding or planting as alternatives.

Materials and methods

Field Work

The UC Davis ampelography learning vineyard has been developed over the past decade to include approximately 300 international varieties planted adjacent to the Viticulture and Enology academic building. The vines are planted in groupings by geographic origin, (e.g. Bordeaux varieties in one row) for the purpose of teaching. The vines are trellised using vertical shoot position (VSP), with regular irrigation, and are treated throughout the growing season with sulfur sprays for pests and disease. The current study of phenology has been tracking over 130 varieties for over four years and measures the response of the varieties through three main phenological stages: budburst, flowering, and veraison. The phenological data has been collected from UC Davis starting in 2014, continued through 2019.

For each of 137 varieties, we recorded the timing of three major phenological stages: Budburst, Flowering, and Veraison. The same individuals were monitored for 5 years. For each vine, three positions on the cordon were chosen at the start of each season before budburst,

following the previous year's recorded positions unless damage had occurred, in which case a nearby cordon was chosen (initial positions were determined randomly). The primary buds from each two-bud spur were chosen at the most basal position. The three buds were tracked through each phase, treated as technical replicates averaged for an overall estimate for each individual vine. Each vine is a biological replicate, and two vines per cultivar were measured.

The timing of budburst was recorded as stages 1-13 (primarily categorized by number of leaves separating from the initial shoot), based on the modified Eichhorn–Lorenz (EL) stage of the three positions monitored for each vine (Coombe 1995). The EL scale describes the phenological stages of grapevine (*Vitis vinifera* L.) and categorizes the stages as follows: budbreak, shoot development, flowering, fruit set, berries pea-sized, veraison, and harvest (Coombe 1995). Flowering was monitored from these same shoot positions, and once clusters started to develop, they were marked with flagging tape. Clusters were chosen from the most basal position on the shoot arising from the most basal bud. Flowering was estimated by percent of the cluster appearing to have caps fallen and flowers showing. At the point where 50% of the caps on flowers have fallen away, called anthesis, the cluster is considered at full bloom (Jones 2013). Flowering is recorded as a percent estimate of the cluster in bloom.

These clusters were then tagged with fluorescent tape loosely and followed subsequently for veraison and maturity. Veraison was recorded as a percent estimate of the cluster with color and softness changes. Records were taken every two to three days during each of the phenological stages. At each stage of monitoring, researchers calibrate observations with each other and with photographs from previous years.

Environmental Data

Environmental data were collected from the nearby California Irrigation Management Information System (CIMIS) weather station (https://cimis.water.ca.gov/WSNReportCriteria.aspx; accessed 8/1/2018) and downloaded as daily and hourly reports for the four years of the study. Temperature was converted to growing degree days (GDD) using the formula [GDD = sum of the average daily temperature – chosen base temperature], and was calculated in two ways: as the sum of average daily temperatures after day 60 (March 1st), (1) with a base temperature of 10°C and (2) with base temperature 0°C (Parker *et al.*, 2011).

The Wang and Engel model uses a maximum temperature of 40°C, which may be the biological threshold for grapevine growth (Wang and Engel, 1998; Luo et al., 2011; Greer 2013). The biological optimal temperature for grapevines is likely around 25°C (Keller 2010), and when temperatures exceed 30°C, there are impacts on anthocyanins (highly volatile phenolic color compounds in berry skin), and temperatures exceeding 37°C decreased coloration in grape berry skin and degradation of aromatic compounds (Bernardo et al., 2018; Venios et al., 2020). Therefore, we include the variable of cumulative number of days when temperature reached a maximum at or over 40°C in our models of veraison, the only phenological stage that encounters these days, with variety as a random effect (Thackeray et al. 2016).

This study spanned four years and is ongoing to evaluate the sensitivity of different varieties to climate change. It is important to note that timing and duration of the winter pruning was variable, which could have introduced error because the timing of pruning can impact budburst (Gatti *et al.*, 2016). Some varieties were discontinued from the study because of death,

disease, or pest damage. Some varieties were only included in later years of the study once they reached maturation.

Estimating GDD of the phenological phases

Measurements of percent budburst, flowering, and veraison were converted to GDD using R (R Core Team 2013). For each stage, a linear model was fit with phenological development as a percent as the response variable and time (in days) as the independent variable. The fitted model was used to estimate the day a cluster reached 50% budburst, flowering, or veraison.

Data were cleaned by removing individuals with illogical estimates for timing. It was determined for these removed points that too few measurements were made for those vines, and the individuals removed were from the year 2015. The limits for estimates were based on observational data. If budburst was predicted earlier than day 60 of the year, this individual was removed, because this was earlier than measurements were recorded. Flowering was limited to day 111 of the year, and veraison was limited to begin at day 175 of the year.

We obtained for each of the four years the GDD's required to reach the three pheno-phases for an individual plant. These GDD's were the response variable of the hierarchical models described in the next section. The days over 40°C from January until September (growing season) were also quantified for each year.

Phenological sensitivity

To determine phenological sensitivity, we calculated the coefficient of variation (CV) of the GDD's across the 4 years of the study, pooling replicates of the same variety. CV is

commonly used to measure the variation of a distribution and, because it is standardized by the mean of the distribution, it allows us to compare the sensitivity of varieties with different mean GDD's from the three distinct stages.

Statistics

To quantify the variation in growing degree days across and within grapevine varieties, we used Bayesian linear mixed effect models as implemented in the package RStanArm (Vehtari *et al.*, 2017). The default set of priors was used for the RStanArm package. A model using GDD's with a base temperature of 10°C were compared against a model with base 0°C temperature. Models were fit using GDD with a base temperature of 0°C on the day of a phenological event as the response variable. Separate models were fit for the three phenological stages: budburst, flowering, and veraison. For the budburst and flowering stages, GDD was the response variable with "utility" as a fixed effect and "geography/variety" as random effects. For veraison, we included "utility" as a fixed effect, "geography/variety" as random, as well as "days above 40°C" as a random effect tied to variety. The climate data were summarized in R from the raw CIMIS data, and the cumulative measurements for each stage included the weeks prior to each stage. The explanatory models of maximum daily temperature, and cumulative number of days with temperatures reaching over 40°C, and year as fixed effects were incorporated into models for each stage. Overall, we added grape utility, in terms of wine or table grape or both, geographic groups, and country of origin as nested random variables (Bacilieri *et al.*, 2013).

The advantage to using a fixed effect model to predict GDD by variety is that we fill gaps by including data from other varieties' responses to predict individual variety response. We quantify variety-level GDD by leveraging information from all varieties together. Rather than

using an average for each variety by year, we utilize the temporal redundancy to estimate consistency across years, and we can see from the average of all varieties together which ones fluctuate the most during years with more change in climate.

We used the posterior predictive check of a PSIS diagnostic plot to ensure khats were all less than 0.7. The preference for rstanarm to evaluate these mixed effects models is based on the Bayesian approach using MCMC, rather than restricted maximum likelihood estimation, which tends to underestimate uncertainties (Goodrich *et al.*, 2018). This Bayesian approach estimates uncertainty for all the model levels, including our random effect of variety which contains 137 or less estimated parameters.

Results

Table 2: Chosen models for each phenological stage are described here. The response variable is growing degree days (GDD) with base temperature 0°C. Models were run in rstanarm using leave one out comparison. The posterior predictive checks showed no Khat values over 0.4 in the PSIS diagnostic plot. The posterior checks for the models show the data is normally distributed. The variable "number of days above 40°C" only explained variation for the model of veraison.

Table 2

Stan Linear Mixed Effects Regression Model	**Stage**
(GDD base 0°C) ~ (1|variety) + (1|geographic group/country of origin) + utility	Budburst
(GDD base 0°C) ~ (1|variety) + (1|geographic group/country of origin) + utility	Flowering
(GDD base 0°C) ~ (1|variety) + (1|geographic group/country of origin) + utility + (1|number of days above 40°C)	Veraison

When ELPD-difference was compared, the differences in log probability for the five models were almost completely within their individual standard errors. For this reason, we can consider all five models substantially predictive, but we chose the top model based on lowest ELPD-difference and biological relevance of the variables in the model.

For veraison, the differences in log probability (−0.6, −4.7, −94.0, and −94.8), were not within their individual standard errors (−1.2, −2.9, −20.7, and −20.7, respectively). The models of veraison were improved by the addition of the variable, "days above 40," referring to the cumulative number of days with daily maximum temperatures at or above 40°C.

The genetically identified geographic origins provided by Bacilieri *et al.* (2013) Supplemental Information added predictive information to our final models for budburst, flowering, and veraison. We see differences in sensitivity to climate across stages for each of the geographic groups, visualized by the coefficient of variation over the four years analyzed (Figure 2). The intercepts reported in Supplementary Table 2, in terms of growing degree days, provide a predictive range to expect phenological variability from these groups.

Figure 2

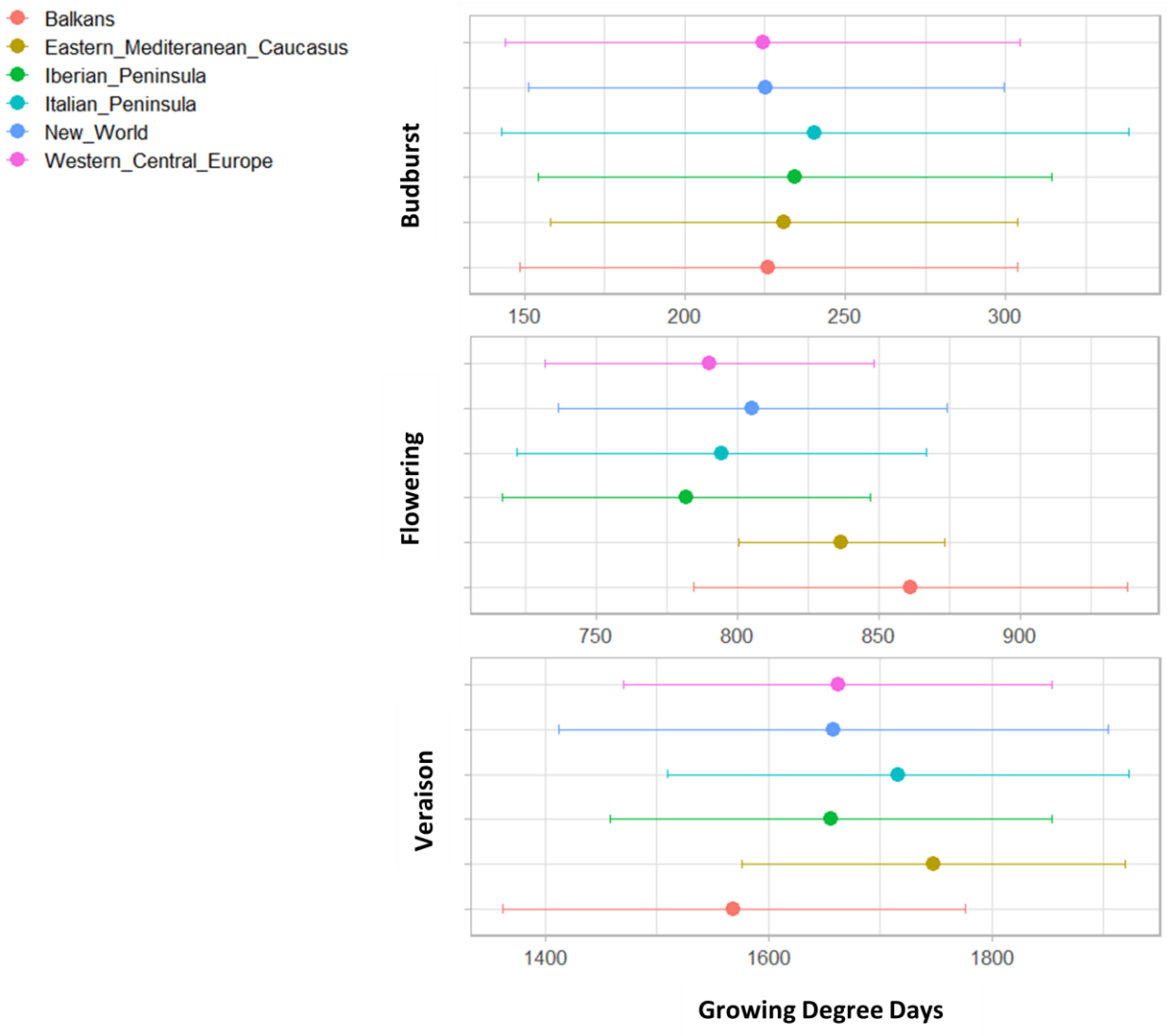

Figure 2: Phenological timing for budburst, flowering, and veraison are shown here grouped by their geographic origin.

The range of phenological timing for specific cultivars can help match varieties with ideal climates and regions. There are varieties from each of these regions with the potential to be late ripening. From the Italian Peninsula, there is Dolcetto with a relatively early veraison and Aglicanico with a relatively late and variable veraison (Figure 2). The timing of stages can be extremely consistent, such as with Gamay Noir from Western Central Europe, but there can also be a wider range of timing like that of Mourvedre, from the same region. Therefore, while region is predictive, analyzing the timing for specific varieties is also useful when selecting alternative varieties for planting.

Table 3: The coefficient of variation for the top five highest ranked by variety, shown here for each of the three phenological stages. The varieties listed in bold are in the top five latest for more than one phenological stage.

Table 3

Variety	Coefficient of variation	Stage
Trebbiano	**0.919**	budburst
Forastera	**0.625**	budburst
Coda di Volpe	**0.585**	budburst
Beauty Seedless	**0.579**	budburst
Carmenere	**0.577**	budburst
Valdepenas	**0.554**	budburst
Aglicanico	**0.278**	veraison
Emerald Seedless	**0.267**	veraison
Dawn Seedless	**0.228**	veraison

Trebbiano	**0.222**	flowering
Pinot blanc	**0.205**	veraison
Canner	**0.193**	veraison
Thompson Seedless	**0.183**	veraison
Scarlett	**0.175**	flowering
Coda di Volpe	**0.170**	flowering
Valdepenas	**0.159**	flowering
Szagos feher	**0.132**	flowering
Carnelian	**0.116**	flowering

A regression of the coefficient of variation across stages (Figure 4) revealed a weak relationship between flowering and veraison, and budburst and veraison, however budburst and flowering did show some trends towards positive relationship. However, several of the varieties with the top sensitivities were in the top five for more than one stage, indicating that while there is not a correlation between geographic region sensitivity across stages, there are some consistently highly sensitive varieties (Table 3). This data suggests that despite geographic trends, each variety responds to climate uniquely. Interestingly, the top highest sensitivities were found for two Italian varieties (Table 3), while table grapes had consistently high sensitivities in flowering and veraison. These estimated sensitivities can be used to predict how robust alternative varieties may be, if planted in California.

While veraison had a larger range for all the varieties combined, the timing of veraison had a relatively low coefficient of variation when looking at each variety's timing over the four

years. Budburst had the highest coefficient of variation, likely due to the impact of conditions during dormancy (Camargo-Alvarez et al., 2020).

Figure 3: The coefficient of variation is used here as a sensitivity index, in terms of calculated growing degree days. The coefficient of variation is response to changes in climate for each year over four years, separated by stage. The sensitivity to climate is shown for the timing of each of the three phenological stage and grouped by geographic origins.

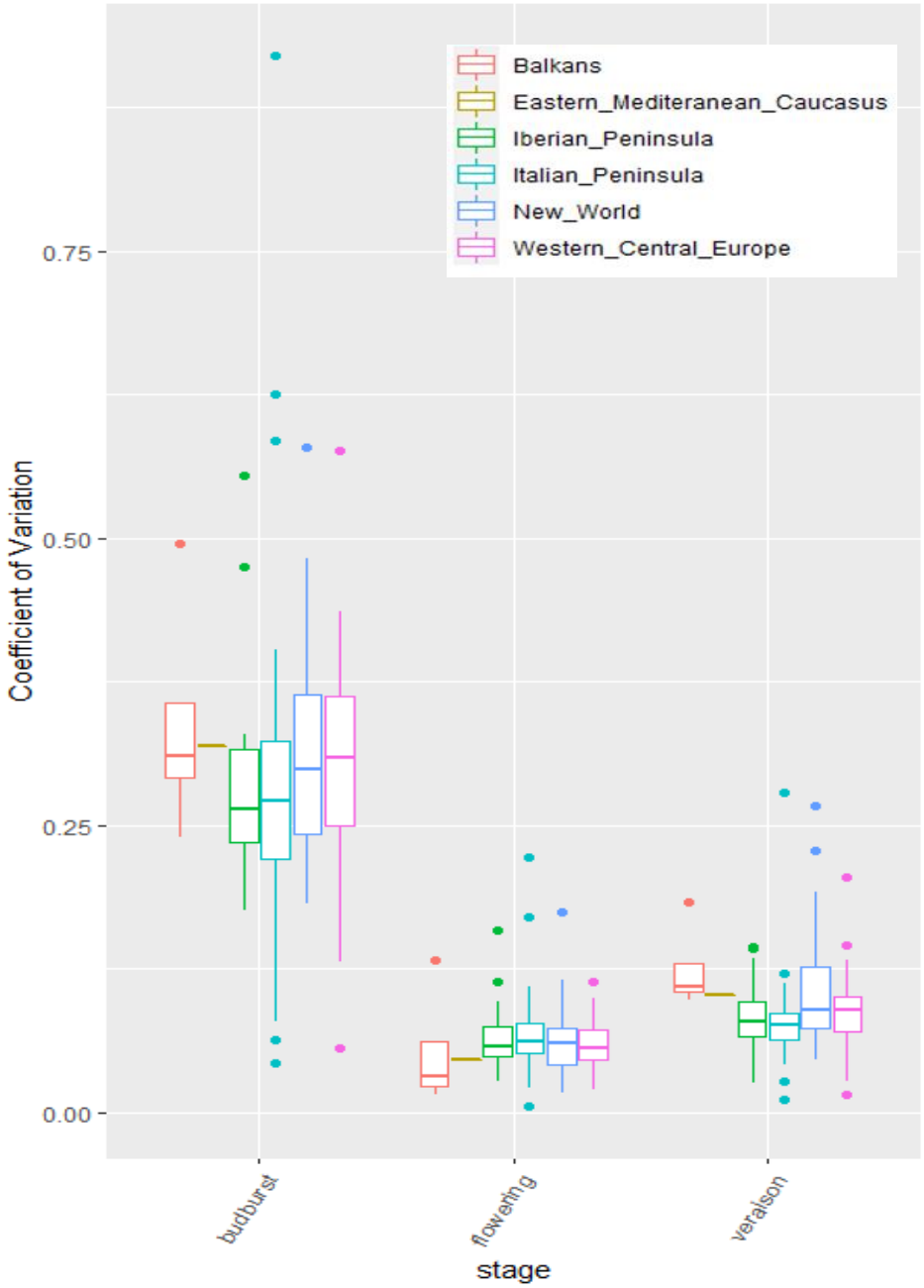

There may also be an accumulation of climatic impacts over the season resulting in the highest variability in timing at veraison. In a previous common garden experiment, the timing of maturity also had the largest standard error with more predictable timing for budburst and flowering (McIntyre *et al* 1982). Sensitivity across stages does not have a strong correlation, but Budburst and Flowering seem to have the strongest relationship, with the highest R^2 for the Balkans geographic region at 96% (Supplementary Table 1). The parameter estimates of the three models reported the highest sigma (indicator of predictiveness for each variable) for variety for all three models.

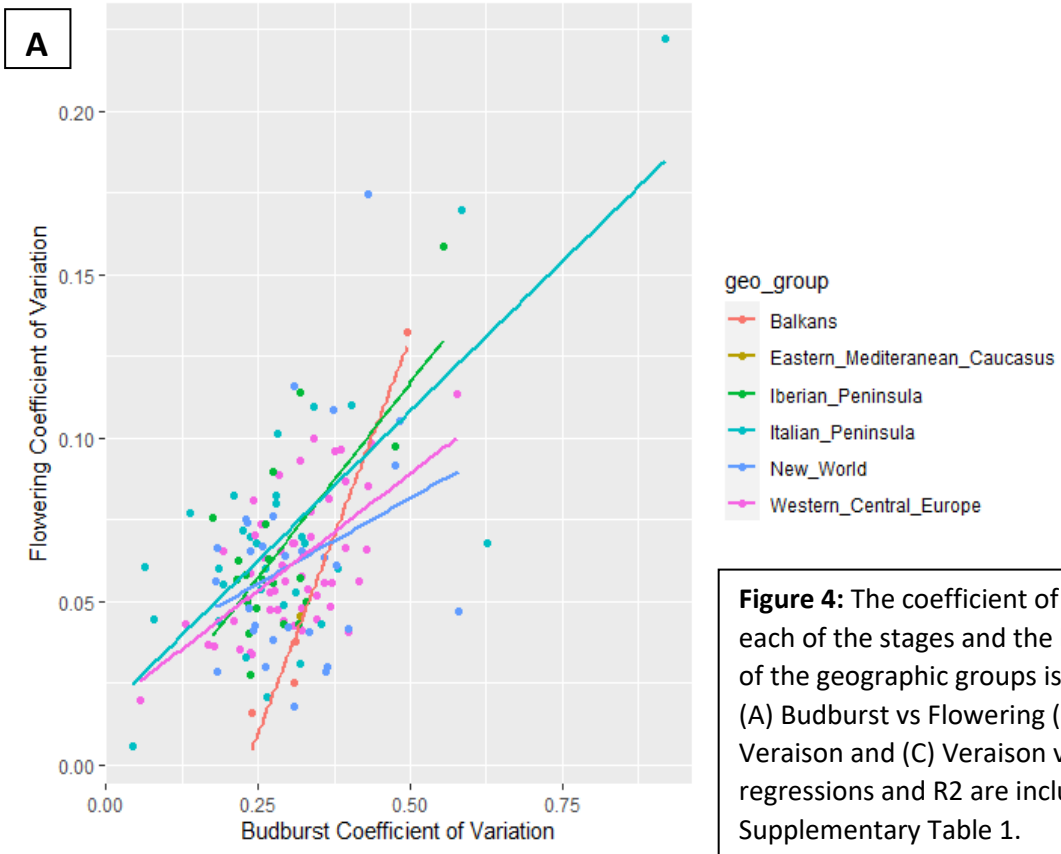

Figure 4: The coefficient of variation for each of the stages and the linear regression of the geographic groups is presented here; (A) Budburst vs Flowering (B) Budburst vs Veraison and (C) Veraison vs Flowering. The regressions and R2 are included in Supplementary Table 1.

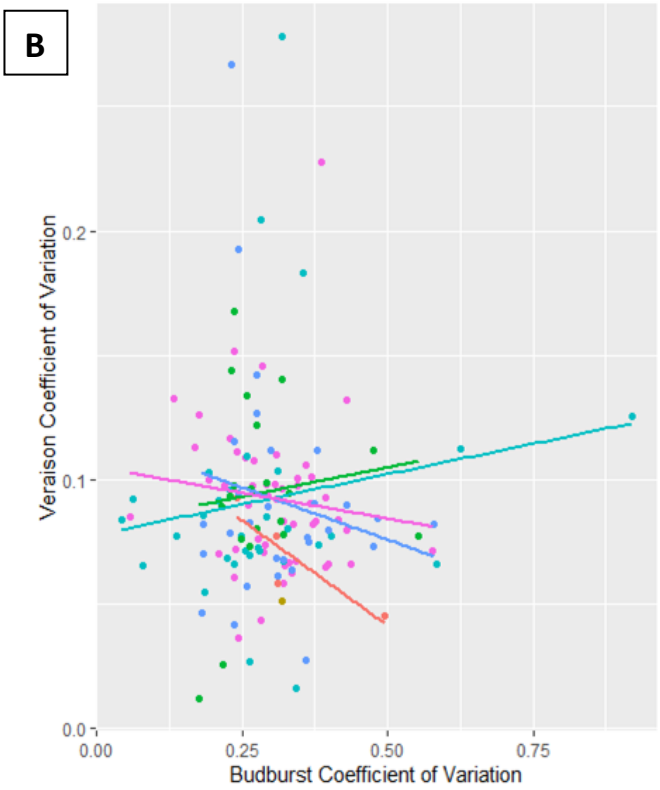

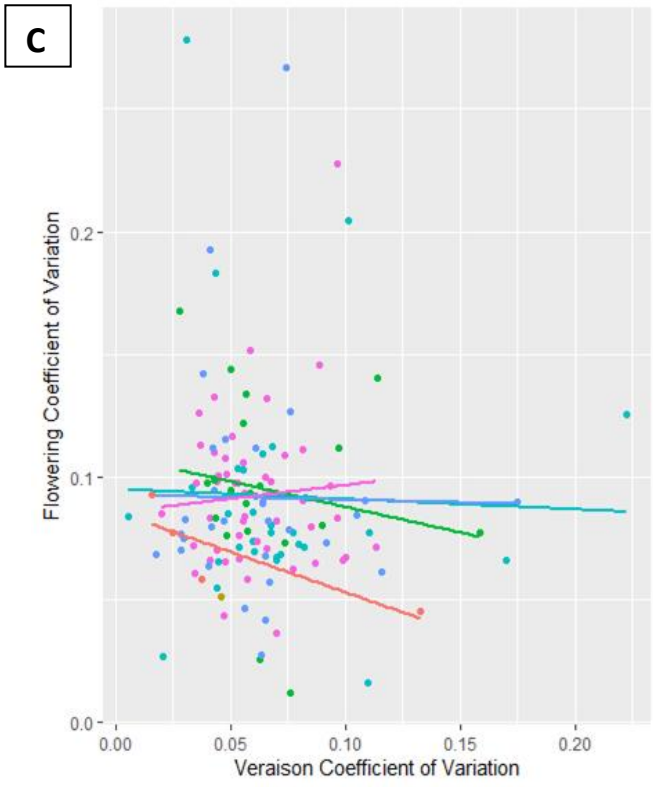

Discussion

From an ecological perspective, a vineyard is a system that responds to its environment. This system includes the soil, international varieties, and the climate. We modelled the response of varieties' phenological timing to climate, and the results present unique sensitivities to climate over 4 years. Geographic origin and cultivated utility of grapes explain some of the variation seen in phenological timing, which we expect is driven by physiological differences.

Accumulation of daily temperature in our model is strongly correlated with phenological stage occurrence, which agrees with past modelling of growing degree days and phenology (Duchêne *et al.*, 2010; Caffara *et al.*, 2010; Parker *et al.*, 2011; Zapata *et al.*, 2017). Previous models have used individual parameters for growing degree days and base temperature based on the cultivar (Zapata *et al.*, 2011). Duchêne *et al.* (2010) used daily maximum temperature rather than GDD in their models to predict phenology, and their models included a stage specific base temperature. Our model is unique by including variety specific response to cumulative days above 40°C. We expected this to impact the timing of veraison for some varieties with higher sensitivity to heat stress.

The chosen model for veraison included the variable of "days above 40°C," which is in part due to the timing of high heat days, typically occurring later in the season, during this stage. This model outranked models for veraison that nested geographic origin, indicating that the effect of high temperature is not variety specific. The general intercepts of the models for each stage predict the mean GDD required to reach each phenological stage, and the intercepts for each variety indicate the specific GDD requirement for each variety (Supplementary Table 2). The general intercept for the three stages was 199 GDD for budburst, 836 GDD for flowering, and 1,699 GDD for veraison (Supplementary Table 2). We may expect for other regions and in

California's future that heat stress may impact flowering as we see an increase in high heat events earlier in the growing season (Monteverde et al., 2020).

The dominant hypotheses indicate that budburst may be less correlated with growing season temperature changes because it is more impacted by viticultural techniques and therefore sensitive to chilling time over dormancy (Moncur *et al.*, 1989; Jones 2013). In the UC Davis ampelography vineyard, all vines are experiencing the same dormancy conditions, so the difference within years in timing of budbreak is explained by the varietal differences (Figure 2). However, across years, the lower sensitivity of budburst timing compared to flowering and veraison may be also be explained in part by the discrepancy in the dominance of climatic versus genetic controls for vegetative versus reproductive growth, respectively (Carmona et al., 2008). Varieties may not be sensitive to temperature in the same way across stages, as the vine switches from vegetative growth to reproductive growth with the onset of flowering (Vasconcelos *et al.*, 2009). The weaker relationship between budburst and cumulative temperature than the subsequent stages may be because flowering time and maturation are more strongly controlled by genetics (Rathcke and Lacey, 1985). Furthermore, the dissociation between vegetative and reproductive growth makes it unclear how plants will adapt to climate change (Franks and Weis, 2008).

While research shows viticulture is expanding to new territories all over the world (Hannah *et al.*, 2013; Moriondo *et al.*, 2013), a crucial aspect to the success of the expanding viticulture into novel territories is matching the phenology to the local climate; agriculture will fail when introduced crops cannot adjust to new seasons (Rathcke and Lacey, 1985). Climate change will not only change the varieties suitable for a region, but also the regions suitable for planting grapes (Hall and Jones, 2009; Morales-Castilla *et al.*, 2020). Failure to choose appropriate

varieties for novel territories can impact natural ecosystems, an unintended adverse effect of expanding viticulture (Hannah *et al.*, 2013).

A recent study modeling changes in viticulture territories under climate change scenarios predicted that 51 % of climatically suitable for growing winegrapes would become unsuitable (Morales-Castilla *et al.*, 2020). The intraspecific variation in heat thresholds for grapevines impacts the adaptation capacity of each cultivar (Parker *et al.*, 2011; Zapata *et al.*, 2017). Previous authors suggest allowing cultivar turnover to prevent these major losses, which will depend heavily on what governments allow in Europe (Morales-Castilla *et al.*, 2020), while we are free to plant many different varieties in California.

Among many strategies of adaptation to climate change, shifting to climatically more appropriate varieties has been widely suggested (Morales-Castilla *et al.*, 2020). Even with our current understanding of varieties' climate niches, only a few existing cultivars are late ripening enough to avoid the warming predicted to occur during maturation in future climate scenarios (Parker *et al.*, 2013; García de Cortázar-Atauri *et al.*, 2017). We identified many late ripening varieties that can be tested in future studies for suitability in California (Supplementary Table 2). International projects such as ADVIDCLIM are currently testing phenological models of grapevine with the expectation that varieties planted will need to change in future climate conditions (Quénol *et al.*, 2014). Hypothetical crosses between very late ripening varieties were modelled and still struggle to be late-ripening enough to endure the predicted 23-day shift and increase of 7°C expected by the end of this century (Duchêne *et al.*, 2010). Within existing varieties, clonal variation does not offer a wide enough plasticity for adapting to climate change, however, taking advantage of existing varieties in warm regions to grow as alternatives is a promising strategy (Delrot *et al.*, 2020, Sargolzaei et al., 2021).

Conclusion

Our study elucidates the differences in varieties' sensitivities to climate and clusters the response by region of origin to explore the plastic phenotypic responses of present-day cultivars. Using published genetic data on thousands of varieties, we were able to incorporate geographic sub-regions of origin into our model comparison and produce predictions on timing for the three phenological stages with unique estimates for all 137 varieties. While geographic origins indicate trends in response to climate, more important are the outliers from the groups that are consistently late ripening with low sensitivity to changes in climate. Our approach to quantifying the responses of hundreds of varieties gives viticulturists insight to future alternative choices, such as the late ripening, heat tolerant Nebbiolo, with veraison predicted at 45-174 GDD later than the mean. Italian varieties also showed the lowest sensitivity to changes in climate, indicated by the relatively low CV compared to other regions. No other phenological studies in California test this many international varieties in the context of the hot central Northern Californian summer growing season with precise observations over years.

Future research will target potential varieties for successful marketing in California under future climate conditions, and potentially elucidate physiological drivers of phenological variation that have been selected unintentionally through grapevine cultivation. These important phenological patterns and sensitivities could be useful for adapting plant material to new regions and new climates.

References

Acevedo-Opazo, C., Ortega-Farias, S. & Fuentes, S. (2010). Effects of grapevine (*Vitis vinifera* L.) water status on water consumption, vegetative growth and grape quality: An irrigation scheduling application to achieve regulated deficit irrigation. *Agricultural Water Management*, (97), 956-964.

Bernardo, S.; Dinis, L.T.; Machado, N.; Moutinho-Pereira, J. Grapevine abiotic stress assessment and search for sustainable adaptation strategies in Mediterranean-like climates. A review. *Agron. Sustain*. 2018, 38, 66.

Bernáth, S., Paulen, O., Šiška, B., Kusá, Z. and F. Tóth. (2021). Influence of Climate Warming on Grapevine (Vitis vinifera L.) Phenology in Conditions of Central Europe (Slovakia). *Plants*, 10: 1020.

Caffarra, A. & Eccel, E. (2010). Increasing the robustness of phenological models for *Vitis vinifera* cv. Chardonnay. *International journal of biometeorology*: 255-267.

Camargo-Alvarez, H., Salazar-Gutiérrez, M., Keller, M. and M. Hoogenboom. (2020). Modeling the effect of temperature on bud dormancy of grapevines. *Agricultural and Forest Meteorology*, 280: 107782.

Cameron, W., Petrie, P. R., Barlow, E., Howell, K., Jarvis, C., & Fuentes, S. (2021). A comparison of the effect of temperature on grapevine phenology between vineyards. *OENO One*, *55*(2), 301–320.

Cameron, W., Petrie, P.R. and E. Barlow. (2022). The effect of temperature on grapevine phenological intervals: Sensitivity of budburst to flowering. *Agricultural and Forest Meteorology*, 315: 108841.

Carmona, M.J., Chaïb, J., Martínez-Zapater, J.M. and M. Thomas. (2008). A molecular genetic perspective of reproductive development in grapevine. *Journal of experimental botany*, *59*: 2579-2596.

CIMIS data report. https://cimis.water.ca.gov/WSNReportCriteria.aspx. CIMIS was established in 1982 as a joint project between the University of California, Davis and DWR. accessed 8/1/2018.

Cook, B.I., & Wolkovich E.M. (2016). Climate change decouples drought from early wine grape harvests in France. *Nature Climate Change* (6), 715.

Coombe, B.G. 1995. Growth stages of the grapevine: adoption of a system for identifying grapevine growth stages. *Australian Journal of Grape and Wine Research,* (1), 104-110.

Coombe, B.G. and Iland, P.G. (2005) Grape berry development and winegrape quality. In: Viticulture. Volume 1 – resources. Eds. P.R. Dry and B.G. Coombe (Winetitles: Adelaide) pp. 210–248.

de Cortázar-Atauri, I. G., Duchêne, E., Destrac-Irvine, A., Barbeau, G., de Rességuier, L., Lacombe, T., Parker, A.K., Saurin, N. & van Leeuwen, C. (2017). Grapevine Phenology in France: From Past Observations to Future Evolutions in the Context of Climate Change. *OENO One*, 51, 115-126.

Costa, R., Fraga, H., Fonseca, A., García de Cortázar-Atauri, I., Val, M.C., Carlos, C., Reis, S. and J. Santos. (2019). Grapevine phenology of cv. Touriga Franca and Touriga Nacional in the Douro wine region: Modelling and climate change projections. *Agronomy*, 9: 210.

Delrot, S., Grimplet, J., Carbonell-Bejerano, P., Schwandner, A., Bert, P. F., Bavaresco, L., Dalla Costa, L., Di Gaspero, G., Duchêne, E., Hausmann, L., & Malnoy, M. (2020). Genetic and Genomic Approaches for Adaptation of Grapevine to Climate Change. In *Genomic Designing of Climate-Smart Fruit Crops*, (pp. 157-270). Springer, Cham.

De Rosa, V., Vizzotto, G. and R. Falchi. (2021). Cold Hardiness Dynamics and Spring Phenology: Climate-Driven Changes and New Molecular Insights Into Grapevine Adaptive Potential. *Frontiers in Plant Science*: 12.

Dinu, D.G., Ricciardi, V., Demarco, C., Zingarofalo, G., De Lorenzis, G., Buccolieri, R., Cola, G. and L. Rustioni. (2021). Climate Change Impacts on Plant Phenology: Grapevine (*Vitis vinifera*) Bud Break in Wintertime in Southern Italy. *Foods* 10: 2769.

Droulia, F. and I. Charalampopoulos. (2021). Future Climate Change Impacts on European Viticulture: A Review on Recent Scientific Advances. *Atmosphere* 12:495.

Duchêne, E., Huard, F., Dumas, V., Schneider, C., & Merdinoglu, D. (2010). The challenge of adapting grapevine varieties to climate change. *Climate research*, 41(3), 193-204.

Duchêne, E., & Schneider, C. (2005). Grapevine and climatic changes: a glance at the situation in Alsace. *Agronomy for Sustainable Development* 25: 93–99.

Estrella, N., Sparks, T.H. and A. Menzel (2007). Trends and temperature response in the phenology of crops in Germany. *Global Change Biology*, 13: 1737-1747.

Franks, S. J., & Weis, A. E. (2008). A change in climate causes rapid evolution of multiple life-history traits and their interactions in an annual plant. *Journal of evolutionary biology*, 21(5), 1321-1334.

Gatti, M., Pirez, F. J., Chiari, G., Tombesi, S., Palliotti, A., Merli, M. C., & Poni, S. (2016). Phenology, canopy aging and seasonal carbon balance as related to delayed winter pruning of *Vitis vinifera* L. cv. Sangiovese grapevines. *Frontiers in plant science*, 7, 659.

Goodrich, B., Gabry, J., Ali, I., & Brilleman, S. (2018). rstanarm: Bayesian applied regression modeling via Stan. R package version 2.17.4. http://mc-stan.org/.

Greer, D.H., (2013). The impact of high temperatures on *Vitis vinifera* cv. Semillon grapevine performance and berry ripening. *Frontiers in Plant Science*, 4, 491.

Hall, A., & Jones, G. V. (2009). Effect of potential atmospheric warming on temperature-based indices describing Australian winegrape growing conditions. *Australian Journal of Grape and Wine Research*, 15(2), 97-119.

Hannah, L., Roehrdanz, P.R., Ikegami, M., Shepard, A.V., Shaw, M.R., Tabor, G., Zhi, L., Marquet, P.A. and Hijmans, R.J. (2013). Climate change, wine, and conservation. *Proceedings of the National Academy of Sciences*, 110(17), 6907-6912.

Hunter, J.J., Volschenk, C.G., Mania, E., Castro, A.V., Booyse, M., Guidoni, S., Pisciotta, A., Di Lorenzo, R., Novello, V. and R. Zorer. (2021). Grapevine row orientation mediated temporal and cumulative microclimatic effects on grape berry temperature and composition. *Agricultural and Forest Meteorology*, 310: 108660.

Jones, G. V. (2013). Winegrape phenology. *In Phenology: An integrative environmental science* (pp. 563-584). Springer, Dordrecht.

Jones, G. V. & Davis, R. E. (2000). Climate influences on grapevine phenology, grape composition, and wine production and quality for Bordeaux, France. *American Journal of Enology and Viticulture*, 51(3), 249-261.

Jones, G. V., White, M. A., Cooper, O. R., & Storchmann, K. (2005). Climate change and global wine quality. *Climatic change*, 73(3), 319-343.

Keller, M. (2010). The science of grapevines. In Anatomy and Physiology, 1st ed.; Keller, M., Ed.; Elsevier Academic Press: London, UK. p. 400.

Luo, H.B., Ma, L., Xi, H.F., Duan, W., Li, S.H., Loescher, W., Wang, J.F. and L.J. Wang. (2011). Photosynthetic responses to heat treatments at different temperatures and following recovery in grapevine (*Vitis amurensis L*.) leaves. *PLoS one:* 23033.

Ma, S., Churkina, G., & Trusilova, K. (2012). Investigating the impact of climate change on crop phenological events in Europe with a phenology model. *International journal of biometeorology*, 56(4), 749-763.

McIntyre, G. N., Lider, L. A., & Ferrari, N. L. (1982). The chronological classification of grapevine phenology. *American Journal of Enology and Viticulture*, 33(2), 80-85.

Moncur, M. W., Rattigan, K., Mackenzie, D. H., & Mc Intyre, G. N. (1989). Base temperatures for budbreak and leaf appearance of grapevines. *American Journal of Enology and Viticulture*, 40(1), 21-26.

Monteverde, C. and F. De Sales. (2020). Impacts of global warming on southern California's winegrape climate suitability. *Advances in Climate Change Research*: 11 279-293.

Morales-Castilla, I., de Cortázar-Atauri, I. G., Cook, B. I., Lacombe, T., Parker, A., van Leeuwen, C., Nicholas, K.A. and Wolkovich, E.M. (2020). Diversity buffers winegrowing regions from climate change losses. *Proceedings of the National Academy of Sciences*, 117: 2864-2869.

Moriondo, M., Jones, G. V., Bois, B., Dibari, C., Ferrise, R., Trombi, G., & Bindi, M. (2013). Projected shifts of wine regions in response to climate change. Climatic change, 119: 825-839.

Mullins, M.G., Bouquet, A., & Williams, L. (1992). Biology of the grapevine. *Cambridge University Press*: Cambridge.

Neethling, E., Petitjean, T., Quénol, H., & Barbeau, G. (2017). Assessing local climate vulnerability and winegrowers' adaptive processes in the context of climate change. *Mitigation and Adaptation Strategies for Global Change*, 22(5), 777-803.

Nicholas, K. A., & Durham, W. H. (2012). Farm-scale adaptation and vulnerability to environmental stresses: Insights from winegrowing in Northern California. *Global Environmental Change*, 22(2), 483-494.

Owens C. (2008) Grapes. In: Hancock J.F. (eds) Temperate Fruit Crop Breeding. Springer, Dordrecht. https://doi.org/10.1007/978-1-4020-6907-9_7

Parker, A., De Cortázar-Atauri, I.G., Chuine, I., Barbeau, G., Bois, B., Boursiquot, J.M., Cahurel, J.Y., Claverie, M., Dufourcq, T., Gény, Le., & Guimberteau, G. (2013). Classification of varieties for their timing of flowering and veraison using a modelling approach: A case study for the grapevine species *Vitis vinifera* L. *Agricultural and Forest Meteorology*, 180, 249-264.

Parker, A. K., De Cortázar-Atauri, I. G., van Leeuwen, C., & Chuine, I. (2011). General phenological model to characterise the timing of flowering and veraison of *Vitis vinifera* L. *Australian Journal of Grape and Wine Research*, 17(2), 206-216.

Parker, A. K., García de Cortázar-Atauri, I. ., Trought, M. C. ., Destrac, A., Agnew, R., Sturman, A., & van Leeuwen, C. (2020). Adaptation to climate change by determining grapevine cultivar differences using temperature-based phenology models: This article is published in cooperation with the XIIIth International Terroir Congress November 17-18 2020, Adelaide, Australia. Guest editors: Cassandra Collins and Roberta De Bei. *OENO One*, *54*(4), 955–974.

Petrie, P. R., & Sadras, V. O. (2008). Advancement of grapevine maturity in Australia between 1993 and 2006: putative causes, magnitude of trends and viticultural consequences. *Australian Journal of Grape and Wine Research*, 14(1), 33-45.

Pipan, P. (2021). Effect of fine scale spatial climate variability on modelled and observed grapevine phenology. Charles Sturt University.

Quénol, H., Marie, G., Barbeau, G., Van Leeuwen, C., Hofmann, M., Foss, C., Irimia, L., Rochard, J., Boulanger, J., Tissot, C., & Miranda, C. (2014). Adaptation of viticulture to climate change: high resolution observations of adaptation scenario for viticulture: the adviclim european project. Bulletin de l'OIV, 87(1001-1002-1003), 395-406.

Rathcke, B., & Lacey, E. P. (1985). Phenological patterns of terrestrial plants. *Annual review of ecology and systematics*, 16(1), 179-214.

R Core Team (2013). R: A language and environment for statistical computing. R Foundation for Statistical Computing, Vienna, Austria. URL http://www.R-project.org/.

Sargolzaei, M., Rustioni, L., Cola, G., Ricciardi, V., Bianco, P.A., Maghradze, D., Failla, O., Quaglino, F., Toffolatti, S.L. and G. De Lorenzis. (2021). Georgian grapevine cultivars: ancient biodiversity for future viticulture. *Frontiers in Plant Science*: 12 94.

Terral, J. F., Tabard, E., Bouby, L., Ivorra, S., Pastor, T., Figueiral, I., Picq, S., Chevance, J.B., Jung, C., Fabre, I., & Tardy, C. (2010). Evolution and history of grapevine (*Vitis vinifera*) under domestication: new morphometric perspectives to understand seed domestication syndrome and reveal origins of ancient European cultivars. *Annals of botany*, 105: 443-455.

Thackeray, S.J., Henrys, P.A., Hemming, D., Bell, J.R., Botham, M.S., Burthe, S., Helaouet, P., Johns, D.G., Jones, I.D., Leech, D.I. and E. Mackay. (2016). Phenological sensitivity to climate across taxa and trophic levels. *Nature*, 535 241-245.

C. van Leeuwen, A. Destrac-Irvine, M. Dubernet, E. Duchêne, M. Gowdy, E. Marguerit, P. Pieri, A. Parker, D.R. LE, N Ollat. (2019). An update on the impact of climate change in viticulture and potential adaptations. *Agronomy*, 9 1-20.

Van Leeuwen, C., Schultz, H. R., de Cortazar-Atauri, I. G., Duchêne, E., Ollat, N., Pieri, P., Bois, B., Goutouly, J.P., Quénol, H., Touzard, J.M., & Malheiro, A. C. (2013). Why climate change will not dramatically decrease viticultural suitability in main wine-producing areas by 2050. *Proceedings of the National Academy of Sciences*, 110(33), E3051-E3052.

Van Leeuwen, C., Trégoat, O., Choné, X., Bois, B., Pernet, D., & Gaudillère, J. P. (2009). Vine water status is a key factor in grape ripening and vintage quality for red Bordeaux wine. How can it be assessed for vineyard management purposes? *OENO One*, 43(3), 121-134.

https://doi.org/10.20870/oeno-one.2009.43.3.798

Vasconcelos, M. C., Greven, M., Winefield, C. S., Trought, M. C., & Raw, V. (2009). The flowering process of *Vitis vinifera*: a review. *American Journal of Enology and Viticulture*, 60(4), 411-434.

https://www.ajevonline.org/content/60/4/411

Vehtari, A., Gelman, A., and Gabry, J. (2017). Practical Bayesian model evaluation using leave-one-out cross-validation and WAIC. *Statistics and Computing*. 27(5), 1413–1432. :10.1007/s11222-016-9696-4.

Venios, X., Korkas, E., Nisiotou, A. and G. Banilas. (2020). Grapevine responses to heat stress and global warming. *Plants*: 1754.

Verdugo-Vásquez, N., Acevedo-Opazo, C., Valdés-Gómez, H., Ingram, B., García de Cortázar-Atauri, I. and B. Tisseyre. (2022). Identification of main factors affecting the within-field spatial variability of grapevine phenology and total soluble solids accumulation: towards the vineyard zoning using auxiliary information. *Precision Agriculture*, 23: 253-277.

Wang, Z.B., Chen, J., Tong, W.J., Xu, C.C. and Chen, F. (2018.) Impacts of climate change and varietal replacement on winter wheat phenology in the North China plain. *International Journal of Plant Production*: 251-263.

Wang, E., & Engel, T. (1998). Simulation of phenological development of wheat crops. *Agricultural systems*, 58(1), 1-24.

Webb, L. B., Whetton, P. H., & Barlow, E. W. R. (2007). Modelled impact of future climate change on the phenology of winegrapes in Australia. *Australian Journal of Grape and Wine Research*, 13(3), 165-175.

L.B. Webb, P.H. Whetton, E.W.R. Barlow. (2011). Observed trends in winegrape maturity in Australia

Global Change Biololgy: 2707-2719

Williams, L. E., & Baeza, P. (2007). Relationships among ambient temperature and vapor pressure deficit and leaf and stem water potentials of fully irrigated, field-grown grapevines. *American journal of enology and viticulture*, 58(2), 173-181.

Winkler, A. J., & Amerine, M. A. (1937). What climate does. *The Wine Review*, 5(6), 9-11.

Wolkovich, E. M., Burge, D. O., Walker, M. A., & Nicholas, K. A. (2017). Phenological diversity provides opportunities for climate change adaptation in winegrapes. *Journal of Ecology*, 105(4), 905-912.

Zapata, D., Salazar-Gutierrez, M., Chaves, B., Keller, M., & Hoogenboom, G. (2017). Predicting key phenological stages for 17 grapevine cultivars (*Vitis vinifera* L.). *American Journal of Enology and Viticulture*, 68(1), 60-72.

Zhongming, Z., Linong, L., Xiaona, Y., Wangqiang, Z. & Wei, L. (2021). AR6 Climate Change 2021: The Physical Science Basis.

Supplementary Table 1: Regression of coefficient of variation for each of the three stages against each other, with R^2

Geographic Region	Budburst vs Flowering	R^2	Budburst vs Veraision	R^2	Flowering vs Veraison	R^2
Balkans	y = -0.111 + 0.483x	0.96	y = 0.126 – 0.169x	0.77	y = 0.0858 – 0.329 x	0.71
Eastern Mediterranean Causasus		NA		NA		NA
Iberian Peninsula	y = -0.0022 + 0.238 x	0.5	y = 0.0812 + 0.0471 x	0.01	y = 0.108 – 0.208x	0.03
Italian Peninsula	y = 0.0166 + 0.183 x	0.56	y = 0.0778 +0.0488x	0.03		<0.01
New World	y = 0.0296 + 0.104x	0.09	y = 0.118 – 0.0836x	0.03		<0.01
Western Central Europe	y = 0.0177 + 0.143 x	0.37	y = 0.105 – 0.0414x	0.01		<0.01

Supplementary Table 2: The general and variety specific intercepts in Growing Degree Days for each stage, as well as the standard distribution between 10-90%.

	Budburst			*Flowering*			*Veraison*		
	mean	0.10	0.90	mean	0.10	0.90	mean	0.10	0.90
General Intercept	199.16	180.39	217.90	836.34	815.84	857.15	1699.46	1441.86	1945.89
Aglicanico	41.43	13.06	70.01	4.33	-17.32	26.04	193.67	120.83	267.24
Albillo Real	-14.14	-45.38	17.20	-26.40	-51.40	-0.62	-221.06	-308.67	-134.60
Aleatico	-21.96	-52.53	8.98	11.03	-12.80	34.26	90.84	13.16	167.47
Alicante Bouschet	-17.41	-46.47	11.58	10.33	-12.78	33.38	-121.76	-183.43	-60.31
Aligote	-24.71	-52.88	4.07	-7.36	-31.28	16.06	27.63	-33.06	87.74
Arneis	-47.75	-77.22	-18.20	1.25	-22.01	25.26	38.71	-23.33	101.09
Auxerrois	-16.46	-44.36	11.54	-5.60	-27.56	16.77	-192.95	-255.22	-129.59
Barbera	-21.60	-50.31	6.94	7.42	-14.89	29.79	22.15	-40.59	84.10
Beauty Seedless	-27.11	-65.75	11.26	6.32	-25.22	37.87	NA	NA	NA
Biancello	-17.67	-45.60	10.91	10.05	-12.79	32.96	41.42	-23.16	106.10
Biancetta trevigniana	-32.78	-61.02	-3.95	-22.98	-44.82	-1.10	37.48	-25.79	100.66
Blush Seedless	19.61	-14.74	54.68	3.25	-23.67	30.50	152.89	65.59	240.90
Bonarda	-7.14	-46.42	32.24	9.83	-21.47	40.76	7.77	-92.51	108.90
Burger	10.65	-16.64	37.94	26.57	4.60	48.41	10.63	-50.96	73.04
Cabernet franc	6.67	-21.23	34.35	-34.33	-57.05	-11.63	104.04	43.03	164.84
Cabernet Sauvignon	36.98	5.09	69.40	-20.63	-46.27	4.33	4.19	-69.19	78.47
Calzin	29.58	0.53	58.69	14.42	-8.55	37.89	-16.05	-81.98	49.78
Canner	3.08	-31.42	37.22	37.50	10.02	64.90	-34.41	-116.32	47.23
Carignane	-12.23	-39.10	15.36	22.66	-0.90	45.63	71.40	8.11	134.36
Carmenere	39.24	11.66	66.87	-55.40	-78.34	-32.28	29.84	-29.23	88.84
Carmine	-6.97	-34.72	20.68	1.58	-20.98	24.69	-47.21	-114.68	18.71
Carnelian	1.40	-27.32	31.29	-1.55	-24.03	21.48	-53.01	-121.53	16.81
Castelao	-22.34	-53.28	7.88	10.89	-14.24	35.58	87.23	11.62	161.63
Centennial Seedless	15.53	-18.92	50.11	-11.11	-38.43	17.00	-273.65	-360.89	-189.66
Centurion	-3.02	-31.59	25.94	-2.75	-26.79	21.30	-21.15	-85.42	41.86
Chardonnay	-59.52	-87.87	-31.32	-6.87	-30.81	16.49	-1.42	-64.17	61.66
Chasselas doree	-28.07	-59.47	2.47	-13.36	-38.55	12.22	-102.71	-179.00	-27.34
Chenin blanc	-52.47	-81.06	-23.50	21.34	-2.52	45.64	33.72	-26.97	92.77
Christmas Rose	1.79	-31.94	34.71	22.73	-3.92	50.21	206.48	119.10	291.67
Ciliegiolo	-12.63	-42.49	16.46	-14.53	-38.01	9.26	-258.61	-337.92	-179.26
Cinsault	5.68	-24.68	35.29	24.59	0.30	48.26	66.27	-7.40	140.47
Coda di Volpe	23.31	-5.49	52.36	1.77	-20.29	24.15	100.12	33.08	166.11

Cornifesto	8.06	-23.12	39.79	-11.97	-37.59	13.22	112.85	37.33	188.19
Cortese	29.02	-10.79	68.75	9.98	-21.13	41.46	-17.77	-120.37	85.44
Cot	-19.68	-47.41	8.19	-4.47	-26.77	18.31	32.28	-30.19	95.77
Counoise	28.45	0.58	55.91	43.14	19.87	66.73	-8.18	-72.91	57.50
Dawn Seedless	17.00	-16.58	51.22	-18.15	-46.83	9.44	126.84	42.32	212.39
Delight	-20.91	-54.94	12.86	-14.28	-42.04	13.67	-200.66	-286.85	-113.49
Dolcetto	11.24	-14.80	37.90	7.66	-14.48	30.25	-59.13	-122.57	2.32
Early Muscat	-16.87	-51.91	18.89	-21.34	-51.09	7.79	-76.00	-176.32	28.29
Emerald Riesling	-6.92	-34.82	20.58	28.93	5.36	52.08	150.61	84.13	214.77
Emerald Seedless	42.09	7.31	76.45	2.15	-25.28	29.05	1.70	-82.31	85.53
Erbaluce	1.49	-28.78	31.33	12.95	-11.38	37.95	4.26	-71.09	79.90
Fiano	-23.32	-51.99	5.55	29.01	6.83	51.26	49.31	-14.13	112.73
Flora	-18.25	-46.09	10.42	16.98	-6.59	40.53	75.16	8.32	143.13
Folle blance	-4.03	-31.72	23.92	8.74	-15.70	33.17	47.43	-15.97	110.77
Forastera	47.46	13.20	81.88	5.00	-23.16	34.10	20.65	-64.84	108.91
Furmint	-8.90	-37.59	19.43	46.04	16.14	75.62	-81.97	-161.41	5.02
Gamay Noir	-7.36	-40.28	25.36	-23.56	-53.42	5.06	-15.56	-94.78	63.60
Gewurztraminer	-34.56	-62.04	-7.44	-5.11	-28.30	17.68	-122.87	-182.92	-61.63
Glennel	7.31	-30.55	45.22	8.59	-20.68	37.60	66.82	-26.30	159.03
Gold	-21.97	-56.20	11.56	42.10	14.04	70.74	-268.84	-349.95	-185.63
Gouveio	-20.27	-48.40	7.75	-7.73	-31.16	15.72	33.39	-33.77	100.03
Graciano	54.32	26.88	81.91	-12.85	-34.80	10.07	98.64	36.55	161.86
Greco di tufo	2.66	-27.90	32.53	2.08	-22.04	27.20	168.23	98.45	239.81
Grenache Noir	6.97	-26.14	39.89	29.32	1.35	57.23	83.55	4.24	163.30
Grignolino	-19.33	-47.52	8.81	33.34	10.45	56.67	1.45	-61.64	65.88
Gruner Veltiner	-18.92	-46.80	10.01	-1.45	-25.24	22.95	-125.45	-201.24	-46.76
Helena	-0.57	-28.40	27.36	-21.55	-44.22	0.97	-112.61	-181.63	-46.46
Juan Garcia	33.53	3.91	62.76	-34.44	-58.46	-10.84	-0.01	-71.22	73.77
July Muscat	-26.04	-54.82	3.10	0.93	-22.93	24.82	22.60	-47.87	95.31
Macabeo	7.34	-20.06	35.54	34.05	11.80	56.51	151.97	90.50	211.60
Malvasia bianca	6.42	-23.53	37.39	19.54	-5.31	44.75	-52.94	-126.27	19.58
Mammolo	19.10	-9.26	47.11	6.41	-15.21	28.71	259.50	197.18	322.23
Marsanne	0.83	-26.82	28.36	-1.69	-23.76	20.07	-51.42	-114.55	13.52
Melon	-34.43	-62.60	-6.42	-5.78	-29.87	18.50	-0.09	-62.55	62.09
Merlot	-0.27	-28.14	26.73	-15.54	-37.02	6.09	-64.19	-126.24	-0.30
Montepulciano	72.98	40.49	105.45	-4.99	-30.48	20.55	44.94	-30.04	118.86
Morrastel	37.49	9.69	64.78	-14.50	-35.73	7.26	62.58	2.72	122.97
Mourvedre	56.71	33.18	79.96	40.51	21.42	60.25	-46.91	-99.44	4.73
Muscadelle du Bordelais	6.41	-22.43	35.88	1.87	-20.29	24.21	12.51	-50.29	74.50
Muscat Ottonel	-4.45	-33.21	24.43	-10.10	-31.78	12.35	-267.76	-332.55	-204.60
Muscato bianco	-15.76	-45.96	13.74	-31.33	-59.95	-2.47	-75.66	-157.44	8.75

Nebbiolo	-28.04	-55.87	-0.16	-32.49	-55.16	-9.65	109.10	45.26	175.24
Negrette	4.42	-22.68	32.15	-0.08	-22.43	22.17	26.06	-35.41	87.09
Negro Amaro	35.87	10.46	61.15	57.71	37.78	78.55	-130.43	-186.42	-73.92
Niabell	44.78	14.03	75.44	-73.24	-98.52	-48.28	291.64	216.35	370.29
Palomino	5.32	-24.70	34.82	27.44	3.43	52.36	31.63	-43.87	105.79
Parellada	2.13	-28.09	31.79	50.17	25.61	74.83	200.13	126.44	273.54
Pedro Ximenez	-16.34	-45.24	12.80	33.60	10.10	56.69	24.21	-43.69	95.28
Periquita	-25.02	-56.90	5.85	11.92	-13.02	37.20	49.60	-25.42	125.57
Perlette	-17.77	-56.76	20.77	-8.81	-39.61	21.87	-126.38	-229.04	-20.20
Petit Manseng	-26.87	-55.44	1.68	-14.66	-38.86	8.99	140.93	79.57	202.62
Petit Verdot	16.69	-11.48	44.19	-27.23	-49.98	-4.78	180.88	116.56	245.20
Picolit	-16.10	-44.64	11.05	-14.28	-36.54	8.17	121.48	56.49	184.95
Pinot blanc	-27.95	-57.82	1.72	-17.49	-43.47	7.93	129.65	60.94	197.08
Pinot gris	-26.28	-54.92	1.89	-47.08	-72.40	-21.82	-37.59	-99.81	23.75
Pinot Meunier	-7.78	-35.19	19.55	-25.39	-49.72	-1.09	-67.08	-130.41	-4.66
Pinot noir	-27.21	-61.14	6.27	-13.38	-41.62	14.89	-87.96	-165.98	-9.13
Pinotage	-17.93	-48.04	12.17	-20.33	-46.20	5.47	-109.90	-191.91	-24.21
Queen	-4.05	-38.54	30.22	-5.70	-33.36	21.96	129.83	45.40	217.03
Refosco	-27.38	-55.23	0.79	-18.41	-40.81	3.78	69.41	6.39	132.95
Ribolla gialla	-15.66	-46.41	15.34	10.00	-13.85	34.06	-93.45	-169.56	-14.44
Riesling	1.24	-33.62	35.27	-10.63	-37.55	15.67	46.91	-32.69	125.90
Riesling Italico	-22.76	-53.78	8.35	2.32	-22.17	27.18	-39.21	-111.64	32.52
Rkatsiteli	-1.32	-30.54	28.27	16.88	-13.25	45.91	54.18	-34.34	139.43
Rondinella	2.66	-37.47	41.39	-6.09	-37.42	24.78	138.37	34.88	239.84
Rotgipfler	8.92	-20.09	38.57	-20.99	-46.01	3.61	0.21	-75.83	78.87
Roussanne	48.55	20.45	77.63	11.97	-9.94	34.00	5.52	-59.25	68.94
Rubired	-7.37	-34.41	20.39	-35.79	-59.09	-13.47	193.68	126.86	259.53
Ruby Cabernet	11.72	-18.75	42.31	16.08	-9.52	41.88	37.21	-41.72	111.73
Ruby Seedless	13.86	-21.20	48.76	16.61	-10.66	44.25	170.96	86.20	254.69
Sagrantino	27.87	0.04	55.94	22.26	-0.66	45.37	-63.11	-125.65	1.33
Sangiovese	-29.18	-53.59	-4.13	-19.77	-38.87	-0.37	-103.80	-156.68	-48.81
Sauvignon blanc	27.55	-1.33	56.86	6.99	-13.90	28.36	-149.06	-209.45	-86.05
Sauvignon gris	4.13	-24.28	32.15	-11.71	-33.88	10.18	-97.42	-158.89	-36.35
Sauvignon vert	11.67	-16.70	40.23	0.18	-22.70	23.06	48.28	-13.43	110.91
Scarlett	5.43	-24.80	34.98	-11.29	-37.66	15.26	-138.35	-221.61	-56.74
Schiopettino	3.49	-24.42	31.21	14.79	-8.15	38.11	46.39	-16.56	108.07
Siegerrebe	-42.00	-70.96	-12.60	6.44	-18.25	31.02	-205.80	-308.33	-103.44
Souzao	105.62	76.11	136.21	-23.83	-47.47	0.20	9.25	-60.85	77.93
Suavis	-23.16	-52.04	5.71	-33.38	-58.33	-8.47	34.66	-44.21	112.44
Sylvaner	-11.87	-45.37	21.32	-5.48	-32.57	22.01	-112.34	-192.66	-31.79
Symphony	-1.36	-29.23	26.97	-3.48	-26.53	19.50	37.98	-29.16	104.01

Syrah	-6.62	-34.52	21.44	58.53	36.37	80.97	-182.46	-242.62	-121.80
Szagos feher	4.06	-25.57	34.51	10.93	-17.34	39.51	-30.50	-111.75	53.65
Tannat	-1.09	-28.12	25.68	18.12	-3.94	40.74	-15.82	-78.32	47.34
Tempranillo	9.12	-19.20	37.95	28.65	5.24	51.93	-178.67	-249.58	-106.10
Teroldego	1.72	-34.24	37.16	2.01	-25.44	29.48	39.87	-38.26	116.93
Thompson Seedless	27.47	-3.85	58.40	39.81	10.66	69.06	17.54	-72.76	108.67
Tinta Amarella	-1.03	-29.32	26.65	-7.64	-30.99	14.83	-61.93	-128.73	3.34
Tinta Barroca	-1.62	-35.06	31.56	-7.11	-35.00	19.64	-130.00	-212.31	-48.34
Tinta Cao	-27.43	-55.91	0.62	-27.68	-51.17	-4.82	150.56	83.75	218.59
Tinta Carvalha	8.48	-20.09	37.18	-19.69	-42.09	2.85	-102.90	-172.16	-34.21
Tinta Francisca	23.64	-5.24	52.40	58.37	34.07	82.65	-21.76	-87.27	44.04
Tinta Madeira	-39.44	-68.87	-9.63	10.30	-12.60	33.22	-117.37	-185.25	-49.01
Tocai Friulano	34.97	7.00	63.58	-2.18	-24.04	19.03	58.02	-5.77	121.32
Touriga Nacional	-1.92	-30.63	26.44	-15.13	-37.83	8.07	23.91	-44.40	91.81
Trebbiano	137.07	110.47	163.61	-26.01	-45.45	-6.47	-78.36	-135.60	-23.41
Trousseau gris	-33.54	-61.89	-4.70	3.94	-19.22	27.14	58.83	-2.87	119.98
Valdepenas	42.03	6.89	77.87	-16.46	-46.47	12.86	-144.07	-235.98	-48.56
Verdejo	-28.37	-57.75	0.92	-12.32	-35.46	11.05	108.53	36.65	181.47
Verdelho	-8.05	-36.39	20.38	-33.05	-55.91	-9.35	82.79	15.35	150.44
Verdello	2.06	-25.60	30.87	-30.61	-52.58	-8.34	-52.49	-115.21	11.10
Vespolina	-25.25	-55.35	4.18	-13.68	-36.73	9.11	80.04	17.39	143.38
Viognier	-20.81	-47.87	6.55	-7.52	-28.87	13.74	-73.39	-135.86	-10.72
Zinfandel/Primitivo	-6.08	-33.87	21.61	-6.54	-29.10	15.53	-113.23	-177.23	-48.35

Chapter 3

VvEPFL9-1 knock-out reduces stomatal density and enhances water use efficiency in grapevine

Molly Clemens[1,2,3], Michele Faralli[1], Jorge Lagreze[1] , Luana Bontempo[1] , Claudio Varotto[1] , Mickael Malnoy[1] , Walter Oechel[2,4] , Annapaola Rizzoli[1] , Lorenza Dalla Costa[1]

1 Research and Innovation Centre, Fondazione Edmund Mach, via E. Mach 1, 38098 San Michele all'Adige, Italia

2 Global Change Research Group, San Diego State University, San Diego, CA 91925, USA

3 Department of Viticulture and Enology, University of California, Davis, CA 91925, USA

4 Department of Geography, University of Exeter, Exeter, EX4 4RJ UK

Journal: Frontiers in Plant Science

Abstract

Epidermal Patterning Factor Like 9 (EPFL9), also known as STOMAGEN, is a cysteine-rich peptide that induces stomata formation in vascular plants, acting antagonistically to other epidermal patterning factors (EPF1, EPF2). In grapevine there are two EPFL9 genes, EPFL9-1 and EPFL9-2 sharing 82% identity at protein level in the mature functional C-terminal domain. In this study, CRISPR/Cas9 system was applied to functionally characterize VvEPFL9-1 in 'Sugraone', a highly transformable genotype. A set of plants, regenerated after gene transfer in embryogenic calli via Agrobacterium tumefaciens, were selected for evaluation. For many lines, the editing profile in the target site displayed a range of mutations mainly causing frameshift in the coding sequence or affecting the second cysteine residue. The analysis of stomata density revealed that in edited plants the number of stomata was significantly reduced compared to control, demonstrating for the first time the role of EPFL9 in a perennial fruit crop. Two edited lines were then assessed for growth, photosynthesis, stomatal conductance, and water use

efficiency in the greenhouse at both controlled ambient conditions and in a natural dry-down experiment. Intrinsic water-use efficiency was significantly improved in edited lines compared to control, indicating possible advantages in reducing stomatal density under future environmental drier scenarios. Our results show the potential of manipulating stomatal density for optimizing grapevine adaptation under changing climate conditions.

Contribution to the field

In this study, we present our findings about the function of a cysteine-rich peptide belonging to the Epidermal Patterning Factor family in grapevine, a perennial fruit crop of high economic and cultural value. In grapevine, we found there are two genes homologous to AtEPF9 and demonstrated that the knock-out of EPFL9-1 reduces stomatal density and plant transpiration and improve water use efficiency. CRISPR/Cas9 system, an outstanding tool allowing to precisely modify genes has been applied to functionally characterize this gene. Predicted climate changes may strongly affect the quality and yield of crops in the near future. The investigation of the genetic mechanisms controlling traits involved in plant adaptability to global warming such as stomatal density, is of primary importance. The role of EPFL9 factor as a positive regulator of stomata formation is well known in Arabidopsis and cereals but in perennial woody crops no information has been collected on its function. In this study, we tried to shed light, for the first time, on the genetic basis of the trait related to stomatal density in a perennial fruit plant.

Introduction

Drought is a threat to the quality and yield of grapevine in the world's important wine grape growing regions (Mosedale et al., 2016; Van Leeuwen and Destrac-Irvine, 2017, Van Leeuwen et al., 2019). These regions are expected to have decreased precipitation with associated risks of developing soil water deficit in coming years (IPCC, 2014; Sherwood and Fu, 2014; Scholasch and Rienth, 2019). One adaptation strategy seen in plants to tolerate water limitation involves stomatal regulation of water loss (Hunt et al., 2010; Hughes et al., 2017; Caine et al., 2019, Bertolino et al., 2019; Dayer et al., 2020; Gambetta et al., 2020). Stomata are pores mainly located in the leaf epidermis. The opening of these pores controls leaf gas exchange (CO_2 uptake for photosynthesis and water loss via transpiration) and is regulated by changes in turgor pressure in the guard cells surrounding these pores. The two guard cells respond to a range of environmental signals, often in conflict with each other, and sometimes rapidly changing (e.g. humidity, CO_2 concentration, light). In drought-stressed grapevine, stomatal closure is triggered by hydraulic signals and maintained by abscisic acid following re-watering (Tombesi et al., 2015). Genotypic variation for stomatal sensitivity to reduced water availability has been shown to exist in grapevine (Schultz, 2003; Soar et al., 2006; Bota et al., 2016; Villalobos-González et al., 2019).

Stomatal density and distribution in the epidermal tissue also plays a critical role in determining transpiration rate per unit of leaf area (Hunt et al., 2010). Previous work focusing on natural variation for stomatal anatomical features provided evidence of a close negative relationship between plant water-use efficiency and stomatal density (Faralli et al., 2019; Bertolino et al., 2019). Stomatal density and distribution are under the control of small cysteine-rich peptides called epidermal patterning factors (EPFs) highly conserved in a wide range of

higher plants (Lu et al., 2019). According to extensive studies carried out in Arabidopsis (Doheny-Adams et al., 2012; Franks et al., 2015; Hepworth et al., 2015; Lee et al., 2015) three members of this family play a key role in the formation of stomata: EPF1, EPF2 and EPFL9. EPF2 and EPF1 are expressed in the epidermis, in the earlier and later stages of leaf development, respectively. EPF2 inhibits the formation of cells considered the precursors of stomata guard cells, while EPF1 inhibits the subsequent differentiation of these same precursors and induces asymmetric cell division (Hara et al., 2009).

Epidermal Patterning Factor Like 9 (EPFL9), also known as STOMAGEN, plays an antagonist role with respect to EPF1 and EPF2 as it induces stomata formation (Kondo et al., 2010). EPF-peptides interact with two transmembrane receptors of epidermal cells, ERECTA and Too Many Mouths (TMM). While EPF1 and EPF2 activate the receptor complex which in turn induces a MAPKs (Mitogen-Activated Protein Kinases) cascade (Morales-Navarro et al., 2018; Zoulias et al., 2018) leading to the destabilization of important transcription factors involved in the formation of stomata (SPEECHLESS, MUTE, FAMA) (Pillitteri et al., 2007; Chen et al., 2020), STOMAGEN inactivates it. STOMAGEN is the only known positive regulator of stomata produced in mesophyll, and was confirmed to act independently of EPF1 and EPF2 (Hunt et al., 2010; Kondo et al., 2010; Sugano et al., 2010; Ohki et al., 2011). Its activity is antagonized by that of EPF2, however, it is not well understood if the antagonistic action is due to the sharing of an identical binding site in the common receptor or to other mechanisms (Ohki et al 2011). An evolutionary model suggests that EPFL9 may derive from the duplication of EPF1/2 with a subsequent alteration in the function (Shimada et al., 2011). This is confirmed by the fact that EPF1/2 are more widespread in higher plants compared to EPFL9 (Lu et al., 2019). Moreover, it is known that cysteine-rich peptides (CRPs) are encoded by genes

usually present in clusters, located in defined chromosomal regions, probably originating from gene duplication (Marshall et al., 2011). Despite the different amino acid composition among the CRP different sub-classes and across species, the members of CRPs have in common a small size, a conserved N-terminal region that include an apoplast secretion signal and a functional C-terminal domain containing cysteine residues (Marshall et al., 2011).

Several functional genomics studies, based on the ectopic expression or silencing of EPF1, EPF2, or EPFL9, have recently demonstrated a highly conserved functional paradigm in Arabidopsis and cereals. In barley, Hughes et al. (2017) proved that *HvEPF1* overexpression limits stomatal development. In a hexaploid bread wheat, Dunn et al. (2019) decreased stomatal density (SD) via the overexpression of *TaEPF1* and *TaEPF2* orthologues and demonstrated improvements in water-use efficiency without affecting yield when SD reduction was moderate. Similarly, in rice Caine et al. (2019) and Mohammed et al. (2019) elucidated the function of *OsEPF1* adopting an over-expression approach. Adding to the studies on rice, Lu et al. (2019) confirmed the role of *OsEPF1*, *OsEPF2* and *OsEPF9* by a dual strategy, both over-expression and down-regulation via RNA interference. Yin and colleagues (2017) were the first to apply the genome editing technology in rice to disrupt *OsEPFL9*.

Gene editing via the clustered regularly interspaced short palindromic repeats (CRISPR)/CRISPR-associated protein 9 (Cas9) (Jinek et al., 2012) is to date the most powerful tool for functional genomics studies in plants (Liu et al., 2016). CRISPR/Cas9 system can efficiently produce nucleotide mutations into precise positions in the genome through the combined action of a specific guide RNA and the Cas9 nuclease which cleaves the DNA eliciting the non-homologous end-joining (NHEJ) pathway for DNA repair (Podevin et al., 2013). NHEJ may produce knock-out (KO) mutants with random insertion or deletion (indels) of

variable lengths at the Cas9 cleavage site causing frameshift mutations or loss of amino acids in protein-coding sequences. These KO mutants are perfect systems to prove the function of a candidate gene (Jain, 2015). This technology is steadily progressing (Hess et al., 2017; Anzalone et al., 2019) and, coupled with the advancements of *in-vitro* culture practices, represents a knowledge-based strategy for the genetic improvements of cultivated plants, with relevant advantages compared to traditional breeding (Chen et al., 2019). In grapevine, CRISPR/Cas9 technology has been successfully applied to evaluate the function of genes involved in susceptibility or tolerance to diseases, mainly caused by fungal pathogens (Malnoy et al. 2016, Giacomelli et al. 2019, Wan et al. 2020, Li et al. 2020, Chen et al. 2021, Scintilla et al. 2021) or to enhance tolerance to cold stress (Wang et al. 2021).

In this study, we inactivated VvEPFL9-1 in a grapevine table grape variety, 'Sugraone', adopting a genome editing approach based on CRISPR/Cas9 technology. Different edited lines with a significant reduction in stomatal density were produced and analyzed to investigate how reducing stomatal density affects grapevine physiological performance under different environmental conditions.

Results

Identification of *AtEPFL9* orthologous genes in grapevine

Two *VvEPFL9* gene variants (hereinafter *VvEPFL9*-1 and *VvEPFL9*-2) were found in contigs of publicly available genomes of different *Vitis vinifera* varieties and of some other species within the same genus (*Vitis sylvestris, Vitis arizonica, Vitis riparia*) (Supplemental Table S1). In the last annotation of the PN40024 grapevine reference genome (PN40024.v4.1, https://integrape.eu/resources/genes-genomes/genome-accessions/, genome assembly version

12X.v4) VvEPFL9-1 (Vitvi05g01370) was localized on chromosome 5 (position 20461188–20461813) while VvEPFL9-2 (Vitvi07g04390) on chromosome 7 (position 17537397–17536466). Interestingly, before the new version of reference genome and related annotation was made publicly available (November 2021, INTEGRAPE Workshop, XIth International Symposium on grapevine physiology and biotechnology 31 Oct-5 Nov 2021, Stellenbosch, South Africa) only VvEPFL9-1 was localized on the genome while the position of VvEPFL9-2 was not assigned (VCost.v3 annotation). According to gene prediction, *VvEPFL9-1*/*-2* have a length of about 330 bp and are composed of three exons encoding for: an N-terminal region with a secretion signal for the apoplast (i.e. first 27 amino acid according to SignalP-5.0 software, Almagro Armenteros et al., 2019, http://www.cbs.dtu.dk/services/SignalP/), a central region likely involved in the processing of the mature peptide and a C-terminal domain of 45 amino acids containing 6 conserved cysteines, that is the functional peptide. A comparison of genomic DNA extracted from a panel of genotypes (i.e. 'Pinot Noir PN40024', 'Riparia Glorie de Montpellier', 'Pinot Noir clone Entav 115', 'Cabernet Sauvignon', 'Chardonnay', 'Merlot', 'Sugraone', 'Syrah' and 'Touriga National'), confirmed the presence of both variants in all the analyzed samples with a very high conservation among genotypes (Supplemental Table S2).

Figure 4

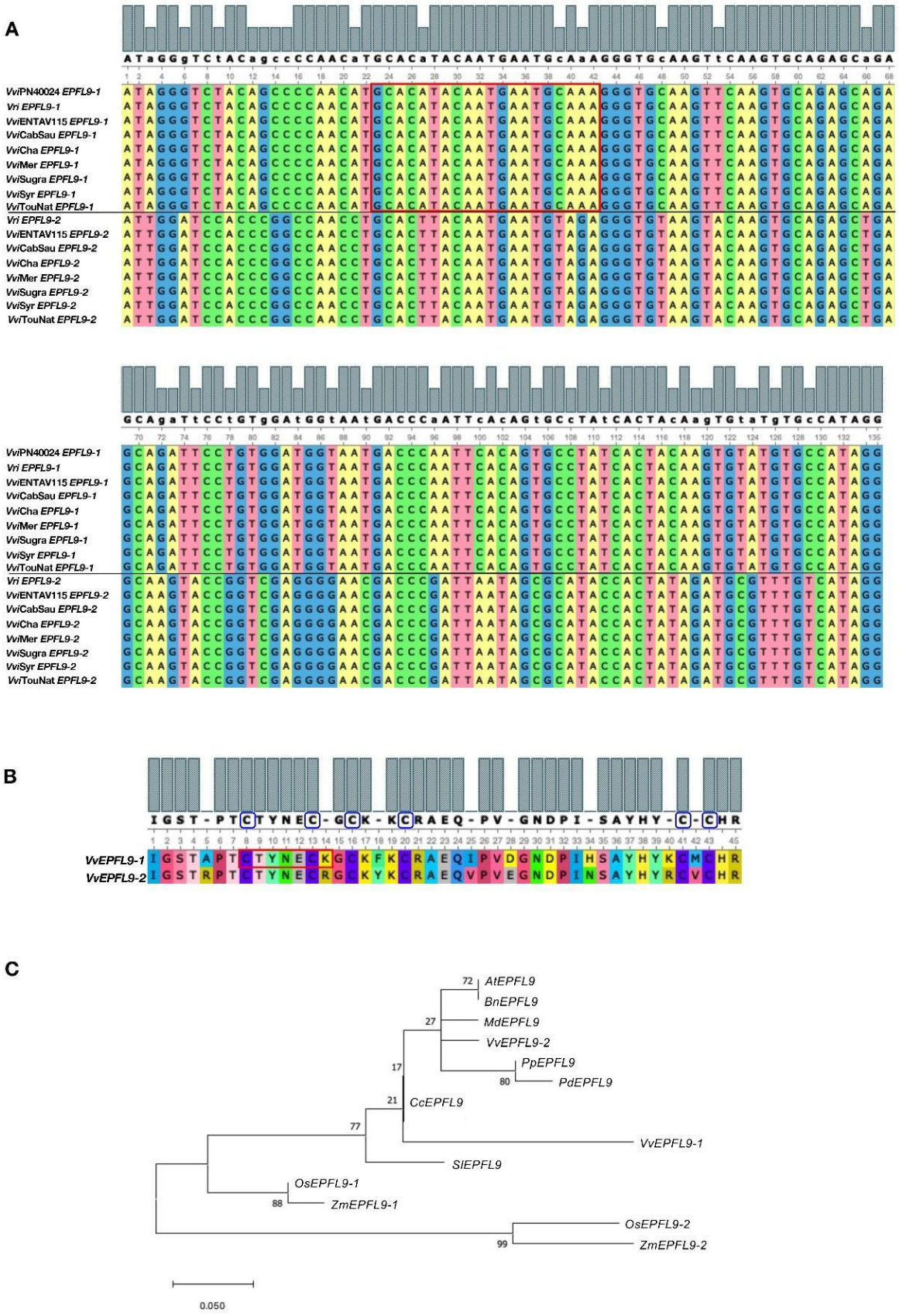
A
VviPN40024 EPFL9-1
Vri EPFL9-1
VviENTAV115 EPFL9-1
VviCabSau EPFL9-1
VviCha EPFL9-1
VviMer EPFL9-1
VviSugra EPFL9-1
VviSyr EPFL9-1
VviTouNat EPFL9-1
Vri EPFL9-2
VviENTAV115 EPFL9-2
VviCabSau EPFL9-2
VviCha EPFL9-2
VviMer EPFL9-2
VviSugra EPFL9-2
VviSyr EPFL9-2
VviTouNat EPFL9-2
B
VvEPFL9-1
VvEPFL9-2
C
AtEPFL9
BnEPFL9
MdEPFL9
VvEPFL9-2
PpEPFL9
PdEPFL9
CcEPFL9
VvEPFL9-1
SlEPFL9
OsEPFL9-1
ZmEPFL9-1
OsEPFL9-2
ZmEPFL9-2
0.050

Figure 4. Analysis of *VvEPFL9* paralogs. A, Alignment of the nucleotide sequence encoding for the C-terminal domain (135 bp) obtained by Sanger sequencing of PCR fragments amplified on genomic DNA with primers VvEPFL9-1_fw; VvEPFL9-1_rv and VvEPFL9-2_fw; VvEPFL9-2_rv (see primer list in Supplemental Table S5). Genomic DNA was extracted from leaves of 'Pinot Noir PN40024', *Vitis riparia* 'Riparia Glorie de Montpellier', 'Pinot Noir clone Entav 115', 'Cabernet Sauvignon', 'Chardonnay', 'Merlot', 'Sugraone', 'Syrah', 'Touriga National'. The red rectangle indicates the 20bp-target site recognized by the sgRNA/Cas9 complex. B, Alignment of the C-terminal protein domain of *VvEPFL9-1* and *VvEPFL9-2*, translated from the 135 bp nucleotide sequences shown in A. Cysteine residues are circled in blue. The red rectangle indicates the peptide region corresponding to the target site. C, Phylogenetic tree of the Arabidopsis *AtEPF9* mature peptide and its orthologs from some dicotyledonous (*Brassica napus*, *Malus x domestica*, *Vitis vinifera*, *Prunus persica*, *Prunus domestica*, *Prunus dulcis*, *Citrus clementina*, *Actinidia chinensis*, *Solanum lycopersicum*) and monocotyledonous (*Orytia sativa*, *Zea mays*) plant species. The alignments were generated with MUSCLE (MEGA X) and visualized with Unipro UGENE (http://ugene.net/faq.html, ADDIN CSL_CITATION {"citationItems":[{"id":"ITEM-1","itemData":{"DOI":"10.1093/bioinformatics/bts091","ISSN":"13674803","PMID":"2236

In all the genotypes no SNPs were detected between the two alleles of both isoforms in the region coding for the C-terminal domain, except in Cabernet Sauvignon where an allelic polymorphism in position 25 was detected in *VvEPFL9-1*, which leads to two different amino acids after the first cysteine of the array (serine or threonine, both polar uncharged). Considering only the region encoding for the C-terminal domain (135 bp), the identity between the two variants was 74%, with a large part of polymorphism leading to synonymous codons (Fig. 4A). At the protein level, the alignment of the C-terminal domains encoded by the two variants showed an identity of 82%, with 8 out of 45 different amino acids (Fig. 4B). In five positions (14, 25, 28, 40, 42) substitutions are conservative, i.e. the pair of amino acids belong to the same class, while in the remaining three positions (5, 18 and 34) the substitutions are non-conservative. A comparison with *AtEPFL9* mature peptide revealed that the identity between

VvEPF9-1 and *AtEPFL9* is 82% while the identity between *VvEPF9-2* and *AtEPFL9* is 95% (Supplemental Fig. S1). Moreover, the relationship of *VvEPFL9-1/-2* with the orthologues of some di- and monocotyledonous plant species including some perennial fruit trees (retrieved from Ensembl Plants genomic database, http://plants.ensembl.org/index.html), is shown in Fig. 4C.

The knock-out of *VvEPF9-1* reduces stomatal density in grapevine

A highly transformable genotype of *Vitis vinifera*, 'Sugraone' was used for gene transfer of the CRISPR/Cas9 machinery in order to obtain edited plants knocked-out for the *VvEPF9-1* gene (Fig. 5). The sgRNA was designed to target a region of 20 nucleotides in the third exon, spanning across "TGC" triplets coding for the first and the second cysteine of the functional C-terminal domain (Fig. 4A, 4B and Table S3). In particular, the cleavage operated by Cas9 was expected to affect the "TCG" triplet coding for the second cysteine, this being located 3 nucleotides upstream of the PAM site (i.e. GGG) (Fig. 4A). The corresponding region of *VvEPF9-2* has 3 mismatches compared with the target site on *VvEPF9-1*, in positions 6, 18 and 20, the last two in the seed region close to the PAM site (Fig. 4A). Several shoots were regenerated from somatic embryos after 7-10 months from Agrobacterium tumefaciens co-culture (Fig. 12), and nine of them were selected for molecular characterization. The Cas9 integration copy number varied in the transgenic lines, ranging from 1 integration copy for line *S-epfl9KO7* to 5 integration copies for line *S-epfl9KO1*, with the majority of lines showing values close to two copies (Fig. 5A). The analysis of the genomic "on-target" site in *VvEPF9-1* proved that all lines were edited, some completely while others showed a degree of wild-type

target sequence, indicated as WT (Fig. 5B; Table S3). In general, the editing profile was highly heterogeneous, with a composite mutation profile for many lines (e.g. *S-epfl9KO2*, *S-epfl9KO5*, *S-epfl9KO6*, *S-epfl9KO7*, *S-epfl9KO9*), including deletions of increasing size (from 1 bp to more than 7 bp), insertions of 1 or 2 bp, and single base substitutions. The most frequent kind of mutations were deletions of 4 or 5 bp (Fig. 5B). The resulting mutations in the protein sequence were frameshift mutations (FS) with or without the formation of premature stop codons (SC), or non-frameshift mutations with loss of the second cysteine due to deletion of 3 or 6 bp or to a single base substitution (Fig. 5C).

Figure 5

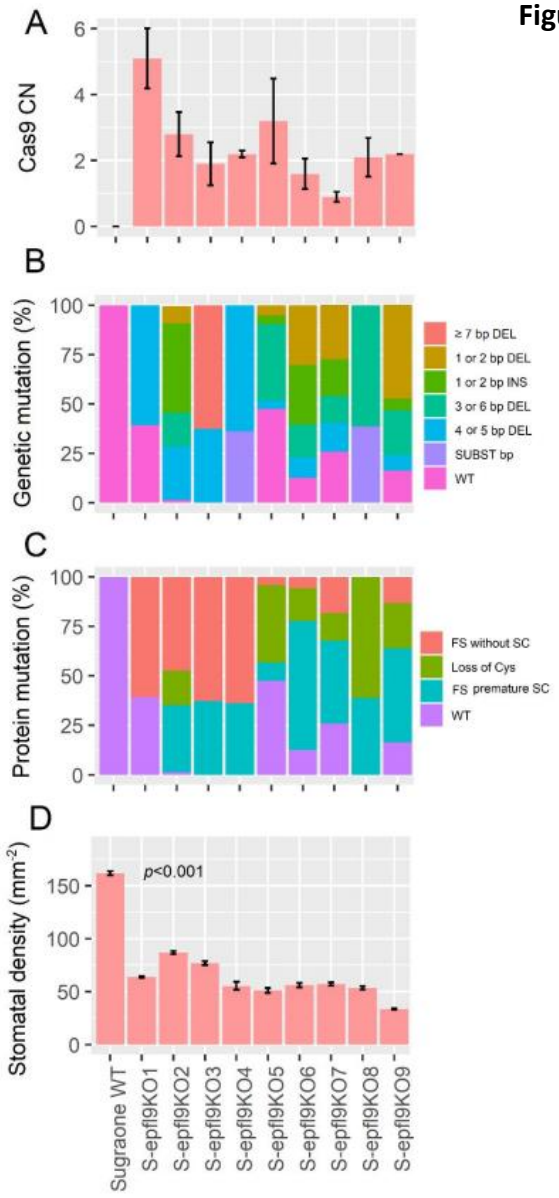

Figure 5. Analysis of stomatal anatomical features confirmed the significant differences for stomatal density and pore length between the selected epfl9-1 knock-out mutants and WT (Fig. 4). S-epfl9KO1 had an average SD of 65 stomata mm-2 while SD for S-epfl9KO2 was 95 stomata mm-2, both significantly lower values than that of Sugraone WT (160 stomata mm-2) respectively by 60% and 40%. Conversely, pore length was significantly higher in S-epfl9KO1 and S-epfl9KO2 than 'Sugraone' WT, by up to 30%.

The analysis of stomatal density in leaves of greenhouse-cultivated plants showed a significant reduction in stomata number in transgenic lines compared to WT (Fig. 6). This reduction was significant even for the lines maintaining a remarkable rate of non-mutated *VvEPF9-1* (i.e. *S-epfl9KO1*, *S-epfl9KO5*, *S-epfl9KO7*) and for lines that went through the loss of the second cysteine of the 6-Cys-array, highlighting the crucial role of such residue (i.e. *S-epfl9KO5* and *S-epfl9KO8*). The editing in the potential "off-target" site in *VvEPFL9-2* was assessed and no mutations were found in all the transgenic lines. This proved that 3 mismatches with respect to the sgRNA, 2 of which close to the PAM site, were enough to avoid Cas9 unspecific cleavage at this site (Fig. S2).

Analysis of stomatal anatomical features confirmed the significant differences for stomatal density and pore length between the selected *epfl9-1* knock-out mutants and WT (Fig. 6). *S-epfl9KO1* had an average SD of 65 stomata mm^{-2} while SD for *S-epfl9KO2* was 95 stomata mm^{-2}, both significantly lower values than that of Sugraone WT (160 stomata mm^{-2}) respectively by 60% and 40%. Conversely, pore length was significantly higher in *S-epfl9KO1* and *S-epfl9KO2* than 'Sugraone' WT, by up to 30%.

Figure 6

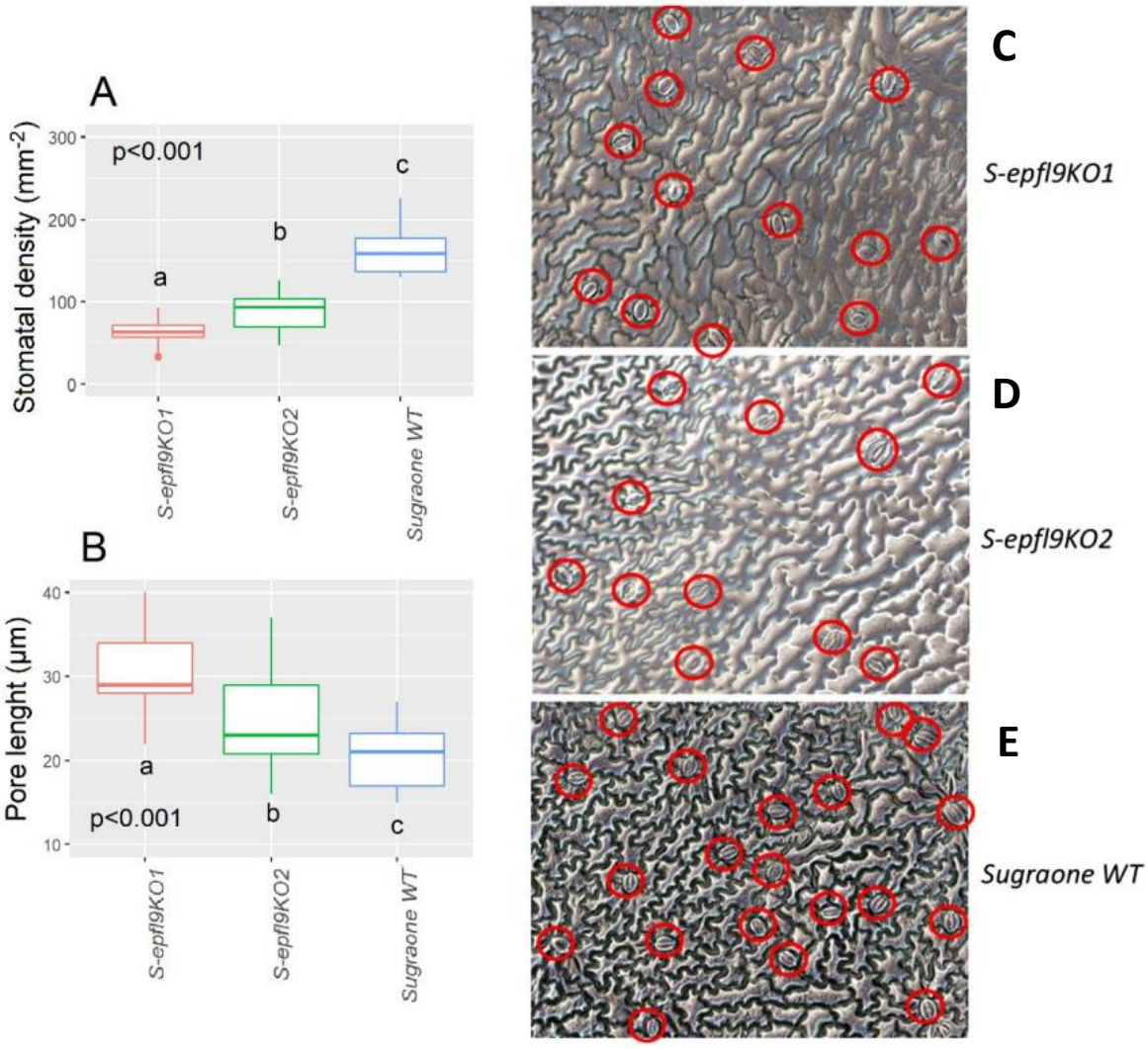

Figure 6. A Stomatal density for S-epfl9KO1, S-epfl9KO2 and Sugraone WT. B Pore length for S-epfl9KO1, S-epfl9KO2 and Sugraone WT. Whiskers indicate the ranges of the minimum and maximum values. Data were analysed with one-way ANOVA (n=6-9). Different letters indicate significantly different values according to Fisher's test. C, D, E Images of nail polish printing of leaf tissue respectively from S-epfl9KO1, S-epfl9KO2 and Sugraone WT.

The knock-out of *VvEPF9-1* enhances plant water use efficiency under optimal growth conditions

A/C_i response curves (net CO_2 assimilation rate, A, versus calculated substomatal CO_2 concentration, C_i) were carried out under optimal environmental conditions and saturating light intensity assessed via light curves (Fig. S3). There were no significant differences for maximum rate of Rubisco-mediated carboxylation (V_{cmax}) between edited lines and WT control ($p>0.05$, Fig. 7A). Similarly, maximum electron transport rate for RuBP regeneration (J_{max}) did not vary between edited lines and WT control ($p>0.05$, Fig. 7B). On the contrary, significant reductions in CO_2 assimilation rate at saturating light (A_{sat}) were detected for *S-epfl9KO1* and, in particular, *S-epfl9KO2* when compared to WT and up to 50% ($p=0.007$, Fig. 7C). *S-epfl9KO1* and *S-epfl9KO2* had significantly lower conductance (g_s) than WT ($p<0.001$) with *S-epfl9KO2* showing the lowest values (0.030 mol m^{-2} s^{-1} on average, Fig. 7D). This led to a significantly higher intrinsic water-use efficiency $_iWUE$ for *S-epfl9KO2* than 'Sugraone' WT ($p=0.024$, Fig. 9E). Accordingly, carbon isotope discrimination ($\delta^{13}C$) analysis detected for *S-epfl9KO2* significant less negative $\delta^{13}C$ values compared to Sugraone WT ($p=0.046$), indicating a higher $_iWUE$ (Fig. 7F). Gravimetric assessments of transpired water normalized for leaf area highlighted significant differences in cumulative transpiration between edited and WT lines. In general, both *S-epfl9KO1* and *S-epfl9KO2* used less water throughout a 14-day experimental period, by up to 21%, compared to 'Sugraone' WT (Fig. 7G).

Figure 7 (next page). Trait assessment under well-watered (WW) conditions. Leaf gas-exchange for S-epfl9KO1, S-epfl9KO2 and 'Sugraone' WT (A, B, C, D, E) and R-epfl9KO1 and 'Riparia' WT (F, G, H, I, J). A and F, Maximum velocity of Rubisco carboxylation (V_{cmax}). B and G, maximum electron transport rate for RuBP regeneration (J_{max}) estimated with A/C_i curves and following curve fitting ADDIN CSL_CITATION {"citationItems":[{"id":"ITEM-1","itemData":{"DOI":"10.1371/journal.pone.0143346","ISSN":"19326203","PMID":"26581080","abstract":"Here I present the R package 'plantecophys', a toolkit to analyse and model leaf gas exchange data. Measurements of leaf photosynthesis and transpiration are routinely collected with portable gas exchange instruments, and analysed with a few key models. These models include the Farquhar-von Caemmerer-Berry (FvCB) model of leaf photosynthesis, the Ball-Berry models of stomatal conductance, and the coupled leaf gas exchange model which combines the supply and demand functions for CO2 in the leaf. The 'plantecophys' R package includes functions for fitting these models to measurements, as well as simulating from the fitted models to aid in interpreting experimental data. Here I describe the functionality and implementation of the new package, and give some examples of its use. I briefly describe functions for fitting the FvCB model of photosynthesis to measurements of photosynthesis-CO2 response curves ('A-Ci curves'), fitting Ball-Berry type models, modelling C3 photosynthesis with the coupled photosynthesis-stomatal conductance model, modelling C4

Figure 7

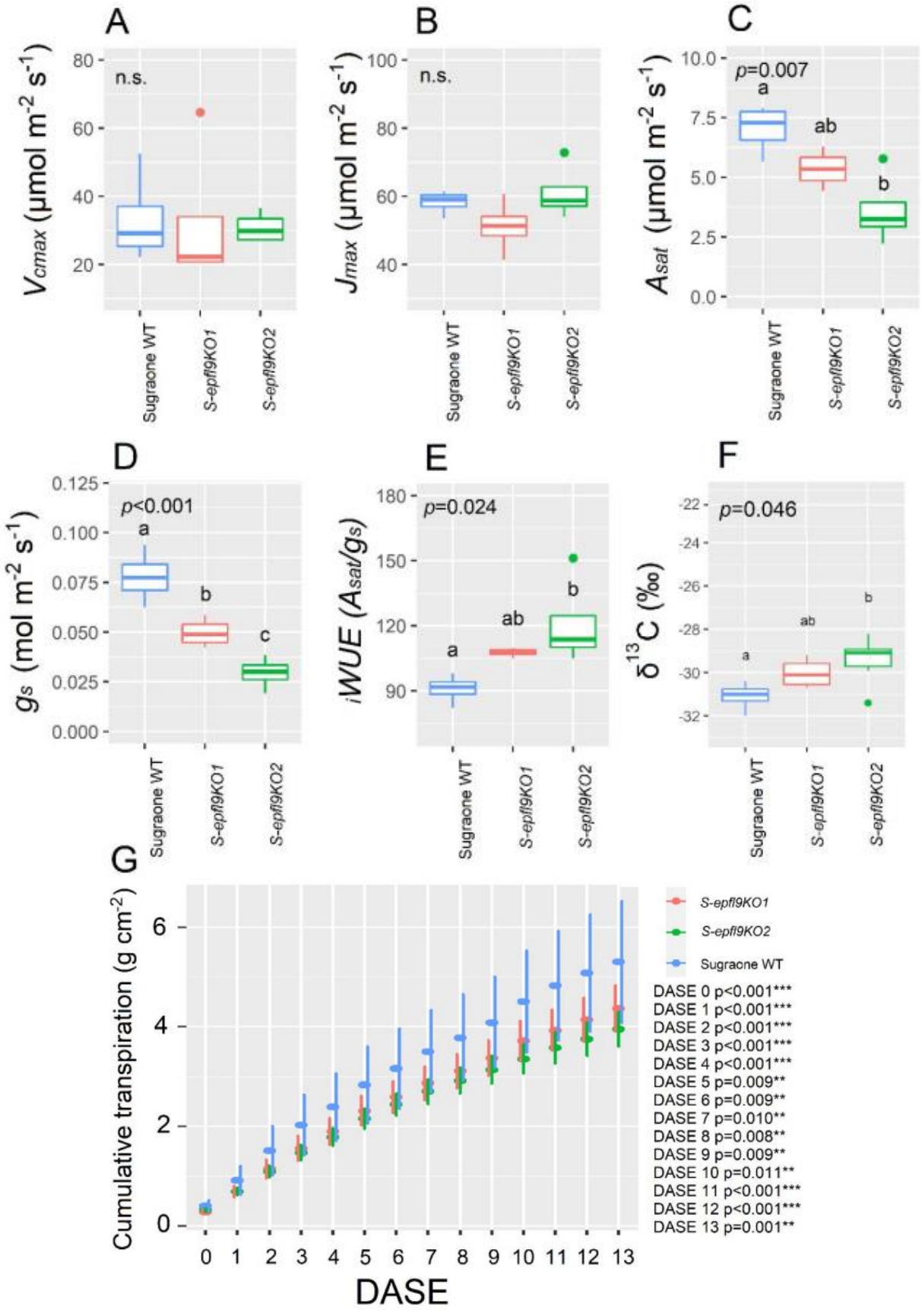
A
B
C
D
E
F
G
n.s.
p=0.007
p<0.001
p=0.024
p=0.046
Sugraone WT
S-epfl9KO1
S-epfl9KO2
DASE
Cumulative transpiration (g cm-2)
DASE 0 p<0.001***
DASE 1 p<0.001***
DASE 2 p<0.001***
DASE 3 p<0.001***
DASE 4 p<0.001***
DASE 5 p=0.009**
DASE 6 p=0.009**
DASE 7 p=0.010**
DASE 8 p=0.008**
DASE 9 p=0.009**
DASE 10 p=0.011**
DASE 11 p<0.001***
DASE 12 p<0.001***
DASE 13 p=0.001**

Gravimetric assessments of transpired water normalized for leaf area highlighted significant differences in cumulative transpiration between edited and WT lines. In general, both *S-epfl9KO1* and *S-epfl9KO2* used less water throughout a 14-day experimental period, by up to 21%, compared to 'Sugraone' WT (Fig. 7G). Moreover, carbon isotope discrimination ($\delta^{13}C$) analysis detected for *S-epfl9KO1* less negative $\delta^{13}C$ values compared to Sugraone WT (p=0.046), indicating a higher *iWUE*. Similarly, less negative $\delta^{13}C$ values were observed in *R-epfl9KO1* when compared to 'Riparia' WT (p=0.025) (Fig. 8).

Figure 8

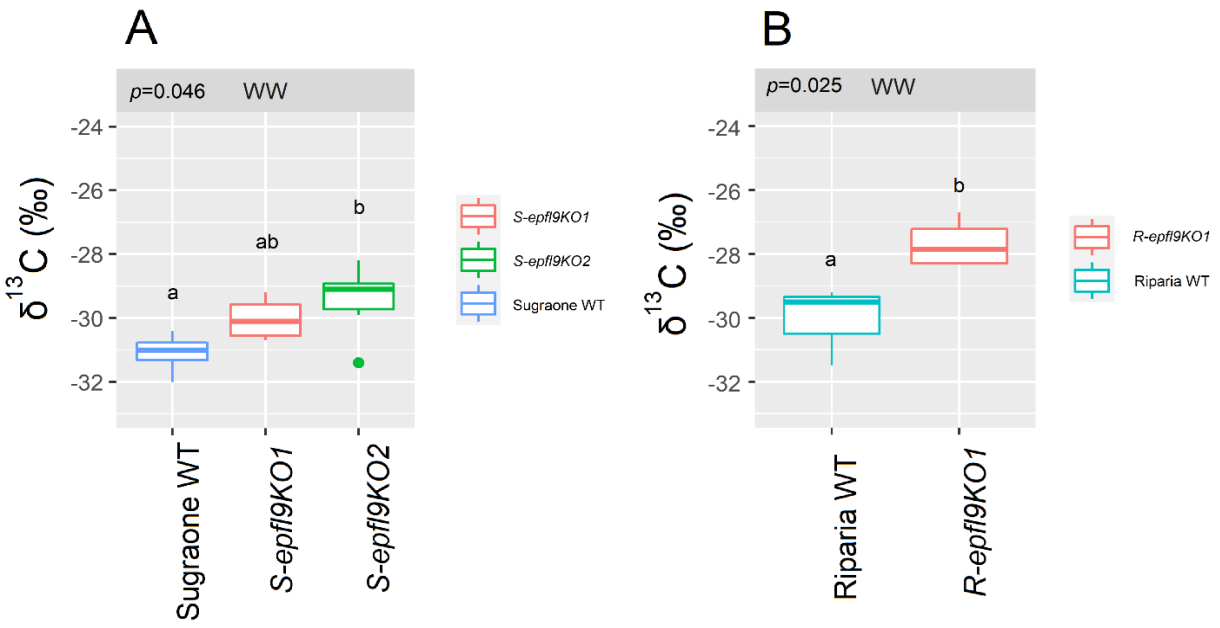

Figure 8. Carbon Isotope discrimination (δ13C) of grapevine leaves assessed before water stress treatment for S-epfl9KO1, S-epfl9KO2 and 'Sugraone' WT (A) and R-epfl9KO1 and 'Riparia' WT (B). Whiskers indicate the ranges of the minimum and maximum values and data were analysed with one-way ANOVA (n=3-6). Different letters indicate significantly different values according to Fisher's test. Data were collected on fully expanded leaves and on day 0 of stress application.

The knock-out of *VvEPF9-1* may reduce impact of water stress in grapevine

In vivo gas-exchange measurements at saturating light were carried out throughout the dry down experiments (Fig. 9). ANOVA output for each day is shown in Table S4. In vivo CO_2 assimilation rate (*A*) was significantly reduced by water stress (WS) in 'Sugraone' WT showing a steeper reduction than knock-out lines, although no significant differences were observed for each day and between lines (Fig. 9A). *S-epfl9KO1* and *2* maintained a lower stomatal conductance (g_s) than 'Sugraone' WT (p= 0.0276, DASA 5, Fig. 7) but intrinsic water-use efficiency $_i$*WUE* resulted not significantly different between the analysed plants (Fig. 9C). Transpiration normalized on leaf area was significantly reduced during the WS and for all the lines (Fig. 11D). The average fraction of transpirable soil water (FTSW) during the dry down is shown in Supplemental Fig. S4. There were significant differences ($p<0.05$) between *S-epfl9KO1* and Sugraone, in particular in the first part of stress application (DASA 1 to 4). Trends ($p<0.1$) were observed under severe WS (DASA 10 to 12) with *S-epfl9KO2* having higher transpiration than Sugraone WT.

Carbon isotope discrimination ($\delta^{13}C$) analysis showed that water stress led to less negative values for all the lines ($p<0.001$) although no significant differences were observed between edited lines and WT (p=0.186) (Supplemental Fig. S5).

Figure 9

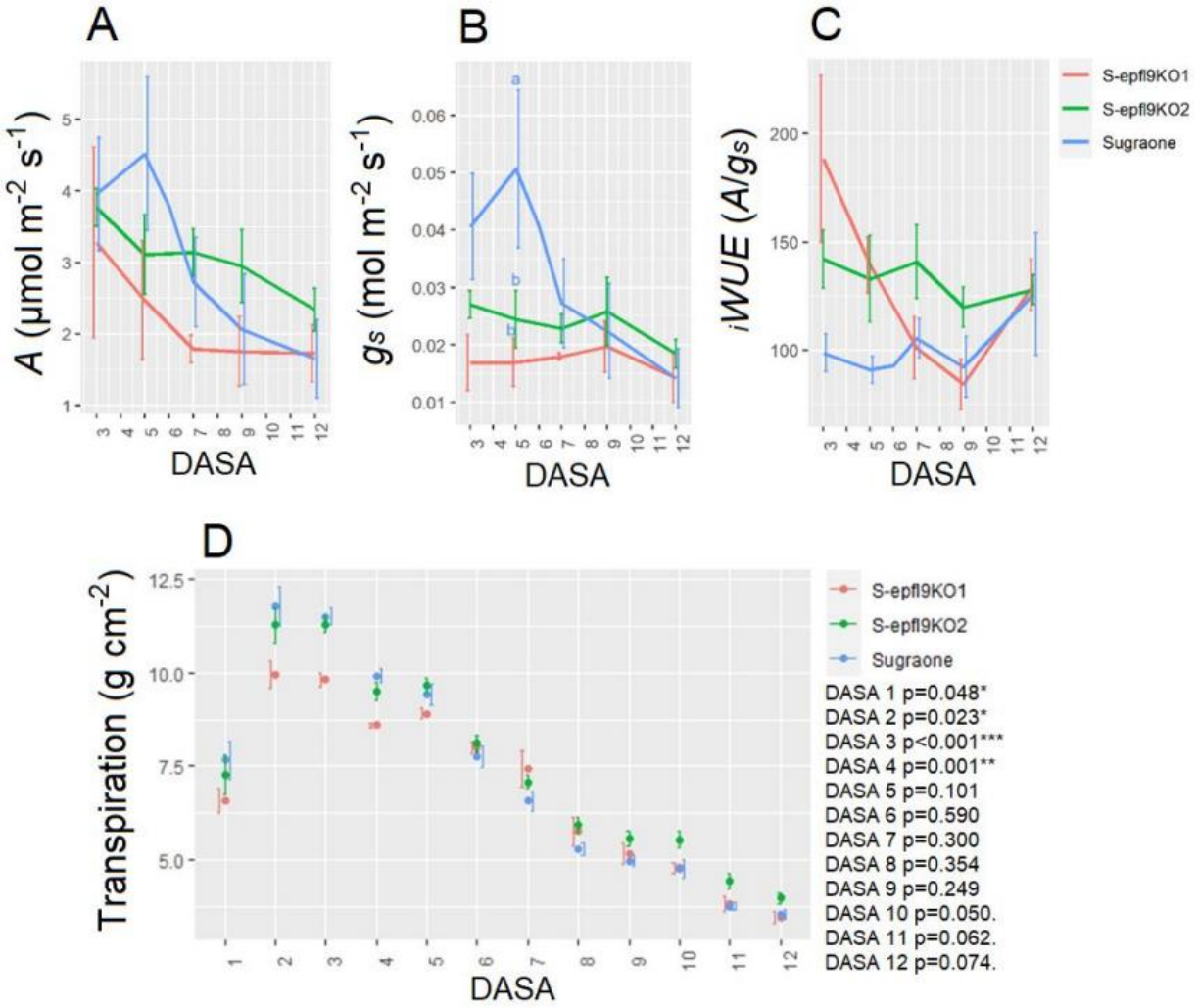

Figure 9. Trait assessment under water stress (WS) conditions, at different days after stress application (DASA). Leaf gas-exchange for S-epfl9KO1, S-epfl9KO2 and 'Sugraone' WT (A, B, C) and R-epfl9KO1 and 'Riparia' WT (E, F, G). *A*= in vivo CO_2 assimilation rate under saturating light, g_s=stomatal conductance, $_iWUE$= intrinsic water-use efficiency. Data are means (n=4-6) ± standard error of the mean (SEM). Data were analysed with one-way ANOVA (p-value in the text) while different letters indicate significant differences between lines according to Fisher's test. Transpiration response to reduced water availability for S-epfl9KO1, S-epfl9KO2 and 'Sugraone' WT (D) and R-epfl9KO1 and 'Riparia' WT (H). Transpiration was assessed gravimetrically and normalized for leaf area estimated via RGB imaging. Data are means ± standard error of the mean (n=5-6). Data were analysed with one-way ANOVA (*** p<0.001, ** p>0.01, * p<0.05, . p<0.1) for each day.

Discussion

Crops worldwide will experience warmer conditions in the next decades, followed by limited water availability and increasing atmospheric CO_2 concentration, leading to possible detrimental effects on yield stability and food security (McGranahan and Poling, 2018). Genetic manipulation of stomatal density and stomatal size have been shown to be an effective approach to increase drought tolerance and reduce water loss in several species (Bertolino et al., 2019; Buckley et al., 2020). Indeed, previous studies in Arabidopsis and grasses showed that water conservation, higher *$_i$WUE* and enhanced tolerance to multiple stresses (e.g. drought stress combined with heat stress) were achieved in lines overexpressing *EPF1/EPF2* or down-regulating *EPFL9*, due to a reduction in stomatal density (Franks et al., 2015; Hughes et al., 2017; Caine et al., 2019; Dunn et al., 2019; Lu et al., 2019).

In the grapevine genus we found two *AtEPFL9* orthologs, we named *VvEPFL9-1* and *VvEPFL9-2*, identical at 82% in the protein region corresponding to the functional peptide and respectively sharing 82% and 95% identity with the same region of AtEPFL9 peptide. So far, two *EPFL9* paralogs have been found in maize and rice (Hepworth et al., 2018; Yin et al., 2017; Lu et al., 2019), showing respectively 84% and 73% (*ZmEPFL9-1* and *ZmEPFL9-2*) and 82% and 73% (*OsEPFL9-1* and *OsEPFL9-2*) identities to AtEPFL9 functional peptide. It has been suggested that *EPFL9* paralogs in cereals might be functionally divergent (Lu et al., 2019) but definitive evidence indicating a different function has never been produced. In the study of Lu et al. (2019), the approach used to silence *OsEPF9-1* was RNA interference with a 450 bp-long hairpin RNA, which hardly discriminated between the two variants. In our study, we focused on *VvEPFL9-1*, localized on chromosome 5 (on the contrary, *VvEPFL9-2* was not anchored to any

chromosome in the grapevine reference genome, probably due to assembling issues) and selectively edited this paralog via CRISPR/Cas9 technology. According to our data, the knock-out of *VvEPFL9-1* can reduce stomatal density by up to 60%, leading to the hypothesis that *VvEPFL9-1* and *VvEPFL9-2* could be both involved in stomatal induction with a redundant function. A similar approach using CRISPR/Cas9 technology to knock-out *EPFL9* in rice achieved nearly 90% of stomatal density reduction compared to control by targeting a site on the first exon encoding for the signal peptide and thus not discriminating between *OsEPFL9* paralogs (Yin et al., 2017).

Our study also confirms the crucial role of cysteine residues in the C-terminal functional peptide. This is demonstrated by the lines *S-epfl9KO5* and *S-epfl9KO8* in which the loss of the second cysteine (due to a 3 bp-deletion or single base substitution) resulted in a stomatal density reduction similar to the one gained by a full frame-shift of the coding sequence. This is consistent with the finding of Ohki et al. (2011) who observed that impairing the formation of a disulphide bond prevented the correct protein folding and function. The design of a sgRNA that directed Cas9 cleavage next to the nucleotide triplet coding for the second cysteine proved to be a good choice for effective 3- and 6- bp deletions. Moreover, our data showed that the retention of almost 50% functional *VvEPFL9-1* in some transgenic lines (S-epfl9KO1 and S-epfl9KO5) due to a partial editing of the target site, with a substantial maintenance of a WT peptide, still resulted in a significant decrease of SD, suggesting that a threshold amount of peptide may be required for EPFL9-1 to be functionally effective.

Reduction in stomatal density following *VvEPFL9-1* knock-out was significant, although partially compensated by an increase in stomatal size (SS, inferred by pore length measurements). The negative yet non-linear association between SD and SS has been frequently

reported in many species (Franks and Beerling, 2009) and often linked to an improved economy of epidermal space allocation with the combination of low SD and high SS as a preferable strategy when low stomatal conductance is required (Doheny-Adams et al., 2012; Lawson and McElwain, 2016). In our work, however, the increase in SS was only a partial compensation for the reduction in SD.

Stomata are the main drivers of transpiration but at the same time are pivotal for CO_2 uptake for mesophyll photosynthesis (Lawson and Blatt, 2014). For instance, in barley and wheat, a reduction in SD by 50% compared to WT led to a significant reduction in carbon assimilation (A_{sat}) and conductance (g_s) and to an enhanced water use efficiency ($_iWUE$) under optimal growth conditions (Hughes et al., 2017; Dunn et al., 2019). Similarly, in 'Sugraone' at well-watered conditions, we found that a 60% reduction in SD lead to a reduced A_{sat} for the edited lines compared to the WT. Additionally, the reduction in g_s was even greater, leading to a higher value of $_iWUE$ (i.e. A_{sat}/ g_s) in edited versus WT lines. Moreover, the reduction in A_{sat} was not concomitant to reductions in Rubisco velocity (V_{cmax}) or to impairment in electron transport chain (J_{max}) suggesting that the knock-out of *VvEPFL9-1* did not affect the photosynthetic machinery, at least at the conditions applied in this work. *Vitis vinifera* genotypes with reduced SD and, in turn, limited A_{sat} and greater $_iWUE$, may be desirable to improve plant water conservation and to delay sugar accumulation under current and future climatic scenarios (Kuhn et al., 2014; Arrizabalaga-Arriazu et al., 2021). Sugars and organic acids along with various secondary metabolites (e.g., tannins, flavonols, anthocyanins, aroma compounds) are determinants of grape berry quality and their accumulation during berry ripening is the result of the interaction between genotype and environment, a relationship made vulnerable by climate change (Bobeica et al., 2015; Rienth et al., 2021).

It is well known that grapevine physiology will be impacted by elevated carbon dioxide, increasing temperatures, and extreme heat events during the growing season (De Cortázar-Atauri et al., 2017; Delrot et al., 2020). In particular, high temperature and increasing CO_2 levels are already affecting viticulture (Mosedale et al., 2016; Cook and Wolkovich, 2016; Edwards et al., 2017; Droulia and Charalampopoulos, 2021) with an evident shift towards an earlier onset of phenological stages (Edwards et al., 2017; Alikadic et al., 2019) and accelerated berry ripening (Jones et al., 2005; Parker et al., 2020; Rienth et al., 2021). High temperatures and water stress slow down vine metabolism resulting in a lower accumulation of polyphenols and aromatic compounds in the berries (Tomasi et al., 2011; Jones, 2013; Pons et al., 2017; Venios et al., 2020). Thus, one of the consequences of a compressed phenology may be an earlier sugar accumulation in the berries that leads to anticipated harvest dates when the secondary metabolites content is sub-optimal (Palliotti et al., 2014; Edwards et al., 2017). Although currently several agronomic approaches of source-limitation (i.e. pre-flowering leaf removal, shading nets, anti-transpirant application, etc) have been set up to delay sugar accumulation in ripening grapes in the field (Palliotti et al., 2014; Prats-Llinàs et al., 2020), stomatal manipulation may be a favorable genetic strategy for the future, that deserves to be further explored also under combined environmental stress and in field trials.

In our study, we further applied a water stress experiment to test if and how a reduced stomatal density can affect plant behavior in drought conditions. During a progressive reduction in soil water availability, significant differences in transpiration rate were observed in ‘Sugraone’ edited lines compared to WT only under moderate water stress (i.e. DASA 3 and 4). Yet, under severe water stress (e.g. DASA 10 to 12), some trends ($p<0.1$) were observed in edited lines showing higher transpiration rate followed by A_{sat} and g_s maintenance. Notably, the reduction in

g_s and A_{sat} during the dry-down was evident for WT plants ($p<0.001$) while this was not significant for edited lines. This conservative behavior induced by reduced SD has been previously associated with a longer period of transpiration maintenance during drought, leading to a prolonged carbon assimilation respect to WT (Caine et al., 2019). In rice, lines overexpressing the *OsEPF1* gene had higher yield than WT when water-stressed at flowering stage (Caine et al., 2019) confirming that water conservation during key-stages of yield formation may be desirable for yield maintenance (Faralli et al., 2019). In addition, limiting plant transpiration could be an advantage for irrigated vineyards in terms of a reduction in water input demand (Keller et al., 2016). In lieu of an increasing number of grapevine growing regions where water resources will become limited (Schultz, 2000; Santillán et al., 2020), genotypes with reduced stomatal density will require less irrigation water per area of cultivation, thereby increasing crop water productivity for farmers (Scholasch and Rienth, 2019).

Conclusion

To our knowledge, this is the first study describing the function of *VvEPFL9-1* in grapevine as well as the physiological advantages of *epfl9-1* knock-out genotypes under different availability of soil water. Reducing stomatal density via *VvEPFL9-1* loss of function can induce water conservation and increase ${}_iWUE$, although an impact of photosynthetic CO_2 absorbance (A_{sat}) was observed in some edited lines. While in several crops, reduced photosynthetic CO_2 uptake can decrease yield and biomass, we speculate that reduced A_{sat} and increased ${}_iWUE$ may be a favorable combination of physiological attributes in grapevine, especially under future climate change scenarios. However, at this stage, further trials in the field under standard management conditions for grapevine are required as well as additional evaluations regarding the

potential effects of reduced stomatal density under natural environmental fluctuations. To conclude, this work reinforces the concept that stomatal anatomical features constitute a promising target for designing climate change-resilient crops (Bertolino et al., 2019; Buckley et al., 2020; Franks et al., 2015; Hughes et al., 2017; Caine et al., 2019; Dunn et al., 2019; Lu et al., 2019) and provides evidence of this in grapevine, the most economically important fruit crop globally.

Materials and methods

Search for the orthologous gene of *AtEPFL9* and experimental confirmation in grapevine genotypes

AtEPFL9 sequence (AT4G12970) was used as a query to interrogate the publicly available genomic databases of *Vitis* spp. (Supplementary Table 1). To experimentally confirm the presence of two *VvEPFL9* paralogs in a set of grapevine genotypes, DNA was extracted from leaf tissue of 'Chardonnay', 'Merlot', 'Syrah', 'Cabernet Sauvignon', 'Touriga National', 'Pinot Noir clone Entav 115', 'Pinot Noir PN40024', 'Sugraone' and 'Riparia Glorie de Montpellier' using Nucleospin Plant II kit (Macherey–Nagel, Düren, Germany) following the manufacturer's instruction. Genomic DNA was quantified using Nanodrop 8800 (Thermo Fischer Scientific, Waltham, MA, USA) and diluted to a final concentration of 30 ng/µL. Two PCR reactions were performed in 25 µl final volume containing 1×PCR BIO (Resnova, Rome, Italy), 30 ng of genomic DNA and 0.5 µM of primers in order to amplify *VvEPFL9-1* (primer VvEPFL9-1_fw and VvEPFL9-1_rv, see Supplementary Table 2) and *VvEPFL9-2* (primer VvEPFL9-2_fw and VvEPFL9-2_rv, see Supplementary Table 2). Amplification products were checked on agarose gel, purified using CleanNGS magnetic beads (CleanNA, Waddinxveen, Netherlands) and sequenced by Sanger sequencing (FEM Sequencing Platform Facility, San Michele all'Adige,

Italy). Sequencing outputs were analyzed with Blast online tool (blast.ncbi.nlm.nih.gov) and for the alignment of the sequences the software MEGAX(Kumar et al., 2018) was used.

Plant material (gene transfer experiments, *in-vitro* and greenhouse growth) (Figure 10)

The CRISPR/Cas9 binary vector with the customized sgRNA was purchased from DNA Cloning Service (Hamburg, Germany). The nucleotide sequence of SpCAS9 and of *NPTII* genes were codon optimized for the plant expression system and their sequences are available on the company website (https://www.dna-cloning.com/). The sequence of the guide RNA carried by the vector was designed with CRISPR-P 2.0 software (http://crispr.hzau.edu.cn/cgi-bin/CRISPR2/CRISPR) and recognizes a region of 20 bp in the third exon of *VvEPFL9-1* (GCACATACAATGAATGCAAA, on-score=0.7058). *Agrobacterium tumefaciens* (A.t.)-mediated gene transfer was performed on embryogenic calli of 'Sugraone' according to Dalla Costa et al. (2022). *NPTII* was used as selectable marker to confer resistance to kanamycin. Regenerated plants were screened by PCR for the presence of SpCAS9 (to select plants which integrated T-DNA) in 20 µl final volume containing 1×PCR BIO (Resnova, Rome, Italy), 0.5 µM of each primer (SpCAS9_Fw and SpCAS9_Rv, see Supplementary Table 2) and 30 ng of genomic DNA. DNA was extracted from freshly frozen leaf tissue (approximately 100 mg) using Nucleospin Plant II kit (Macherey–Nagel, Düren, Germany) following the manufacturer's instruction, quantified using Nanodrop 8800 (Termo Fischer Scientific, Waltham, MA, USA) and diluted to a final concentration of 30 ng/µL.

Edited lines and WT control were propagated *in-vitro* in sterilized jars containing WP medium (McCown and Lloyd, 1981) in a growth chamber at 100 photosynthetic photon flux density (PPFD) ± 20 (µmol m^{-2} s^{-1}), 24 °C and a 16/8 light/dark photoperiod. Four biological replicates

of healthy developed edited lines and of the WT control were acclimatized in the greenhouse using 0.25 L plastic pots with three holes in the bottom to allow for water drainage, filled with a similar amount of growing substrate (Extra quality - Semina, TerComposti, Calvisano, Italy) and covered by parafilm on the top. Plants were kept in a growth chamber (PPFD 100 +/- 20 µmol m^{-2} s^{-1}, 24 °C, 16/8 light/dark photoperiod) and after one week, holes were gradually made in the top of the parafilm over the course of two weeks. After 17 days, plants were repotted into 0.75 L pots all containing growing substrate (Extra quality - Special Cactus, TerComposti, Calvisano, Italy). Pots were kept in the same growth chamber for a subsequent ten days before moving to the greenhouse. In the greenhouse, plants were grown under natural light supplemented by high-pressure sodium lamps system (PPFD 200-250 µmol m^{-2} s^{-1}) with a 16-h/8-h light–dark photoperiod. Environmental conditions including temperature and humidity during the growth chamber and greenhouse cultivation are shown in Supplementary Figure 1.

Molecular characterization of edited lines

Transgene copy number quantification

The quantification of SpCAS9 copy number (CN) in grapevine lines was carried out according to real-time PCR method developed by Dalla Costa et al. (2009). Reactions were performed in a 96-well plate on a C1000 thermal cycler (Bio-Rad, Hercules, USA) equipped with CFX96 real-time PCR detection system (Bio-Rad, Hercules, USA). The real-time PCR singleplex reaction was carried out in a 10 µl final volume containing 1×SsoAdvanced Universal Probes Supermix (Bio-Rad, Hercules, USA), 40 ng of genomic DNA, 0.3 µM primers (Sigma, Haver hill, UK) and a 0.2 µM specifc Taqman probe (Sigma, Haverhill, UK). The thermal protocol was as follows: polymerase activation for 3 min at 95 °C followed by 40 cycles of denaturation of 10 s at 95 °C,

annealing of 5 s at 58 °C and 5 s at 60 °C and an elongation of 30 s at 72 °C. Primers and Taqman probes used to amplify grapevine endogenous *VvCHI* (VvChiRT_fw; VvChiRT_rv; VvChiRT_Probe) and *SpCAS9* (SpCas9RT_fw; SpCas9RT_rv; SpCas9RT_Probe) were reported in Supplementary Table 2. The standard curves (four points, starting from 106 plasmid molecules and adopting a serial dilution of 1:5) were built with a plasmid pGEM-T easy (Promega, Madison, Wisconsin, USA), in which we cloned a fragment of *VvCHI* and *SpCAS9.* For each sample, the *SpCAS9* CN was calculated using the following formula: (transgene total copies/ endogenous gene total copies)×2. The total copies of transgene and endogenous gene were calculated on the basis of the mean values of the quantification cycles (Cq) of two technical replicates.

On- and off target editing evaluation

In the grapevine lines integrating T-DNA, a region of the gene *VvEPFL9-1* containing the site targeted by the sgRNA/Ca9 complex, was amplified with primers VvEPFL9-1_fw and VvEPFL9-1_rv (see Supplementary Table 2) both elongated with overhang Illumina adapters. PCR was carried out in 20 µl final volume containing 1×PCR BIO (Resnova, Rome, Italy), 0.4 µM of each primer and 30 ng of genomic DNA. The Illumina library was sequenced on an Illumina MiSeq (PE300) platform at the Sequencing Platform Facility of Fondazione Edmund Mach (San Michele all'Adige, Italy). CRISPResso2 pipeline (https://crispresso.pinellolab.partners.org/submission) (Clement et al., 2019) was used to process the raw paired end reads with default parameters and to visualize the mutations profiles in the target sequences. For the analysis of the off-target site in the gene VvEPFL9-2, a PCR was carried out in 25 µl final volume containing 1×PCR BIO (Resnova, Rome, Italy), 0.5 µM of each primer (VvEPFL9-2_fw and VvEPFL9-2_rv, see Supplementary Table 4) and 30 ng of genomic

DNA. Amplification products were checked on agarose gel, purified using CleanNGS magnetic beads (CleanNA, Waddinxveen, Netherlands) and sequenced by Sanger sequencing (FEM Sequencing Platform Facility). Sequencing outputs were analyzed with Blast online tool (blast.ncbi.nlm.nih.gov).

T-DNA integration site identification

T-DNA integration points (IP) were determined following the method described in Dalla Costa et al. (2020). The library was sequenced by Illumina MiSeq (PE300) platform at the Sequencing Platform Facility of Fondazione Edmund Mach (San Michele all'Adige, Italy). The putative genomic regions identified were validated by PCR amplification. PCR was performed in a 20 µl final volume containing 1×PCR BIO (Resnova, Rome, Italy), 40 ng of genomic DNA and 0.5 µM of the primers reported in Supplementary Table 4. Amplification products were checked on agarose gel, purified using PureLink Quick Gel Extraction (Invitrogen, Carlsbad, CA, USA) and sequenced by Sanger sequencing (FEM Sequencing Platform Facility). Sequencing outputs were analyzed with the Blast sequence server (using the database PN40024.v4_REF_genome) available online at the European network INTEGRAPE website (https://integrape.eu/resources/genes-genomes/genome-accessions/).

Experimental conditions and physiological analysis

Experiment 1: well-watered (WW) conditions in greenhouse. Biological replicates of edited lines S-*epfl9*KO1 (n=4) and S-*epfl9*KO2 (n=4), and of 'Sugraone' WT (n=4) kept in a greenhouse for two months were used. Pots were covered in aluminum foil and wrapped in plastic to limit soil evaporation (Supplementary Figure 2). All plants were measured daily for 11 days at the same time each morning for mass of water loss.

Experiment 2: water-stress (WS) conditions in greenhouse. The same plants used in Experiment 1 were used in Experiment 2. Control pots (soil-filled pots without plants) were placed at the end of each row in randomized positions, weighed by balance and returned to the same positions every day to assess soil evaporation. Pots dried down naturally for a subsequent 15 days.

Experiment 3: well-watered (WW) conditions in an automated high-throughput phenotyping platform. Biological replicates of the edited line S-*epfl9*KO6 (n=6) and 'Sugraone' WT (n=4), maintained in greenhouse for 12 months, with a height range of 60-70 cm and a weight brought to 3000 g (in 5L pots) were used. Plants were moved inside the phenotyping platform (WIWAM, Gand, Belgium) at the Plant Phenotyping Facility of Fondazione Edmund Mach where temperature was set to 28/25°C, photoperiod to 16/8h and average PPFD to 300 µmol m^{-2} s^{-1} at apical leaf level. Plants were automatically watered every day at 6:00 AM to target weight (3000g) and pot weight was evaluated before and after watering for 12 days.

Soil water content, transpiration, and leaf area determination.

In Experiment 1 and 2, total transpirable soil water (TTSW) was calculated as the difference between pot mass at day 1, fully watered (100% capacity), and the pot mass at the end of the natural dry down when transpiration reached a minimum. Fully watered plants (100% relative soil water content) were weighted after watering to capacity and allowing pots to drain for 2 hours. The fraction of transpiration soil water (FTSW) was calculated as a daily ratio between the amount of soil water remaining in the pot left for transpiration and the TTSW using the equation: FTSW = (PMn - PMfinal)/TTSW, where PMn is the pot mass for each day, and

PMfinal is the pot mass at the end of the day 11. FTSW data were reported in Supplementary Figure 3. At day 12 (i.e. after Experiment 1), plants were unwrapped from the aluminum and plastic coverings, re-watered to 100% of their initial weight using syringes and weighed as a starting mass for the stress application. In both Experiment 1 and 2, transpiration (g/cm2) was measured as the grams of water lost daily, normalized by the relative leaf area for each individual [T= (mass 0 - mass 1)/relative leaf area, where 0 and 1 represent the days in consecutive order]. Growth was measured as a relative leaf area every other day for a period of 28 days using RGB imaging. The software Easy Leaf Area (Easlon and Bloom, 2014) was used for analysis. Photos of the plants were taken at the same distance and tripod angle (45°) to provide uniform and consistent assessment of relative leaf area (example in Supplementary Figure 4A). A biomass-leaf area estimated curve was constructed using eight plants of varying sizes validating the non-destructive approach (Supplementary Figure 5). In Experiment 3, daily water-use was automatically calculated as daily pot weight loss (g). In addition, projected leaf area (pixels) was calculated at the beginning and at the end of the experiment (day 1 and day 12 respectively) as the average green pixels in four RGB images collected at different pot angles and analyzed with the WIWAM software (example in Supplementary Figure 4B).

Stomatal characterization

Samples for stomatal characterization were taken at well-watered conditions as well as at the end of the drought treatment (i.e. Experiment 1 and 2). Leaves were chosen with the same size and position, typically leaf three, unless abnormal. Clear gel nail polish was applied to the abaxial and adaxial surfaces of the leaf to create an imprint of the leaf surface and allowed to dry. Clear tape was used to peel off the nail polish, and the tape was mounted on a microscope slide. Slides

were imaged using a compound microscope (DM, Leica Microsystems, Wetzlar, Germany) at 40x and at five different technical positions of the same area (0.3 mm^2) on the four biological replicates for a total of twenty measurements of stomata density per individual. Stomatal size (SS) was characterized from three technical replicates from three biological replicates for a total of 9 replicates per individual. These 9 replicates were averaged to create an average radius (r) for reach individual, and the stomatal size was subsequently calculated as $SS = 0.5\pi r^2$; stomatal size is equal to 0.5 multiplied by the average length of stomata squared multiplied by π.

Gas-exchange analysis, SPAD and leaf temperature

For Experiment 1, 2 and 3, gas-exchange measurements were carried out using a portable infra-red gas analyzer and a 2 cm^2 leaf cuvette with an integral blue–red LED light source (LiCOR 6400-40XT, Lincoln, NE, USA). Inside the cuvette, flow rate was set at 400 µmol s^{-1}, leaf temperature at 24°C, PPFD to 1500 µmol m^{-2} s^{-1} and C_a of 400 µmol mol^{-1}. In Experiment 1, measurements of the response of photosynthesis (A) to sub-stomatal CO_2 concentrations (C_i) curves (A/C_i) were performed between 9:00 and 12:00, on the most expanded leaf from each plant. For A/C_i, C_a was sequentially decreased to 300, 200, 150, 75 and 50 µmol mol^{-1} before returning to the initial concentration of 400 µmol mol^{-1}. This was followed by a sequential increase to 500, 700, 900, 1100, 1300, and 1500 µmol mol^{-1}. Readings were recorded when A reached steady state. The maximum velocity of Rubisco for carboxylation (V_{cmax}) and the maximum rate of electron transport demand for Ribulose 1,5-bisphosphate (RuBP) regeneration (J_{max}) were estimated as described by Duursma (2015). A_{sat} represents CO_2 assimilation rate at saturating PPFD while g_s represents stomatal conductance at ambient CO_2 (C_a). Intrinsic water-use efficiency ($_iWUE$) was calculated as $=A_{sat}/g_s$. During Experiment 2, measurements of A and

g_s were taken every day on fully expanded leaves for the first 3 days to record a baseline gas-exchange before water stress was applied. Subsequently gas-exchange data were recorded every two days in fully expanded leaves. In Experiment 3, gas-exchange parameters (A and g_s), leaf temperature and leaf chlorophyll content were measured at day 5 on the same leaves respectively with LiCOR 6400-40XT (Lincoln, NE, USA), an infra-red thermometer (62 MAX+, FLUKE Corporation, Everett, Washington USA) and a SPAD (Minolta SPAD 502).

Carbon Isotope Composition

Carbon isotope composition was estimated in leaves with the same leaf size and position, count as leaf three unless abnormal. Samples for stomatal characterization were taken first, and the remaining fresh leaf tissue was dried at 80°C for two days to be used for $\delta^{13}C$ determination. $\delta^{13}C$ was analyzed in 2 mg aliquots of leaf sample weighed in tin capsules. Samples were combusted in an elemental analyzer (Thermo Flash EA 1112 Series, Bremen, Germany), CO_2 was separated by chromatography and directly injected into a continuous-flow isotope ratio mass spectrometer (Thermo Finnigan Delta V, Bremen, Germany) through the interface ConFlo IV dilutor device (Thermo Finningan, Bremen, Germany). Samples were measured in duplicate. The isotope ratios were expressed in δ‰ against Vienna-Pee Dee Belemnite for $\delta^{13}C$ according to the following equation: $\delta‰ = (R_{SA} - R_{REF}) / R_{REF}$ where R_{SA} is the isotope ratio measured for the sample and R_{REF} is the international standard isotope ratio. The isotopic values were calculated using a linear equation against working in-house standards, which were themselves calibrated against the international reference materials L-glutamic acid USGS 40 (U.S. Geological Survey, Reston, VA, USA), fuel oil NBS-22 and IAEA-CH-6. The uncertainty of measurement (calculated as 2 standard deviations) was 0.1‰.

Statistics

Statistical analyses were performed using R software (R Core Team 2020). A one-way ANOVA was conducted to compare differences in cumulative transpiration, conductance, photosynthesis, and water use efficiency between edited and WT lines for each day of measurement. Post hoc comparisons using Fisher's LSD test were carried out to assess group differences. *P* values lower than 0.05 were considered significant.

Figure 10

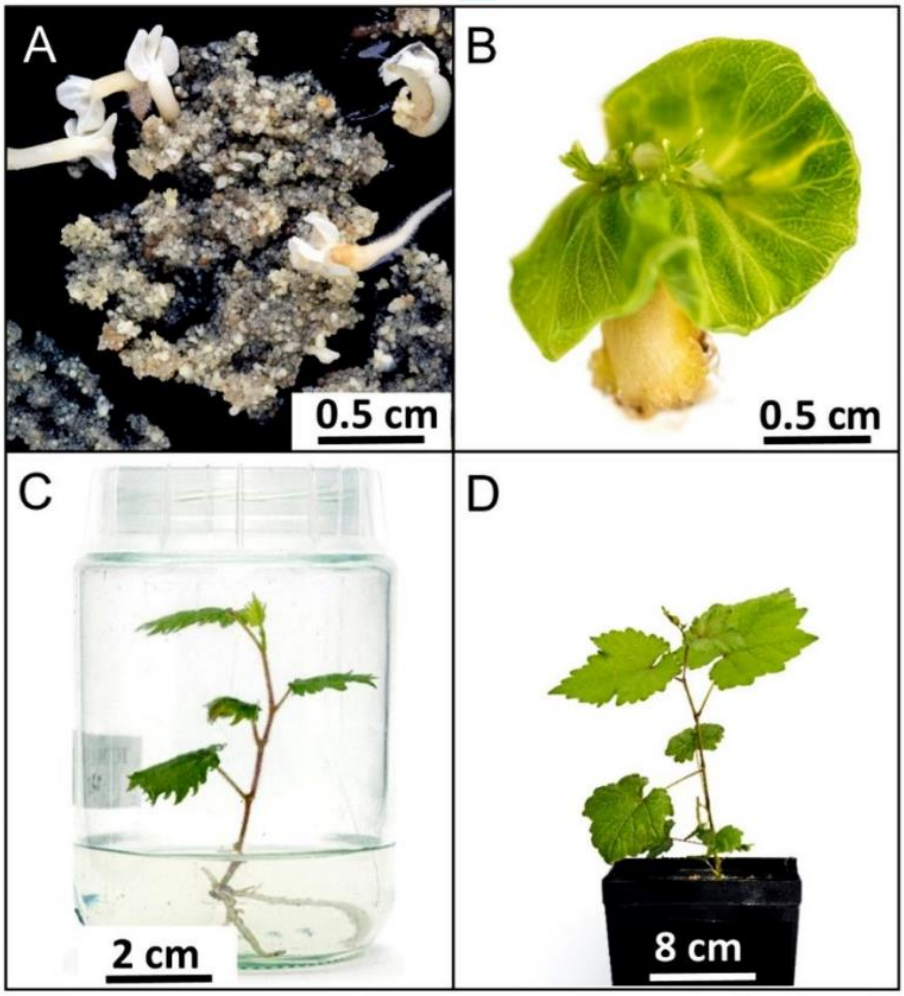

Figure 10. Pipeline to obtain epfl9-1 mutants for physiological characterization. (A) Embryogenic callus of 'Sugraone' 7 months after co-cultivation with Agrobacterium tumefaciens. Some embryos are developing on a homogeneous callus mainly formed by small globular embryos. (B) Embryo producing shoot. (C) In vitro plantlet cultivated in baby jars. (D) Greenhouse plant after 2 months from acclimatization of an in vitro plantlet

Accession Numbers

VvEPFL9-1 (*Vitis vinifera*; Vitvi05g01370; Chr. 5:20,673,140-20,673,946)

VvEPFL9-2 (*Vitis vinifera*; contig VV78X057312.8. BioProject PRJEA18357)

AtEPFL9 (*Arabidopsis thaliana*; AT4G12970; Chr. 4:7,585,869-7,587,099)

BnEPFL9 (*Brassica napus*; BnaA08g04900D-1; SuperContig LK032336: 217,786-218,791)

OsEPFL9-1 (*Oryza sativa*; BGIOSGA005039-TA; Chr. 1: 43,547,940-43,548,849)

OsEPFL9-2 (*Oryza sativa*; BGIOSGA026626-TA; Chr. 8: 27,848,069-27,849,071)

ZmEPFL9-2 (*Zea mays*; Zm00001d049795_T001; Chr. 4: 44,952,499-44,952,735)
ZmEPFL9-1 (*Zea mays*; Zm00001d012079_T001; Chr. 8: 167,759,340-167,760,532)
SlEPFL9 (*Solanum lycopersicum*; Solyc08g066610.3.1; Chr. 8: 55,431,397-55,432,638)
MdEPFL9 (*Malus domestica*; mRNA:MD10G0128800; Chr. 10: 24,119,461-24,120,875)
CcEPFL9 (*Citrus clementina*; ESR50459; SuperContig KI536726: 16,315,957-16,317,054)
PpEPFL9 (*Prunus persica* ; ONH92727; Chr. 8: 18,622,099-18,623,493)
PdEPFL9 (*Prunus dulcis*; VVA33635; SuperContig pdulcis26_s0297: 70,503-71,904)
AcEPFL9 (*Actinidia chinensis*; PSR86312; Chr. 28: 8,025,811-8,028,082)

Acknowledgments

We thank Valentino Poletti for his technical help with culture media preparation and Dr. Lisa Giacomelli and Dr. Massimiliano Trenti for sharing with us embryogenic calli of 'Sugraone' and 'Riparia', respectively. We would like to thank Damiano Gianelle for lending the Li-Cor 6400. A special thanks to Dr. Claudio Moser for useful suggestions and discussion. This research was supported by the Autonomous Province of Trento (Project Vitis&CC).

References

Alikadic A, Pertot I, Eccel E, Dolci C, Zarbo C, Caffarra A, De Filippi R, Furlanello C (2019) The impact of climate change on grapevine phenology and the influence of altitude: A regional study. Agric For Meteorol 271: 73–82

Almagro Armenteros JJ, Tsirigos KD, Sønderby CK, Petersen TN, Winther O, Brunak S, von Heijne G, Nielsen H (2019) SignalP 5.0 improves signal peptide predictions using deep neural networks. Nat Biotechnol 37: 420–423

Anzalone A V., Randolph PB, Davis JR, Sousa AA, Koblan LW, Levy JM, Chen PJ, Wilson C, Newby GA, Raguram A, et al (2019) Search-and-replace genome editing without double-strand breaks or donor DNA. Nature 576: 149–157

Arrizabalaga-Arriazu M, Morales F, Irigoyen JJ, Hilbert G, Pascual I (2021) Growth and physiology of four *Vitis vinifera* L. cv. Tempranillo clones under future warming and water deficit regimes. Aust J Grape Wine Res 27: 295–307

Bertolino LT, Caine RS, Gray JE (2019) Impact of stomatal density and morphology on water-use efficiency in a changing world. Front Plant Sci 10: 225

Bobeica N, Poni S, Hilbert G, Renaud C, Gomès E, Delrot S, Dai Z (2015) Differential responses of sugar, organic acids and anthocyanins to source-sink modulation in Cabernet Sauvignon and Sangiovese grapevines. Front Plant Sci 6: 14

Bota J, Tomás M, Flexas J, Medrano H, Escalona JM (2016) Differences among grapevine cultivars in their stomatal behavior and water use efficiency under progressive water stress. Agric Water Manag 164: 91–99

Buckley CR, Caine RS, Gray JE (2020) Pores for thought: can genetic manipulation of stomatal density protect future rice yields? Front Plant Sci 10: 1783

Caine RS, Yin X, Sloan J, Harrison EL, Mohammed U, Fulton T, Biswal AK, Dionora J, Chater CC, Coe RA, et al (2019) Rice with reduced stomatal density conserves water and has improved drought tolerance under future climate conditions. New Phytol 221: 371–384

Canaguier A, Grimplet J, Di Gaspero G, Scalabrin S, Duchêne E, Choisne N, Mohellibi N, Guichard C, Rombauts S, Le Clainche I, et al (2017) A new version of the grapevine reference genome assembly (12X.v2) and of its annotation (VCost.v3). Genomics Data 14: 56–62

Chen K, Wang Y, Zhang R, Zhang H, Gao C (2019) CRISPR/Cas genome editing and precision plant breeding in agriculture. Annu Rev Plant Biol 70: 667–697

Chen L, Wu Z, Hou S (2020) SPEECHLESS speaks loudly in stomatal development. Front Plant Sci 11: 114

Clement K, Rees H, Canver MC, Gehrke JM, Farouni R, Hsu JY, Cole MA, Liu DR, Joung JK, Bauer DE, et al (2019) CRISPResso2 provides accurate and rapid genome editing sequence analysis. Nat Biotechnol 37: 224–226

Cook BI, Wolkovich EM (2016) Climate change decouples drought from early wine grape harvests in France. Nat Clim Chang 6: 715–719

De Cortázar-Atauri IG, Duchêne É, Destrac-Irvine A, Barbeau G, De Rességuier L, Lacombe T, Parker AK, Saurin N, Van Leeuwen C (2017) Grapevine phenology in France: from past observations to future evolutions in the context of climate change. Oeno One 51: 115–126

Dalla Costa L, Pinto-Sintra AL, Campa M, Poletti V, Martinelli L, Malnoy M (2014) Development of analytical tools for evaluating the effect of T-DNA chimeric integration on transgene expression in vegetatively propagated plants. Plant Cell, Tissue Organ Cult 118: 471–484

Dalla Costa L, Vaccari I, Mandolini M, Martinelli L (2009) Elaboration of a reliable strategy based on real-time PCR to characterize genetically modified plantlets and to evaluate the efficiency of a marker gene removal in grape (*Vitis spp.*). J Agric Food Chem 57: 2668–77

Dayer S, Herrera JC, Dai Z, Burlett R, Lamarque LJ, Delzon S, Bortolami G, Cochard H, Gambetta GA (2020) The sequence and thresholds of leaf hydraulic traits underlying grapevine varietal differences in drought tolerance. J Exp Bot 71: 4333–4344

Delrot S, Grimplet J, Carbonell-bejerano P, Schwandner A, Bert P, Bavaresco L, Costa LD, Gaspero G Di, Duchêne E, Hausmann L, et al (2020) Genetic and genomic approaches for adaptation of grapevine to climate change. *In* C Kole, ed, Genomic designing of climate-smart fruit crops. Springer International Publishing, Switzerland, pp 157–270

Doheny-Adams T, Hunt L, Franks PJ, Beerling DJ, Gray JE (2012) Genetic manipulation of stomatal density influences stomatal size, plant growth and tolerance to restricted water supply across a growth carbon dioxide gradient. Philos Trans R Soc B Biol Sci 367: 547–555

Droulia F, Charalampopoulos I (2021) Future climate change impacts on european viticulture: a review on recent scientific advances. Atmosphere 12: 495

Dunn J, Hunt L, Afsharinafar M, Meselmani M Al, Mitchell A, Howells R, Wallington E, Fleming AJ, Gray JE (2019) Reduced stomatal density in bread wheat leads to increased water-use efficiency. J Exp Bot 70: 4737–4747

Duursma RA (2015) Plantecophys - An R package for analysing and modelling leaf gas exchange data. PLoS One 10: 1–13

Edwards EJ, Unwin D, Kilmister R, Treeby M, Ollat N (2017) Multi-seasonal effects of warming and elevated CO2 on the physiology, growth and production of mature, field grown, Shiraz grapevines. J Int des Sci la Vigne du Vin 51: 127–132

Faralli M, Matthews J, Lawson T (2019) Exploiting natural variation and genetic manipulation of stomatal conductance for crop improvement. Curr Opin Plant Biol 49: 1–7

Franks PJ, Beerling DJ (2009) Maximum leaf conductance driven by CO2 effects on stomatal size and density over geologic time. Proc Natl Acad Sci U S A 106: 10343–10347

Franks PJ, W. Doheny-Adams T, Britton-Harper ZJ, Gray JE (2015) Increasing water-use efficiency directly through genetic manipulation of stomatal density. New Phytol 207: 188–

195

Gambetta GA, Herrera JC, Dayer S, Feng Q, Hochberg U, Castellarin SD (2020) The physiology of drought stress in grapevine: towards an integrative definition of drought tolerance. J Exp Bot 71: 4658–4676

Hara K, Yokoo T, Kajita R, Onishi T, Yahata S, Peterson KM, Torii KU, Kakimoto T (2009) Epidermal cell density is autoregulated via a secretory peptide, EPIDERMAL PATTERNING FACTOR 2 in Arabidopsis leaves. Plant Cell Physiol 50: 1019–1031

Hepworth C, Caine RS, Harrison EL, Sloan J, Gray JE (2018) Stomatal development: focusing on the grasses. Curr Opin Plant Biol 41: 1–7

Hepworth C, Doheny-Adams T, Hunt L, Cameron DD, Gray JE (2015) Manipulating stomatal density enhances drought tolerance without deleterious effect on nutrient uptake. New Phytol 208: 336–341

Hess GT, Tycko J, Yao D, Bassik MC (2017) Methods and applications of CRISPR-mediated base editing in eukaryotic genomes. Mol Cell 68: 26–43

Hughes J, Hepworth C, Dutton C, Dunn JA, Hunt L, Stephens J, Waugh R, Cameron DD, Gray JE (2017) Reducing stomatal density in barley improves drought tolerance without impacting on yield. Plant Physiol 174: 776–787

Hunt L, Bailey KJ, Gray JE (2010) The signalling peptide EPFL9 is a positive regulator of stomatal development. New Phytol 186: 609–614

IPCC (2014) Climate Change 2014: synthesis report. Contribution of working groups I, II and III to the fifth assessment report of the intergovernmental panel on climate change. IPCC, Geneva, Switzerland

Jain M (2015) Function genomics of abiotic stress tolerance in plants: a CRISPR approach. Front Plant Sci 6: 375

Jinek M, Chylinski K, Fonfara I, Hauer M, Doudna JA, Charpentier E (2012) A Programmable Dual-RNA – Guided DNA Endonuclease in Adaptive Bacterial Immunity Guided. Science 337: 816–822

Jones G (2013) Winegrape phenology. *In* MD Schwartz, ed, Phenology: an integrative environmental science, second edition. Springer, Dordrecht, pp 563–584

Jones G V., White MA, Cooper OR, Storchmann K (2005) Climate change and global wine quality. Clim Change 73: 319–343

Keller M, Romero P, Gohil H, Smithyman RP, Riley WR, Casassa LF, Harbertson JF (2016) Deficit irrigation alters grapevine growth, physiology, and fruit microclimate. Am J Enol Vitic 67: 426–435

Kondo T, Kajita R, Miyazaki A, Hokoyama M, Nakamura-Miura T, Mizuno S, Masuda Y, Irie K, Tanaka Y, Takada S, et al (2010) Stomatal density is controlled by a mesophyll-derived signaling molecule. Plant Cell Physiol 51: 1–8

Kuhn N, Guan L, Dai ZW, Wu BH, Lauvergeat V, Gomès E, Li SH, Godoy F, Arce-Johnson P,

Delrot S (2014) Berry ripening: recently heard through the grapevine. J Exp Bot 65: 4543–4559

Kumar S, Stecher G, Li M, Knyaz C, Tamura K (2018) MEGA X: Molecular evolutionary genetics analysis across computing platforms. Mol Biol Evol 35: 1547–1549

Lawson T, Blatt MR (2014) Stomatal size, speed, and responsiveness impact on photosynthesis and water use efficiency. Plant Physiol 164: 1556–1570

Lawson T, McElwain JC (2016) Evolutionary trade-offs in stomatal spacing. New Phytol 210: 1149–1151

Lee JS, Hnilova M, Maes M, Lin YCL, Putarjunan A, Han SK, Avila J, Torii KU (2015) Competitive binding of antagonistic peptides fine-tunes stomatal patterning. Nature 522: 439–443

Van Leeuwen C, Destrac-Irvine A (2017) Modified grape composition under climate change conditions requires adaptations in the vineyard. Oeno One 51: 147–154

Van Leeuwen C, Destrac-Irvine A, Dubernet M, Duchêne E, Gowdy M, Marguerit E, Pieri P, Parker A, De Rességuier L, Ollat N (2019) An update on the impact of climate change in viticulture and potential adaptations. Agronomy 9: 1–20

Liu D, Hu R, Palla KJ, Tuskan GA, Yang X (2016) Advances and perspectives on the use of CRISPR/Cas9 systems in plant genomics research. Curr Opin Plant Biol 30: 70–77

Lu J, He J, Zhou X, Zhong J, Li J, Liang YK (2019) Homologous genes of epidermal patterning factor regulate stomatal development in rice. J Plant Physiol 234–235: 18–27

Marshall E, Costa LM, Gutierrez-Marcos J (2011) Cysteine-Rich Peptides (CRPs) mediate diverse aspects of cell-cell communication in plant reproduction and development. J Exp Bot 62: 1677–1686

McCown BH, Lloyd G (1981) Woody plant medium (WPM) - a mineral nutrient formulation for microculture of woody plant-species. Hortic Sci 16: 453

McGranahan DA, Poling BN (2018) Trait-based responses of seven annual crops to elevated CO2 and water limitation. Renew Agric Food Syst 33: 259–266

Mohammed U, Caine RS, Atkinson JA, Harrison EL, Wells D, Chater CC, Gray JE, Swarup R, Murchie EH (2019) Rice plants overexpressing OsEPF1 show reduced stomatal density and increased root cortical aerenchyma formation. Sci Rep 9: 5584

Morales-Navarro S, Pérez-Díaz R, Ortega A, de Marcos A, Mena M, Fenoll C, González-Villanueva E, Ruiz-Lara S (2018) Overexpression of a SDD1-like gene from wild tomato decreases stomatal density and enhances dehydration avoidance in arabidopsis and cultivated tomato. Front Plant Sci 9: 940

Mosedale JR, Abernethy KE, Smart RE, Wilson RJ, Maclean IMD (2016) Climate change impacts and adaptive strategies: lessons from the grapevine. Glob Chang Biol 22: 3814–3828

Ohki S, Takeuchi M, Mori M (2011b) The NMR structure of stomagen reveals the basis of

stomatal density regulation by plant peptide hormones. Nat Commun 2: 512

Okonechnikov K, Golosova O, Fursov M, Varlamov A, Vaskin Y, Efremov I, German Grehov OG, Kandrov D, Rasputin K, Syabro M, et al (2012) Unipro UGENE: a unified bioinformatics toolkit. Bioinformatics 28: 1166–1167

Palliotti A, Tombesi S, Silvestroni O, Lanari V, Gatti M, Poni S (2014) Changes in vineyard establishment and canopy management urged by earlier climate-related grape ripening: A review. Sci Hortic 178: 43–54

Parker AK, de Cortázar-Atauri IG, Trought MCT, Destrac A, Agnew R, Sturman A, van Leeuwen C (2020) Adaptation to climate change by determining grapevine cultivar differences using temperature-based phenology models. Oeno One 54: 955–974

Pillitteri LJ, Sloan DB, Bogenschutz NL, Torii KU (2007) Termination of asymmetric cell division and differentiation of stomata. Nature 445: 501–507

Podevin N, Davies H V., Hartung F, Nogué F, Casacuberta JM (2013) Site-directed nucleases: A paradigm shift in predictable, knowledge-based plant breeding. Trends Biotechnol 31: 375–383

Pons A, Allamy L, Schüttler A, Rauhut D, Thibon C, Darriet P (2017) What is the expected impact of climate change on wine aroma compounds and their precursors in grape? Oeno One 51: 141–146

Prats-Llinàs MT, Nieto H, DeJong TM, Girona J, Marsal J (2020) Using forced regrowth to manipulate Chardonnay grapevine (*Vitis vinifera* L.) development to evaluate phenological stage responses to temperature. Sci Hortic 262: 109065

Rienth M, Vigneron N, Darriet P, Sweetman C, Burbidge C, Bonghi C, Walker RP, Famiani F, Castellarin SD (2021) Grape berry secondary metabolites and their modulation by abiotic factors in a climate change scenario–a review. Front Plant Sci 12: 643258

Santillán D, Garrote L, Iglesias A, Sotes V (2020) Climate change risks and adaptation: new indicators for Mediterranean viticulture. Mitig Adapt Strateg Glob Chang 25: 881–899

Scholasch T, Rienth M (2019) Review of water deficit mediated changes in vine and berry physiology; Consequences for the optimization of irrigation strategies. Oeno One 3: 423–444

Schultz HR (2003) Differences in hydraulic architecture account for near-isohydric and anisohydric behaviour of two field-grown Vitis vinifera L. cultivars during drought. Plant, Cell Environ 26: 1393–1405

Schultz HR (2000) Climate change and viticulture: A European perspective on climatology, carbon dioxide and UV-B effects. Aust J Grape Wine Res 6: 2–12

Sherwood S, Fu Q (2014) A drier future? Science 343: 737–739

Shimada T, Sugano SS, Hara-Nishimura I (2011) Positive and negative peptide signals control stomatal density. Cell Mol Life Sci 68: 2081–2088

Soar CJ, Dry PR, Loveys BR (2006) Scion photosynthesis and leaf gas exchange in *Vitis vinifera*

L. cv. Shiraz: Mediation of rootstock effects via xylem sap ABA. Aust J Grape Wine Res 12: 82–96

Sugano SS, Shimada T, Imai Y, Okawa K, Tamai A, Mori M, Hara-Nishimura I (2010) Stomagen positively regulates stomatal density in Arabidopsis. Nature 463: 241–244

Tomasi D, Jones G V., Giust M, Lovat L, Gaiotti F (2011) Grapevine phenology and climate change: relationships and trends in the Veneto region of Italy for 1964-2009. Am J Enol Vitic 62: 329–339

Tombesi S, Nardini A, Frioni T, Soccolini M, Zadra C, Farinelli D, Poni S, Palliotti A (2015) Stomatal closure is induced by hydraulic signals and maintained by ABA in drought-stressed grapevine. Sci Rep 5: 12449

Venios X, Korkas E, Nisiotou A, Banilas G (2020) Grapevine responses to heat stress and global warming. Plants 9: 1–15

Villalobos-González L, Muñoz-Araya M, Franck N, Pastenes C (2019) Controversies in midday water potential regulation and stomatal behavior might result from the environment, genotype, and/or rootstock: evidence from Carménère and Syrah grapevine varieties. Front Plant Sci 10: 1522

Yin X, Biswal AK, Dionora J, Perdigon KM, Balahadia CP, Mazumdar S, Chater C, Lin HC, Coe RA, Kretzschmar T, et al (2017) CRISPR-Cas9 and CRISPR-Cpf1 mediated targeting of a stomatal developmental gene EPFL9 in rice. Plant Cell Rep 36: 745–757

Zoulias N, Harrison EL, Casson SA, Gray JE (2018) Molecular control of stomatal development. Biochem J 475: 441–454

Supplementary Figures

Supplementary Figure 1. Alignment of *AtEPFL9* against *VvEPF9-1* and *VvEPF9-2*. The alignment was made using Unipro UGENE software (Okonechnikov et al., 2012). The red rectangle indicates the designed target site for the CRISPR/Cas9 system.

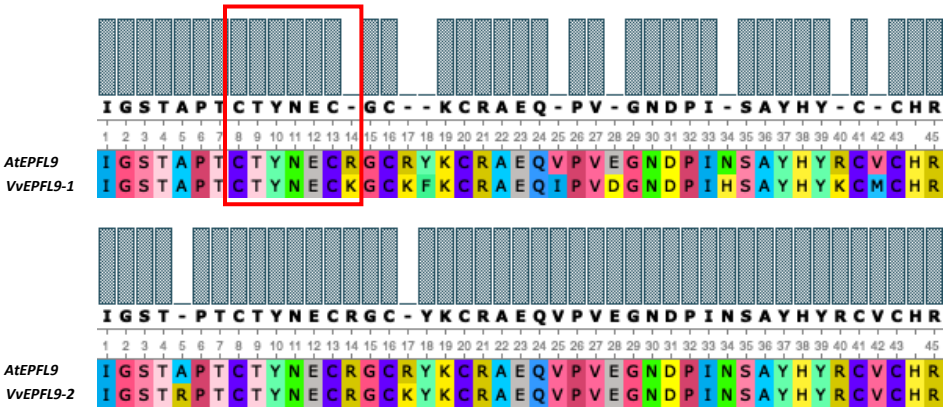

Okonechnikov, K. *et al.* Unipro UGENE: a unified bioinformatics toolkit. *Bioinformatics* **28**, 1166–1167 (2012).

Supplementary Figure 2. Analysis of CRISPR/Cas9 editing in the potential "off-target" site in *VvEPFL9-2* in nine transgenic lines

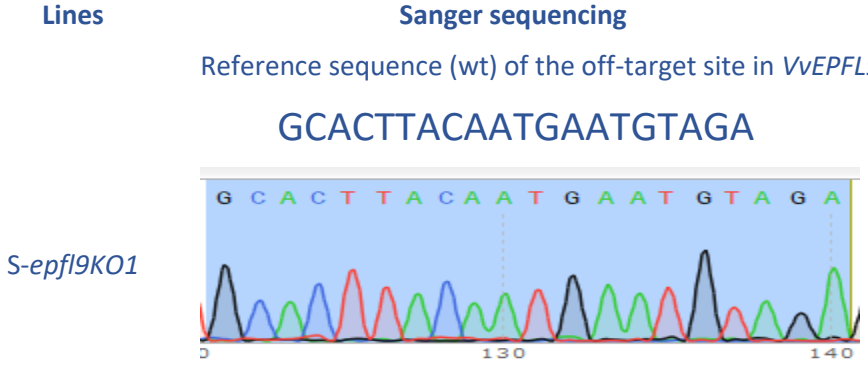

S-epfl9KO2

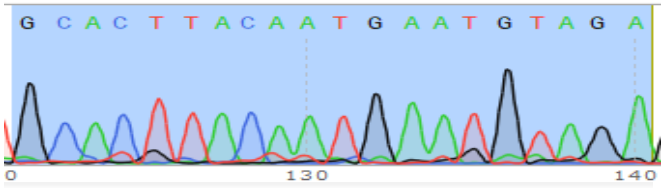

S-epfl9KO3

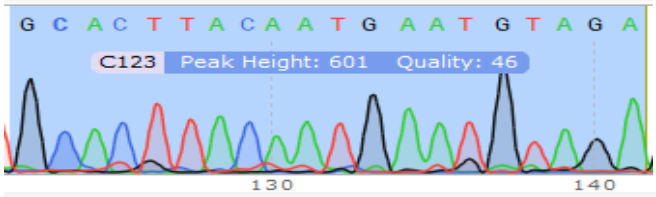

S-epfl9KO4

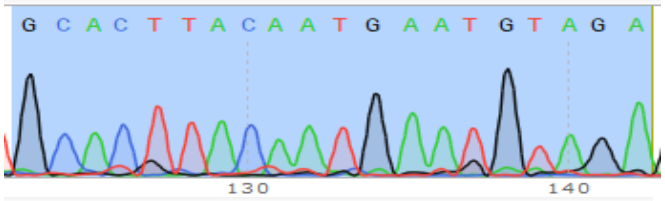

S-epfl9KO5

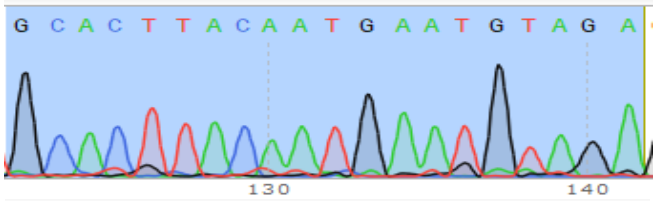

S-epfl9KO6

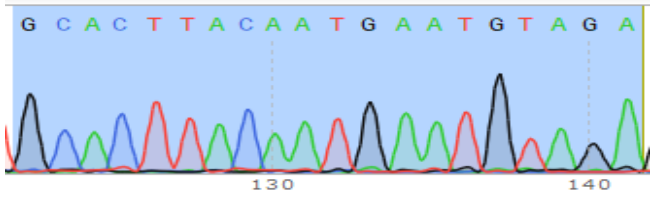

S-epfl9KO7

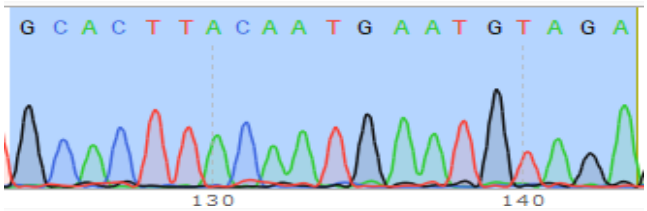

S-epfl9KO8

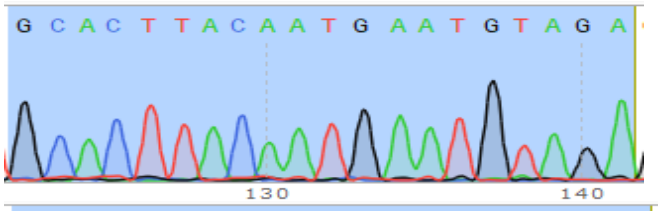

S-epfl9KO9

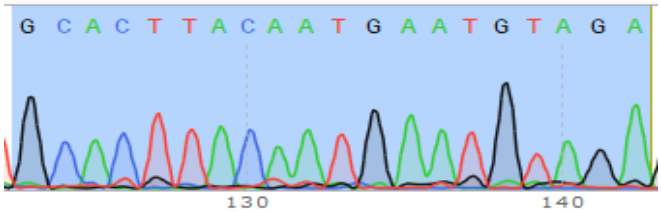

Supplementary Figure 3. Example of photosynthetic CO_2 response curves (*A*/*Ci*). Curves were carried out in Sugraone (**a**), *S-epfl9KO1* (**b**) and *S-epfl9KO2* (**c**). Fitted limiting rate for photosynthesis is shown as black line. Colored lines indicate the two photosynthesis rates of the model (Ac and Aj). **d** an example of light curve for *S-epfl9KO2* is shown. PPFD= Photosynthetic Photon Flux Density.

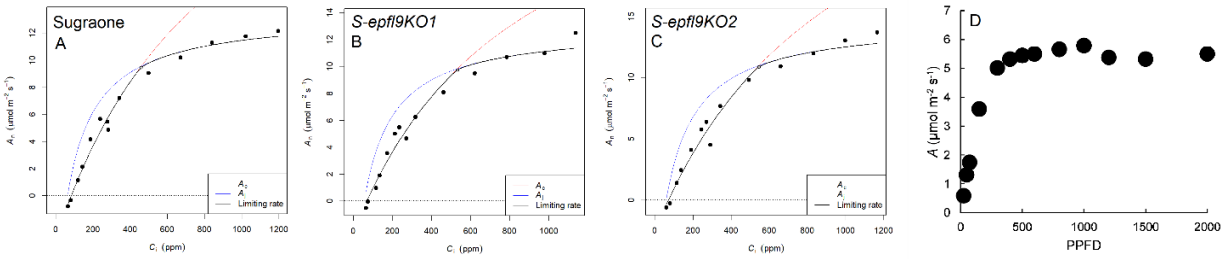

Supplementary Figure 4. Fraction of Transpirable Soil Water (FTSW) for days 1-11 of well-watered conditions and days 12-27 of the natural dry-down. The red vertical line indicated the timing of unwrapping the pots to begin the natural dry down, after full re-watering based on initial pot weights. The average FTSW is shown by the point, with the standard error indicated by the whiskers.

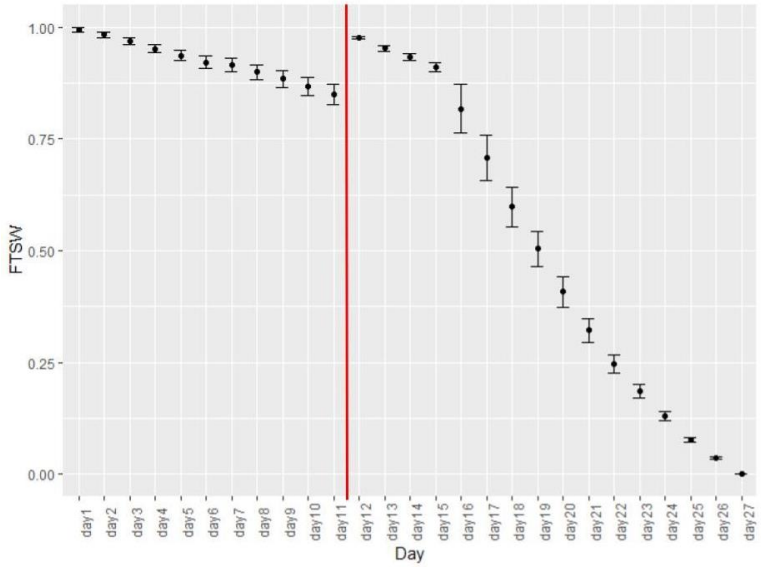

Supplementary Figure 5. Carbon Isotope discrimination (δ13C) of grapevine leaves assessed after the water stress treatment. Whiskers indicate the ranges of the minimum and maximum values and data were analyzed with one-way ANOVA (n=3-6). Different letters indicate significantly different values according to Fisher's test. Data were collected on fully expanded leaves.

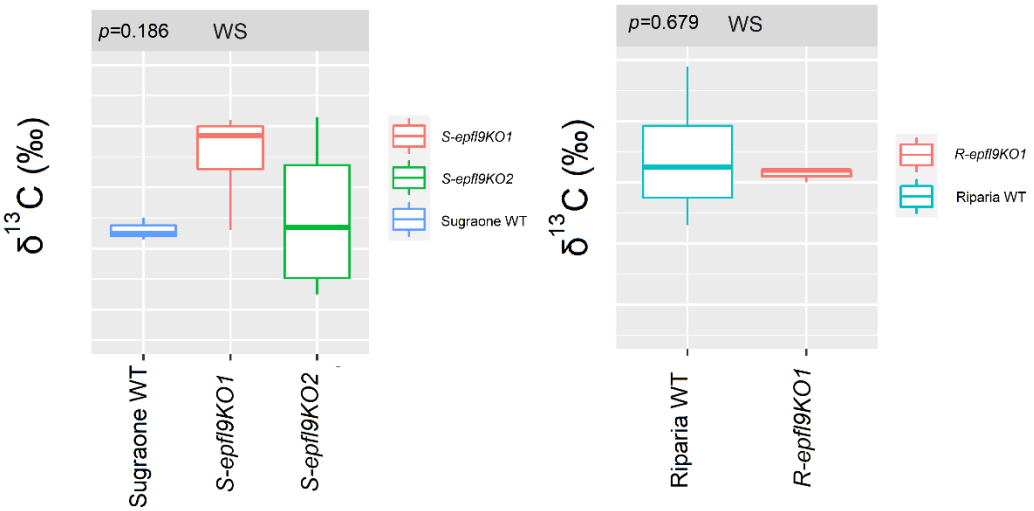

Supplementary Figure 6. Environmental data for the growth chamber and greenhouse during plant phenotyping. **(A)** Temperature and **(B)** humidity were recorded inside the growth chamber from October 29/2020- to November 17/2020 (grey shading) and in greenhouse from November 18- to December 14/2020. Red dotted line indicated the starting of the water stress experiment when the plastic and aluminum coverings were removed from the plants in well-watered conditions to begin the natural dry down.

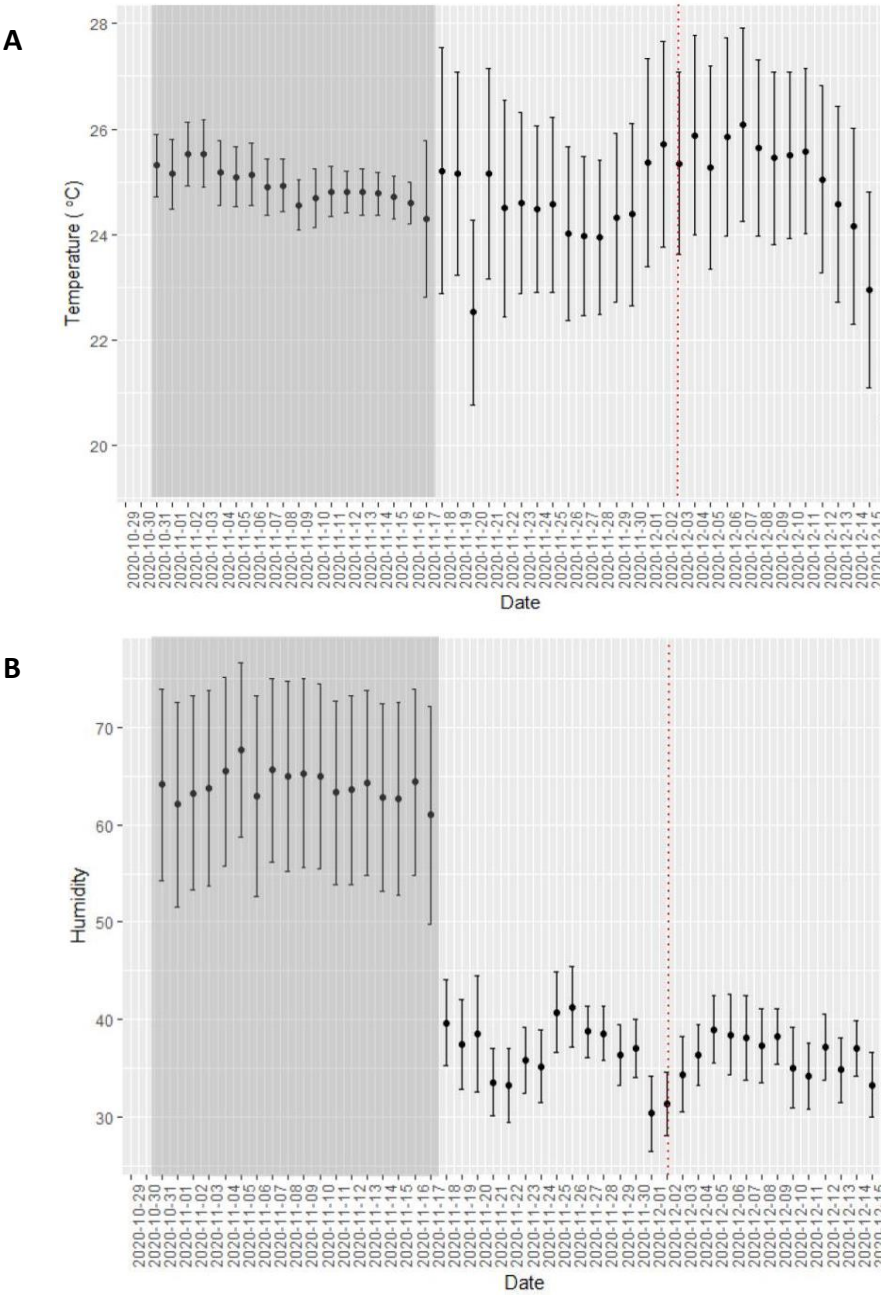

Supplementary Figure 7. Method for measuring transpiration. Aluminum foil and an additional plastic bag were used to prevent any water loss through evaporation. Plants were weighed at the same time daily to measure water lost through transpiration. 133-3 is *S-epfl9KO2*.

Supplementary Figure 8. Method for assessing leaf area using Easy Leaf Area software. Plants were photographed at the same distance and angle, and compared to the same standard area (square in red=4 cm^2) to retrieve total relative leaf area. 133-3 is *S-epfl9KO2*.

Supplementary Figure 9. Estimation of the relationship between non-destructive and destructive biomass estimation methods. **(A)** Leaf area estimate via RGB imaging (45° angle) *versus* leaf area estimated via RGB imaging (90° angle). **(B)** Leaf area estimate via RGB imaging (45° angle) *versus* fresh weight. **(C)** Leaf area estimate via RGB imaging (45° angle) *versus* and dry weight. **(D)** Fresh weight *versus* dry weight. Leaf area was calculated using Easy Leaf Area (Ealson and Bloom 2014). Linear regression was significant ($p<0.05$) for all the correlations (R^2 between 0.82 and 0.89) thus validating the non-destructive approach used in this work to estimate leaf area accumulation dynamics.

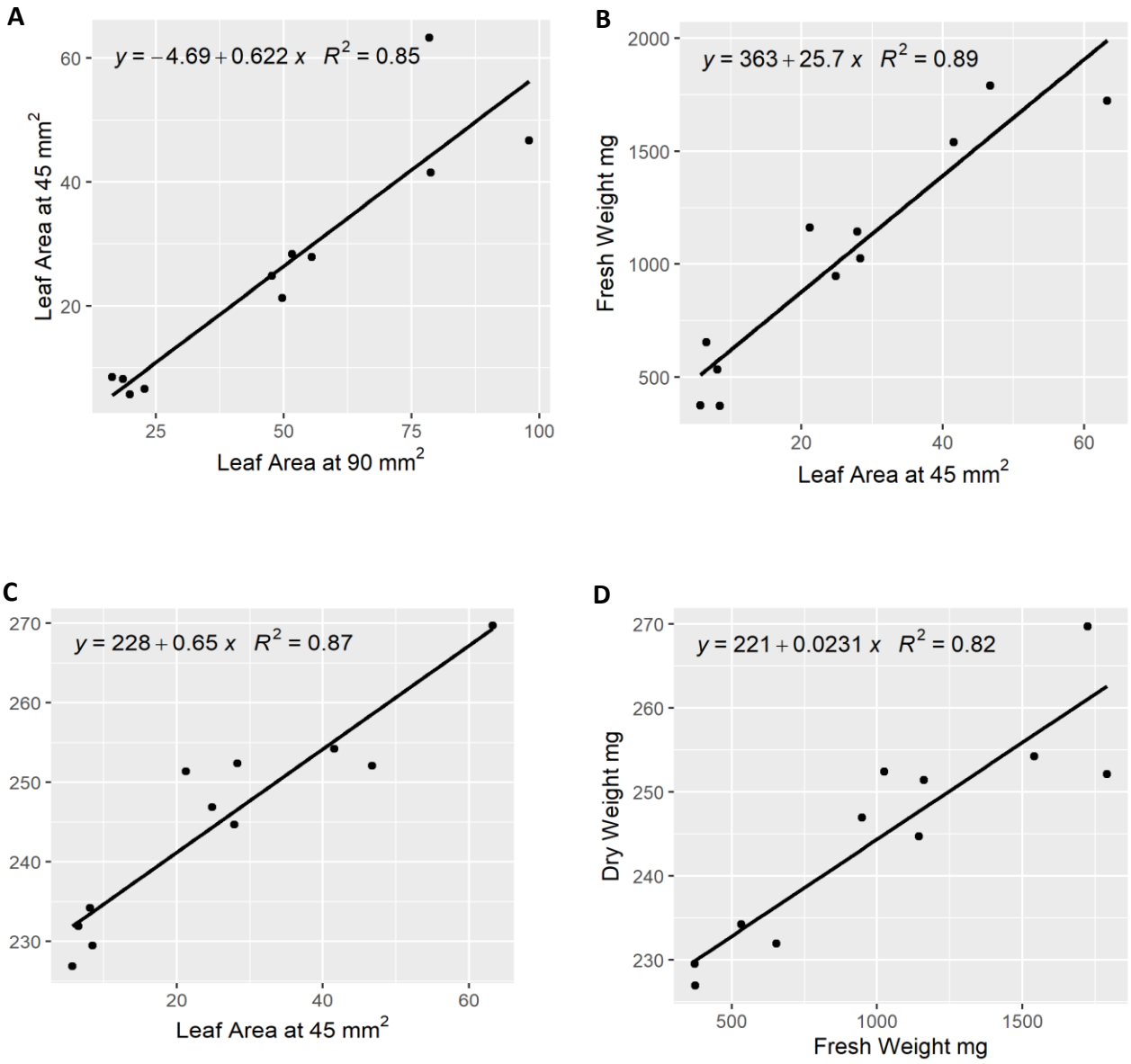

Supplementary Table 3. Publicly available genomic databases of different *Vitis Spp.* and *Vitis vinifera* varieties.

Species	Cultivar	Reference	Web site
Vitis arizonica	-	[1]	http://www.grapegenomics.com/pages/Vari/
Vitis riparia	Gloire de Montpellier	[2]	https://www.ncbi.nlm.nih.gov/assembly/GCF_004353265.1
Vitis sylvestris	DVIT3351.27	[1]	http://www.grapegenomics.com/pages/VvSyl/
	DVIT3603.07	[1]	http://www.grapegenomics.com/pages/VvSyl/
	DVIT3603.16	[1]	http://www.grapegenomics.com/pages/VvSyl/
	O34-16	[1]	http://www.grapegenomics.com/pages/VvSyl/
Vitis vinifera	Black Corinth Seeded	[1]	http://www.grapegenomics.com/pages/VvBlaCori/
	Black Corinth Seedless	[1]	http://www.grapegenomics.com/pages/VvBlaCori/
	Cabernet Sauvignon	[3]	http://www.grapegenomics.com/pages/VvCabSauv/
	Carménère	[4]	http://www.grapegenomics.com/pages/VvCar/
	Merlot	[1]	http://www.grapegenomics.com/pages/VvMerl/
	Riesling	[5]	http://www.grapegenomics.com/pages/VvRies/
	Pinot Noir ENTAV115	[6]	https://www.ncbi.nlm.nih.gov/bioproject/PRJEA18357
	Pinot Noir (PN40024)	[7,8]	https://urgi.versailles.inra.fr/Species/Vitis/Data-Sequences/Genome-sequences

2. Girollet, N. *et al.* De novo phased assembly of the *Vitis riparia* grape genome. *Sci. Data* **6**, 1–8 (2019).

3. Chin, C. S. *et al.* Phased diploid genome assembly with single-molecule real-time sequencing. *Nat. Methods* **13**, 1050–1054 (2016).

4. Minio, A., Massonnet, M., Figueroa-Balderas, R., Castro, A. & Cantu, D. Diploid genome assembly of the wine grape carménère. *G3 Genes, Genomes, Genet.* **9**, 1331–1337 (2019).

5. Zou, C. *et al.* Multiple independent recombinations led to hermaphroditism in grapevine. *Proc. Natl. Acad. Sci. U. S. A.* **118**, (2021).

6. Velasco, R. *et al.* A high quality draft consensus sequence of the genome of a heterozygous grapevine variety. *PLoS One* **2**, (2007).

7. Vitulo, N. *et al.* A deep survey of alternative splicing in grape reveals changes in the splicing machinery related to tissue, stress condition and genotype. *BMC Plant Biol.* **14**, 20–30 (2014).

8. Canaguier, A. *et al.* A new version of the grapevine reference genome assembly (12X.v2) and of its annotation (VCost.v3). *Genomics Data* **14**, 56–62 (2017).

Supplementary Table 4.

Grapevine variety	Sequence ID	Sanger sequenced region	Allelic polymorphism
Cabernet Sauvignon	*>VviCabSau_EPFL9-1*	TTCATATCCATCACAAAGAATAGTATCAGTTCA GGTGAGAAATGCAAACATTAATGAAGATCAAA ACCAGTCCCATATTCCTTGATTTTTTTCAATAAG TATGTGCTTATATTTAGGGTTCTTGGGTGCTAG AACAATGGAGATGGAGGATGGAGAAAATGGG GTTCAAGAAGAGAGATGATAGGGTCTACAGCC CCAACATGCTCATACAATGAATGCAAAGGGTG CAAGTTCAAGTGCAGAGCAGAGCAGATTCCTG TGGATGGTAATGACCCAATTCACAGTGCCTATC ACTACAAGTGTATGTGCCATAGGTAATTCAATT AGTGGCTCCTTTTTTTTTTTTTGGGTTCTTTTTG GAAAGTTT	2 SNPs: G + T (position -97); T + A (position 25)
	>VviCabSau_EPFL9-2	TGGGAACAAGTAGTATCTATGCCTGAAAATTT GTTCAATTATACTCGAGTATACTTACTTTTGACC ATTTTTGAGCCTGCAGGGCAGTGGTGAACAAT GGATGAATAGGAATTCAAGGAGACTGATGATT GGATCCACCCGGCCAACCTGCACTTACAATGA ATGTAGAGGGTGTAAGTACAAGTGCAGAGCTG AGCAAGTACCGGTCGAGGGGAACGACCCGATT AATAGCGCATACCACTATAGATGCGTTTGTCAT AGGTAAAGATGAACCAAAGTTAAGGCTAAGGC TCAGTGTTGTGTTGATCAA	1 SNP: G + A (position -45)
Sugraone	*>VviSugra_EPFL9-1*	TTCATATCCATCACAAAGAGTAGTATCAGTTCA GGTGAGAAATGCAAACATTAATGAAGATCAAA ACCAGTCCCATATTCCTTGATTTTTTTCAATAAG TATGTGCTTATATTTAGGGTTCTTGGGTGCTAG AACAATGGAGATGGAGGATGGAGAAAATGGG TTTCAAGAAGAGAGATGATAGGGTCTACAGCC CCAACATGCACATACAATGAATGCAAAGGGTG CAAGTTCAAGTGCAGAGCAGAGCAGATTCCTG TGGATGGTAATGACCCAATTCACAGTGCCTATC ACTACAAGTGTATGTGCCATAGGTAATTCAATT AGTGGCTCCTTTTTTTTTTTTTGGGTTCTTTTTG GTAAGTTTT	2 SNPs: G + T (position -97); G + T (position -17)
	>VviSugra_EPFL9-2	TGGGAACAAGTAGTATCTATGCCTGAAAATTT GTTCAATTATACTCGAGTATACTTACTTTTGACC ATTTTTGAGCCTGCAGGGCAGTGGTGAACAAT GGATGAATAGGAATTCAAGGAGACTGATGATT GGATCCACCCGGCCAACCTGCACTTACAATGA ATGTAGAGGGTGTAAGTACAAGTGCAGAGCTG AGCAAGTACCGGTCGAGGGGAACGACCCGATT AATAGCGCATACCACTATAGATGCGTTTGTCAT AGGTAAAGATGAACCAAAGTTAAGGCTAAGGC TCAGTGTTGTGTTGATCAA	1 SNP: G + A (position -45)

Pinot Noir (PN40024)	***>VviPN40024_EPFL9-1***	TTCATATCCATCACAAAGAGTAGTATCAGTTCA GGTGAGAAATGCAAACATTAATGAAGATCAAA ACCAGTCCCATATTCCTTTATTTTTTTCAATAAG TATGTGCTTATATTTAGGGTTCTTGGGTGCTAG AACAATGGAGATGGAGGATGGAGAAAATGGG GTTCAAGAAGAGAGATGATAGGGTCTACAGCC CCAACATGCACATACAATGAATGCAAAGGGTG CAAGTTCAAGTGCAGAGCAGAGCAGATTCCTG TGGATGGTAATGACCCAATTCACAGTGCCTATC ACTACAAGTGTATGTGCCATAGGTAATTCAATT AGTGGCTCCTTTTTTTTTTT	No SNP
	>VviPN40024_EPFL9-2	TGGGAACAAGTAGTATCTATGCCTGAAAATTT GTTCAATTATACTCGAGTATACTTACTTTTGACC ATTTTTGAGCCTGCAGAGCAGTGGTGAACAAT GGATGAATAGGAATTCAAGGAGACTGATGATT GGATCCACCCGGCCAACCTGCACTTACAATGA ATGTAGAGGGTGTAAGTACAAGTGCAGAGCTG AGCAAGTACCGGTCGAGGGGAACGACCCGATT AATAGCGCATACCACTATAGATGCGTTTGTCAT AGGTAAAGATGAACCAAAGATAAGGCTAAGG CTCAGTGTTGTGATGATCA	No SNP
Pinot Noir (ENTAV115)	***>VviPN-ENTAV115_EPFL9-1***	TTCATATCCATCACAAAGAGTAGTATCAGTTCA GGTGAGAAATGCAAACATTAATGAAGATCAAA ACCAGTCCCATATTCCTTTATTTTTTTCAATAAG TATGTGCTTATATTTAGGGTTCTTGGGTGCTAG AACAATGGAGATGGAGGATGGAGAAAATGGG GTTCAAGAAGAGAGATGATAGGGTCTACAGCC CCAACATGCACATACAATGAATGCAAAGGGTG CAAGTTCAAGTGCAGAGCAGAGCAGATTCCTG TGGATGGTAATGACCCAATTCACAGTGCCTATC ACTACAAGTGTATGTGCCATAGGTAATTCAATT AGTGGCTCCTTTTTTTTTTT	No SNP
	>Vvi-ENTAV115_EPFL9-2	TGGGAACAAGTAGTATCTATGCCTGAAAATTT GTTCAATTATACTCGAGTATACTTACTTTTGACC ATTTTTGAGCCTGCAGAGCAGTGGTGAACAAT GGATGAATAGGAATTCAAGGAGACTGATGATT GGATCCACCCGGCCAACCTGCACTTACAATGA ATGTAGAGGGTGTAAGTACAAGTGCAGAGCTG AGCAAGTACCGGTCGAGGGGAACGACCCGATT AATAGCGCATACCACTATAGATGCGTTTGTCAT AGGTAAAGATGAACCAAAGATAAGGCTAAGG CTCAGTGTTGTATTGATCAA	No SNP
Merlot	***>VviMer_EPFL9-1***	TTCATATCCATCACAAAGAGTAGTATCAGTTCA GGTGAGAAATGCAAACATTAATGAAGATCAAA ACCAGTCCCATATTCCTTGATTTTTTTCAATAAG TATGTGCTTATATTTAGGGTTCTTGGGTGCTAG AACAATGGAGATGGAGGATGGAGAAAATGGG GTTCAAGAAGAGAGATGATAGGGTCTACAGCC	1 SNP: G + T (position -97)

		CCAACATGCACATACAATGAATGCAAAGGGTG CAAGTTCAAGTGCAGAGCAGAGCAGATTCCTG TGGATGGTAATGACCCAATTCACAGTGCCTATC ACTACAAGTGTATGTGCCATAGGTAATTCAATT AGTGGCTCCTTTTTTTTTTTT	
	>VviMer_EPFL9-2	TGGGAACAAGTAGTATCTATGCCTGAAAATTT GTTCAATTATACTCGAGTATACTTACTTTTGACC ATTTTTGAGCCTGCAGGGCAGTGGTGAACAAT GGATGAATAGGAATTCAAGGAGACTGATGATT GGATCCACCCGGCCAACCTGCACTTACAATGA ATGTAGAGGGTGTAAGTACAAGTGCAGAGCTG AGCAAGTACCGGTCGAGGGGAACGACCCGATT AATAGCGCATACCACTATAGATGCGTTTGTCAT AGGTAAAGATGAACCAAAGTTAAGGCTAAGGC TCAGTGTTGTATTGATCAA	1 SNP: G + A (position -45)
***Vitis riparia* 'Glorie de Montpellier'**	***>Vri _EPFL9-1***	TTCATATCCATCACAAAGAGTAGTATCAGTTCA GGTGAGAAATGCAAACATTAATGAAGATCAAA ACCAGTCCCATATTCCTTTATTTTTTTCAATAAG TATGTGCTTATATTTAGGGTTCTTGGGTGCTAG AACAATGGAGATGGAGGATGGAGAAAATGGG GTTCAAGAAGAGAGATGATAGGGTCTACAGCC CCAACATGCACATACAATGAATGCAAAGGGTG CAAGTTCAAGTGCAGAGCAGAGCAGATTCCTG TGGATGGTAATGACCCAATTCACAGTGCCTATC ACTACAAGTGTATGTGCCATAGGTAATTCAATG AGTGGCTCCTTTTTTTTTTTTTTT	No SNP
	>Vri _EPFL9-2	TGGGAACAAGTAGTATCTATGCCTGAAAATTT GTTCAATTATACTCGAGTATACTTACTTTTGACC ATTTTTGAGCCTGCAGAGCAGTGGTGAACAAT GGATGAATAGGAATTCAAGGAGACTGATGATT GGATCCACCCGGCCAACCTGCACTTACAATGA ATGTAGAGGGTGTAAGTACAAGTGCAGAGCTG AGCAAGTACCGGTCGAGGGGAACGACCCGATT AATAGCGCATACCACTATAGATGCGTTTGTCAT AGGTAAAGATGAACCAAAGTTAAGGCTAAGGC TCAGTGTT	No SNP
Chardonnay	***>VviCha_EPFL9-1***	TTCATATCCATCACAAAGAGTAGTATCAGTTCA GGTGAGAAATGCAAACATTAATGAAGATCAAAA CCAGTCCCATATTCCTTTATTTTTTTCAATAAG TATGTGCTTATATTTAGGGTTCTTGGGTGCTA GAACAATGGAGATGGAGGATGGAGAAAATGGG GTTCAAGAAGAGAGATGATAGGGTCTACAGCC CCAACATGCACATACAATGAATGCAAAGGGTGC AAGTTCAAGTGCAGAGCAGAGCAGATTCCTGT GGATGGTAATGACCCAATTCACAGTGCCTATCA CTACAAGTGTATGTGCCATAGGTAATTCAATTA GTGGCTCCTTTTTTTTTTTTT	1 SNP: G + T (position -97)

	>VviCha_EPFL9-2	TGGGAACAAGTAGTATCTATGCCTGAAAATTT GTTCAATTATACTCGAGTATACTTACTTTTGACC ATTTTTGAGCCTGCAGAGCAGTGGTGAACAAT GGATGAATAGGAATTCAAGGAGACTGATGATT GGATCCACCCGGCCAACCTGCACTTACAATGA ATGTAGAGGGTGTAAGTACAAGTGCAGAGCTG AGCAAGTACCGGTCGAGGGGAACGACCCGATT AATAGCGCATACCACTATAGATGCGTTTGTCAT AGGTAAAGATGAACCAAAGTTAAGGCTAAGGC TCAGTGTTGTGTTGATCAA	No SNP
Syrah	***>VviSyr_EPFL9-1***	TTCATATCCATCACAAAGAGTAGTATCAGTTCA GGTGAGAAATGCAAACATTAATGAAGATCAAA ACCAGTCCCATATTCCTTGATTTTTTTCAATAAG TATGTGCTTATATTTAGGGTTCTTGGGTGCTAG AACAATGGAGATGGAGGATGGAGAAAATGGG GTTCAAGAAGAGAGATGATAGGGTCTACAGCC CCAACATGCACATACAATGAATGCAAAGGGTG CAAGTTCAAGTGCAGAGCAGAGCAGATTCCTG TGGATGGTAATGACCCAATTCACAGTGCCTATC ACTACAAGTGTATGTGCCATAGGTAATTCAATT AGTGGCTCCTTTTTTTTTTTT	1 SNP: G + T (position -97)
	>VviSyr_EPFL9-2	TGGGAACAAGTAGTATCTATGCCTGAAAATTT GTTCAATTATACTCGAGTATACTTACTTTTGACC ATTTTTGAGCCTGCAGGGCAGTGGTGAACAAT GGATGAATAGGAATTCAAGGAGACTGATGATT GGATCCACCCGGCCAACCTGCACTTACAATGA ATGTAGAGGGTGTAAGTACAAGTGCAGAGCTG AGCAAGTACCGGTCGAGGGGAACGACCCGATT AATAGCGCATACCACTATAGATGCGTTTGTCAT AGGTAAAGATGAACCAAAGTTAAGGCTAAGGC TCAGTGTTGTGTTGATCAA	1 SNP: G + A (position -45)
Touriga Nacional	***>VviTouNat_EPFL9-1***	TTCATATCCATCACAAAGAGTAGTATCAGTTCA GGTGAGAAATGCAAACATTAATGAAGATCAAA ACCAGTCCCATATTCCTTGATTTTTTTCAATAAG TATGTGCTTATATTTAGGGTTCTTGGGTGCTAG AACAATGGAGATGGAGGATGGAGAAAATGGG GTTCAAGAAGAGAGATGATAGGGTCTACAGCC CCAACATGCACATACAATGAATGCAAAGGGTG CAAGTTCAAGTGCAGAGCAGAGCAGATTCCTG TGGATGGTAATGACCCAATTCACAGTGCCTATC ACTACAAGTGTATGTGCCATAGGTAATTCAATT AGTGGCTCCTTTTTTTTTTT	1 SNP: G + T (position -97)
	>VviTouNat_EPFL9-2	GGGGAACAAGTAGTATCTATGCCTGAAAATTT GTTCAATTATACTCGAGTATACTTACTTTTGACC ATTTTTGAGCCTGCAGAGCAGTGGTGAACAAT GGATGAATAGGAATTCAAGGAGACTGATGATT	

		GGATCCACCCGGCCAACCTGCACTTACAATGA ATGTAGAGGGTGTAAGTACAAGTGCAGAGCTG AGCAAGTACCGGTCGAGGGGAACGACCCGATT AATAGCGCATACCACTATAGATGCGTTTGTCAT AGGTAAAGATGAACCAAAGTTAAGGCTAAGGC TCAGTGTTGTGTTGATCAA	

Supplementary Table 4. Sanger sequencing of the *VvEPFL9-1* PCR amplified fragment from genomic DNA extracted from leaves of different grapevine varieties. Primer used in the PCR were reported in Supplemental Table S5 (VvEPFL9-1_fw; VvEPFL9-1_rv; VvEPFL9-2_fw; VvEPFL9-2_rv). In red the coding sequence for the functional domain of the protein. The position of the SNPs is assigned considering the coding region in red; upstream of that region, SNP position is identified as the bases of distance from the beginning of the red region preceded by a minus (-).

Supplementary Table 5. Primers and probes used in the PCR reactions for different applications.

Primer name	Primer sequence	PCR product lenght	Application
VvEPFL9-1_fw	5′-GGGACTGCAACTCATTCAGAACT-3′	450 bp	(i) Sequencing of the VvEPFL9 genes in genotypes of interest (ii) check of the editing in the target site (on/off target)
VvEPFL9-1_rv	5′-TCTCCTACATCCCACATGCATCT-3′		
VvEPFL9-2_fw	5′-GGGAACAAGTAGTATCTATGCCT-3′	308 bp	
VvEPFL9-2_rv	5′- TGATCAACACAACACTGAGCCT-3′		
SpCas9_Fw	5′-CTTCAGAAAGGACTTCCAATTC-3′	693 bp	Screening of the transgenic plants
SpCas9_Rv	5′-ATGATCAAGTCCTTCTTCACTT-3′		
VvChiRT_fw	5′-GAGGCTGGGGATGAGAAAATTG-3′		
VvChiRT_rv	5′-CCCATCTCTCCTTCAACCACCT-3′	75 bp	
VvChiRT_Probe	FAM-5′-AAGCTGAGAAGG TTGCTCCGGT-3′-TAMRA		CN quantification by Real-time PCR
SpCas9RT_fw	5′- TACGCTGACCTTTTCTTGG-3	87 bp	
SpCas9RT_rv	5′-CTTGGTGATCTCAGTGTTCA-3′		

SpCas9RT_Probe	FAM-5'-CCTCTCCGACGCTATTCTGCTCTCC-3'

Supplementary Table 5. Outputs of CRISPResso2 software for the analysis of CRISPR/*Cas9* genome editing outcomes from Illumina sequencing data for all the edited lines obtained. For each transgenic line, the distribution of identified alleles around the predicted Cas9 cleavage position is reported (column 2). The 20bp-target site in the exon3 of VvEPFL9-1 (i.e. GCACATACAATGAATGCAAA) is indicated with a grey horizontal bar on each plot. Nucleotides are indicated by unique colors (A = green; C = red; G = yellow; T = purple). Substitutions are shown in bold font. Red rectangles highlight inserted sequences. Horizontal dashed lines indicate deleted sequences. The vertical dashed line indicates the predicted cleavage site. For the 9 selected lines reported in Fig. 2, mutated alleles were translated in protein with the software EMBO Transeq (https://www.ebi.ac.uk/Tools/st/emboss_transeq/) and the kind of mutation classified as (i) frameshift mutation with premature stop codons (F-S with SC); (ii) frameshift mutation without stop codons (F-S without SC); (iii) loss of the second Cysteine of the 6 –Cys-array (Loss of Cys). The presence of a non-mutated allele resulted in a % of WT (wild type) peptide. Alleles with a reduced number of reads (i.e. values of percentages that are below 1) were not considered (most of them showed some polymorphisms far away from the Cas9 cleavage site that are probably due to technical errors of the PCR reaction or of the sequencing procedure). According to the plot, the sum of the percentages for each kind of mutation does not reach 100% (column 5), so, for clarity of presentation and to normalize the outputs among lines, percentages were proportionally increased to reach a total of 100% (column 6, P%= proportionally increased percentages).

Supplementary Table 6. One-way ANOVA outputs for gas-exchange analysis collected at different days of water stress application (with reference to **Figure 6**).

Figure 6A:

Day 3 :	Df Sum Sq Mean Sq F value Pr(>F)
	line 2 0.985 0.492 0.15 0.863
	Residuals 9 29.644 3.294
Day 5:	Df Sum Sq Mean Sq F value Pr(>F)
	line 2 9.48 4.739 1.885 0.191
	Residuals 13 32.69 2.515

Day 7:	Df Sum Sq Mean Sq F value Pr(>F)
	line 2 3.843 1.9215 2.402 0.141
	Residuals 10 7.998 0.7998
Day 9:	Df Sum Sq Mean Sq F value Pr(>F)
	line 2 3.783 1.891 1.37 0.294
	Residuals 11 15.189 1.381
Day 12:	Df Sum Sq Mean Sq F value Pr(>F)
	line 2 1.127 0.5633 0.767 0.493
	Residuals 9 6.614 0.7349

Figure 6B:

Day 3 :	Df Sum Sq Mean Sq F value Pr(>F)
	line 2 0.001135 0.0005674 3.727 0.0662 .
	Residuals 9 0.001370 0.0001522
Day 5:	Df Sum Sq Mean Sq F value Pr(>F)
	line 2 0.002864 0.0014318 4.792 0.0276 *
	Residuals 13 0.003884 0.0002988
Day 7:	Df Sum Sq Mean Sq F value Pr(>F)
	line 2 0.0001901 9.506e-05 0.928 0.427
	Residuals 10 0.0010240 1.024e-04
Day 9:	Df Sum Sq Mean Sq F value Pr(>F)
	line 2 0.0000942 4.71e-05 0.304 0.744
	Residuals 11 0.0017051 1.55e-04
Day 12:	Df Sum Sq Mean Sq F value Pr(>F)
	line 2 0.0000485 2.423e-05 0.357 0.709
	Residuals 9 0.0006112 6.791e-05

Figure 6C:

Day 3 :	Df Sum Sq Mean Sq F value Pr(>F)
	line 2 16041 8021 3.495 0.0753 .
	Residuals 9 20651 2295
Day 5:	Df Sum Sq Mean Sq F value Pr(>F)
	line 2 6671 3335 3.305 0.0691 .
	Residuals 13 13119 1009
Day 7:	Df Sum Sq Mean Sq F value Pr(>F)
	line 1 4458 4458 1.751 0.234
	Residuals 6 15277 2546
Day 9:	Df Sum Sq Mean Sq F value Pr(>F)
	line 2 3442 1721.0 3.221 0.0792 .
	Residuals 11 5876 534.2
Day 12:	Df Sum Sq Mean Sq F value Pr(>F)
	line 2 37 18.6 0.014 0.986
	Residuals 9 11763 1307.0

CONCLUSION

Climate change is reshaping the vineyard system. Elevated levels of carbon dioxide are increasing growing season temperatures, fueling unwanted growth, and altering the balance of sugar acid ratios at harvest. On a physiological scale, elevated carbon dioxide and temperature impact the water use dynamics of the vineyard system, and depending on soil water availability, gains in water use efficiency may be limited. This thesis identified several challenges to modern viticulture, modelled the phenological response of potential alternative varieties, and explored a solution by genetically modifying grapevine for reduced stomatal density.

Elevated carbon dioxide impacts grapevine more negatively than crops like corn or potatoes because grapes are cultivated for qualities resulting from chemical balance, rather than cultivated for high yield. The penultimate harvest depends on phenological timing, which elevated carbon is advancing, along with increasing growing season temperatures. One response has been to cultivate alternative varieties, utilizing the expansive diversity available within the thousands of existing grapevine varieties. Alternative varieties may have qualities such as late ripening, heat tolerance, salt tolerance, and drought tolerance. It is important to note that high quality wine is produced when grapevine phenology is accurately matched to the local climate, so that maturation occurs during the late summer when temperatures begin to drop. Varieties have different requirements for accumulated heat, making some perfectly suited to long hot summers while others thrive in short cooler growing seasons.

While growers launch into the next generation of varieties, research like this thesis supports the expansion of lesser known varieties by providing predictions of sensitivity to climate. The diversity plots like the Ampelography vineyard at University of California Davis and the San Diego State University Santa Margarita Ecological Reserve, “The Grove,” provide a

side by side comparison of cultivars responding to climate within two important wine grape growing regions in California. The Grove provides a baseline for research on two important varieties for Southern California, Syrah and Cabernet Sauvignon, and is testing the response of Nebbiolo, Nero d'Avola, Touriga Nacional, Vermentio, Assyrtiko, Fiano, and Moschofilero. These alternatives will be the models for future studies as well, which will build on the phenological sensitivities modelled for the main geographical origins. As grapevine material continues to be adapted to new regions, these phenological models are informative for farmers by providing precise estimates of timing for the three main life cycle stages.

Finally, in the first study to describe and manipulate the epidermal patterning factor in grapevine (*VvEPFL9-1)*, I explored the possibility of designing well known grapevine cultivars to have desirable traits. These knock-out transformations were evaluated under well-watered and soil water deficit conditions. There was a reduction of stomatal density resulting from the knock-out of *EPFL-1*, and a subsequent increase in intrinsic water use efficiency for young (less than 3-month-old) grapevines in greenhouse. This study is foundational for stomatal manipulation in grapevine for climate change resilience in the industry, in particular, for well-known varieties with susceptibility to drought. Most vineyards in Europe continue to be dry-farmed, so we must consider mitigations that do not include increasing irrigation. The use of irrigation in New World territories such as California can also have cascading detrimental ecological impacts on surrounding natural environments. Our successful transformation demonstrated that altering stomatal density can improve water use traits in grapevine.

There will be many pathways to adapting grapevine to climate change. Evaluating the phenological and physiological response to create accurate and reliable predictions for future climate scenarios is essential to creating an achievable path forward. Additionally, innovative

solutions such as genetic transformations can be pivotal when attempting to provide resilience to centuries old cultivars.